

**ROLES OF CYCLIC GMP-AMP SYNTHASE
IN IMMUNE DEFENSE AGAINST RETROVIRUSES AND AUTOIMMUNITY**

APPROVED BY SUPERVISORY COMMITTEE

Dr. Zhijian Chen (Mentor)

Dr. Nan Yan

Dr. Lora Hooper

Dr. Chandrashekhar Pasare

DEDICATION

I would like to thank my family, my mentor, my graduate committee, and the people who participated in my projects for their support. I would like to thank Nicole Varnado and Philip Cheng for the editing.

ROLES OF CYCLIC GMP-AMP SYNTHASE
IN IMMUNE DEFENSE AGAINST RETROVIRUSES AND AUTOIMMUNITY

by

DAXING GAO

DISSERTATION

Presented to the Faculty of the Graduate School of Biomedical Sciences
The University of Texas Southwestern Medical Center at Dallas
In Partial Fulfillment of the Requirements
For the Degree of

DOCTOR OF PHILOSOPHY

The University of Texas Southwestern Medical Center at Dallas
Dallas, Texas
December, 2015

Copyright

by

Daxing Gao, 2015

All Rights Reserved

ROLES OF CYCLIC GMP-AMP SYNTHASE
IN IMMUNE DEFENSE AGAINST RETROVIRUSES AND AUTOIMMUNITY

Daxing Gao, Ph.D.

The University of Texas Southwestern Medical Center at Dallas, 2015

Supervising Professor: Zhijian “James” Chen, Ph.D.

The presence of DNA in the cytosol is known to trigger robust innate immunity. Cyclic GMP-AMP synthase (cGAS) is the sensor of cytosolic DNA and activation of cGAS initiates cytokine production. Here we show cGAS plays essential roles in immune defense against retroviruses as well as in autoimmune diseases caused by self-DNA.

HIV infection abrogates adaptive immunity by the depletion of CD4 T cells. However, innate immune defense mechanisms against HIV are largely unknown. We show

that pseudotyped HIV can infect human and mouse cell lines, leading to the production of interferons (IFN) and other antiviral cytokines. Activation of innate immunity by HIV requires viral cDNA synthesis but not cDNA integration. Furthermore, retrotranscribed HIV cDNA is sensed by the cytosolic DNA sensor cGAS, which then produces the second messenger 2'3'-cyclic GMP-AMP (cGAMP) to activate the adaptor STING. Importantly, wild-type HIV also triggers cGAMP production in human primary macrophages, underscoring the key role of cGAS in HIV sensing. Moreover, cytosolic sensing of other retroviruses such as murine leukemia virus and simian immunodeficiency virus also depends on cGAS.

cGAS is important for the immune response against retroviruses, however, overactive cGAS causes autoimmunity. TREX1 is a cytosolic DNase which clears mislocalized DNA in the cytosol. Loss-of-function mutations in TREX1 cause the human disease Aicardi–Goutières syndrome (AGS). AGS manifests with abnormal type I IFN production and inflammation in multiple organs. *Trex1*^{-/-} mice exhibit autoimmune and inflammatory phenotypes that are associated with elevated expression of IFN-induced genes (ISGs). Here we show that genetic ablation of cGAS in *Trex1*^{-/-} mice eliminates all detectable pathological and molecular phenotypes, including ISG induction, autoantibody production, aberrant T-cell activation, and lethality. Similarly, deletion of cGAS in mice lacking DNaseII, a lysosomal enzyme that digests DNA, rescues the lethal autoimmune phenotype of the *DnaseII*^{-/-} mice. Also, polyarthritis in *DnaseII*^{-/-} *Ifnar1*^{-/-} mice is dependent on cGAS.

These results improve our understanding of immune detection of HIV and provide cGAMP as a new adjuvant for developing HIV vaccines. Moreover, our results suggest that inhibition of cGAS may lead to new treatments of some human autoimmune diseases caused by self-DNA.

Contents

CHAPTER ONE: Introduction	1
CHAPTER TWO: cGAS is the sensor of retroviruses	26
Results.....	26
Conclusions and discussion	41
Materials and methods	49
CHAPTER THREE: cGAS initiates autoimmunity caused by self-DNA	54
Results.....	54
Conclusions and discussion	74
Materials and methods	80
References.....	87

PRIOR PUBLICATIONS

Gao D, Wu J, Wu YT, Du F, Aroh C, Yan N, Sun L, Chen ZJ. Cyclic GMP-AMP synthase is an innate immune sensor of HIV and other retroviruses. **Science**. 2013 Aug 23;341(6148):903-6. doi: 10.1126/science.1240933.

Gao D, Li T, Li XD, Chen X, Li QZ, Wight-Carter M, Chen ZJ. Activation of cyclic GMP-AMP synthase by self-DNA causes autoimmune diseases. **Proc Natl Acad Sci U S A**. 2015 Sep 14. pii: 201516465. DOI: 10.1073/pnas.1516465112

Li XD, Wu J, **Gao D**, Wang H, Sun L, Chen ZJ. Pivotal roles of cGAS-cGAMP signaling in antiviral defense and immune adjuvant effects. **Science**. 2013 Sep 20;341(6152):1390-4. doi: 10.1126/science.1244040.

LIST OF FIGURES

Figure 1	7
Figure 2	12
Figure 3	18
Figure 4	27
Figure 5	28
Figure 6	29
Figure 7	31
Figure 8	32
Figure 9	33
Figure 10	35
Figure 11	37
Figure 12	38
Figure 13	40
Figure 14	40
Figure 15	42
Figure 16	54
Figure 17	55
Figure 18	56
Figure 19	58
Figure 20	59
Figure 21	60

Figure 22	61
Figure 23	62
Figure 24	63
Figure 25	64
Figure 26	65
Figure 27	66
Figure 28	67
Figure 29	68
Figure 30	69
Figure 31	70
Figure 32	71
Figure 33	72
Figure 34	73
Figure 35	74
Figure 36	76

LIST OF TABLES

Table 1	51
Table 2	81

LIST OF DEFINITIONS

- cGAS – cyclic GMP-AMP synthase
- cGAMP – cyclic GMP-AMP
- TLR – Toll-like receptor
- STING – Stimulator of interferon genes protein
- IFN – interferon
- IKK – I κ B kinase
- NF- κ B – Nuclear Factor kappa B
- TBK1 – TANK-Binding Kinase 1
- Mtb – Mycobacterium tuberculosis
- HIV – Human Immunodeficiency Virus
- IRF3/7 – Interferon Regulatory Factor 3/7
- RIG-I – Retinoic acid-inducible gene 1
- MDA5 – Melanoma Differentiation-Associated protein 5
- MAVS – mitochondrial antiviral signaling protein
- MyD88 – Myeloid differentiation primary response gene 88
- TRIF – TIR-domain-containing adaptor-inducing interferon- β
- CARD – Caspase activation and recruitment domains
- TNF – Tumor necrosis factors
- TRAF – TNF receptor associated factor
- ISG – IFN stimulated gene

SAMHD1 – SAM domain and HD domain-containing protein 1

TREX1 – Three prime repair exonuclease 1

CXCL10 – C-X-C motif chemokine 10

IFIT3 – Interferon-induced protein with tetratricopeptide repeats 3

SLE – Systemic lupus erythematosus

AGS – Aicardi-Goutieres syndrome

CHAPTER ONE: Introduction

Innate immunity and adaptive immunity

Numerous microbes such as bacteria, viruses and fungi from the environment frequently invade our bodies but only occasionally lead to signs and symptoms of infectious diseases. Two distinct systems of immunity - innate immunity and adaptive immunity in vertebrates contribute to the defense against pathogen invasion.

Innate immunity serves as the frontier to keep microbial invaders in check and acts in a fast manner to eliminate the pathogens. As the first line of protection, innate immunity has been extensively studied in the past. The innate immune system employs a series of pathogen recognition receptors (PRRs) to recognize conserved molecules from pathogens, which are known as pathogen-associated molecular patterns (PAMPs) (Medzhitov and Janeway 1997). Upon activation, PRRs transduce signals through adaptor proteins, kinases or transcription factors, ultimately leading to anti-pathogen activity, such as cytokine production. Type I interferon (IFN) is one of the key cytokines in the antiviral response (Grandvaux, tenOever et al. 2002). Type I IFN acts in autocrine and paracrine manners and alerts neighboring uninfected cells. Type I IFN binds to the interferon- α/β receptor (IFNAR) and activates the JAK-STAT signaling pathway. Subsequent phosphorylation of signal transducer and activator of transcription 1 (STAT1) and STAT2 leads to the formation of STAT1–STAT2–IFN-regulatory factor 9 (IRF9) complexes, turning on transcription of IFN stimulated genes (ISGs) which restrict viral replication (Platanias 2005).

The second phase of the immune response is taken over by the adaptive immune system later on (Le Bon and Tough 2002). The adaptive immune system involves the humoral response and the cell-mediated response. B cells and antibodies participate in the humoral response. The cell-mediated response primarily requires T cells and phagocytes. Compared to innate immunity, adaptive immunity generates a more specific response to pathogens through somatic mutations in T cells and B cells. T cells are primarily composed of CD8+ cytotoxic T lymphocytes (CTL) and CD4+ T helper (Th) cells. CD8+ T cells kill cancer cells or pathogen-infected cells directly. CD4+ T cells play various helper roles in adaptive immunity, such as selection of B cells, antibody class switching and activation of CD8+ T cells. CD4+ T cells differentiate into distinct subtypes which are defined by a combination of cell surface markers, transcription factors and effector cytokines (Zhu, Yamane et al. 2010). T-bet is a key transcription factor for the activation of the Th1 response, and mature Th1 cells secrete IFN γ . Th2 cells require GATA3 for differentiation, and they produce interleukin (IL)-4, IL-5, and IL-13. Different T cell cytokines regulate corresponding antibody class switching. For instance, the Th1 response is associated with isotypes of IgG2a and IgG2b in mouse, whereas Th2 cytokines promote IgG1 production.

Innate immunity has been shown to influence different aspects of adaptive immunity. Dendritic cells and macrophages are the main professional antigen presenting cells (APC). Both types of cells phagocytose cell debris, foreign substances or microbes. They express major histocompatibility complex class (MHC) II molecules and CD86 on their cell surface. Engulfed antigens are processed into peptides and loaded onto MHC II molecules. TCR from CD4+ T cells recognizes MHC II-presented foreign peptide on APCs and induces T cell

activation. CD86 on APCs interacts with CD28 on T cells, providing the survival and proliferation signal for T cells. Upon activation, T cell surface markers, such as CD69, are upregulated (Maino, Suni et al. 1995). Some of the activated T cells further become memory cells, which express high levels of CD44 and low levels of CD62L, compared to CD44^{low}CD62^{high} naïve cells (Swain and Bradley 1992). CD8+ memory T cells also upregulate Ly6c (Walunas, Bruce et al. 1995). Memory responses enable adaptive immunity to last for years or decades. Cytokines produced by APCs, such as IL-12, IL-4 and IL-6 also affect differentiation of T cells. For instance, IL-12 promotes the Th1 response, while IL-4 enhances the Th2 response (Murphy and Reiner 2002).

Overall, innate immunity controls pathogen propagation in early infection. Most pathogens are detected and resolved by innate immune responses within hours. In comparison, adaptive immunity targets pathogens more efficiently but requires a longer time to develop. The two immune systems cooperate with and compensate for each other to provide immune protection.

Toll-like receptor-mediated sensing of nucleic acids

Among different PRRs, Toll-like receptors are membrane bound receptors expressed by certain types of immune cells, such as dendritic cells (DCs), macrophages and B cells. There are ten TLRs identified in humans and each recognizes distinct PAMPs (Akira, Uematsu et al. 2006). Nucleic acids from pathogens serve as PAMPs and can be sensed by TLRs on the endosomal compartment (Fig 1). TLR3 detects dsRNA and signals through the adaptor TRIF, which activates the transcription factor IRF3. TLR7 and human TLR8

recognize viral ssRNA. TLR9 senses unmethylated CpG-DNA from bacteria. TLR7 and TLR9 are highly expressed in a small subset of DCs, known as plasmacytoid DCs (pDCs) (Muzio, Polentarutti et al. 2000, Akira and Takeda 2004). pDCs are particularly efficient in producing large amounts of Type I IFN despite their low cell count in blood. TLR7, TLR8, and TLR9 share a common adaptor MyD88 which activates the transcription factor IRF7. Both TRIF and Myd88 activation induces production of downstream Type I IFN and inflammatory cytokines. In this process, endoplasmic reticulum (ER)-resident membrane protein Unc-93 homolog B1 (UNC93B1) specifically interacts with endosomal TLRs and regulates trafficking of these receptors in cells (Tabeta, Hoebe et al. 2006).

TLRs engage in immune defense against a variety of pathogens. *TLR3*-deficient mice are more susceptible than wild-type mice following infection with murine cytomegalovirus (MCMV). And *TLR3* deficiency is associated with herpes simplex encephalitis in children (Tabeta, Georgel et al. 2004, Zhang, Jouanguy et al. 2007). However, rather than assuming a protective role, TLR3 is involved in pathogenesis of influenza A virus and West Nile virus (WNV) (Wang, Town et al. 2004, Le Goffic, Balloy et al. 2006). TLR7 recognizes guanosine (G)-rich and uridine (U)-rich ssRNA ligands derived from HIV, influenza virus, and synthetic polyuridine ssRNA (Kadowaki, Ho et al. 2001, Diebold, Kaisho et al. 2004). Influenza virus and VSV potently stimulate TLR7 in DCs to mount IFN production (Ahmed, Mitchell et al. 2009). Homologous to TLR7, human TLR8 preferentially mediates recognition of bacterial RNA, as well as ssRNA from HIV, SeV, VSV and influenza A virus (Diebold, Kaisho et al. 2004, Lund, Alexopoulou et al. 2004, Melchjorsen, Jensen et al. 2005, Kruger, Oldenburg et al. 2015). TLR9, a receptor expressed by diverse cell types, such as B

lymphocytes, pDCs, monocytes and natural killer cells, accounts for detection of various DNA viruses and bacterial DNA (Bauer, Kirschning et al. 2001).

Additionally, TLRs also play multiple roles in the progression of autoimmune disease, such as systemic lupus erythematosus (SLE). DNA-containing immune complexes from SLE patients stimulate DCs through Fc γ receptors (Fc γ R) and TLR9 (Boule, Broughton et al. 2004). SLE patients also have high titers of anti-small nuclear ribonucleoproteins (snRNPs) antibodies. These immune complexes contain small nuclear RNA (snRNA) which potentially activates TLR7 (Vollmer, Tluk et al. 2005). An in vivo study has demonstrated that TLR7 exacerbates the disease and conversely, TLR9 ameliorates the disease in a lupus model with lymphoproliferation (LPR) mutations even though the production of dsDNA-specific antibodies depends on TLR9 (Christensen, Kashgarian et al. 2005, Christensen, Shupe et al. 2006, Lartigue, Courville et al. 2006). In another model of SLE, additional loss of *TLR9* dramatically improves the survival of *Fc γ RIIb*^{-/-} C57BL/6 mice (Ehlers, Fukuyama et al. 2006). All in all, TLRs have complicated functions in autoimmunity of different models.

Cytosolic RNA sensing pathway

In addition to TLRs, nucleic acids can be sensed by cytosolic PRRs (Fig 1). Compared to TLRs, cytosolic receptors are broadly expressed by different cell types and detect derivatives from microbes in the cytosol. Retinoic acid-inducible gene I (RIG-I), encoded by *DDX58* gene, is ubiquitously expressed in most somatic cell types and is responsible for sensing of RNA viruses (Yoneyama, Kikuchi et al. 2004). RIG-I detects virus-derived short dsRNA with uncapped 5'-triphosphate and blunt ends, which has different features from

RNA in eukaryotic cells (Hornung, Ellegast et al. 2006, Pichlmair, Schulz et al. 2006).

Additionally, RIG-I is able to recognize 5' triphosphate RNA transcribed from AT-rich dsDNA by DNA polymerase III (Chiu, Macmillan et al. 2009). MDA5, another RIG-I-like receptor (RLR), preferentially binds to long dsRNA (>1000bp) with no end specificity (Kato, Takahasi et al. 2011). Laboratory of genetics and physiology 2 (LGP2), the third RLR, lacks signaling effector domains and functions as a modulator in the RNA sensing pathway. LGP2 has been shown to inhibit the RIG-I pathway but is actually a positive regulator in MDA5 signaling (Satoh, Kato et al. 2010). A cell-intrinsic role for LGP2 in supporting survival and effector functions of CD8+ T cells during RNA infection has been described (Suthar, Ramos et al. 2012). All three RLR proteins share considerable homology, with a C-terminal regulatory domain (CTD) that has been implicated in autoregulation and DECH box helicase domain regions which have RNA binding and ATP hydrolysis activity. Unlike LGP2, only RIG-I and MDA5 have N-terminal CARD motifs which are essential for downstream activation.

CARD domains of RIG-I and MDA5 interact with the helicase domain in an autoinhibited state without ligand interaction. RNA binding of RIG-I and MDA5 leads to a conformational change that releases the auto-inhibition and allows association of unanchored K63 polyubiquitin chains to the CARD domain (Reikine, Nguyen et al. 2014). Ubiquitin is involved in multiple aspects of RIG-I activation. Tripartite motif-containing protein (TRIM) 25 is an E3 ligase that interacts with RIG-I and is critical for RIG-I activation (Gack, Shin et al. 2007). Production of IFN in *Trim25*^{-/-} cells in response to SeV infection is compromised.

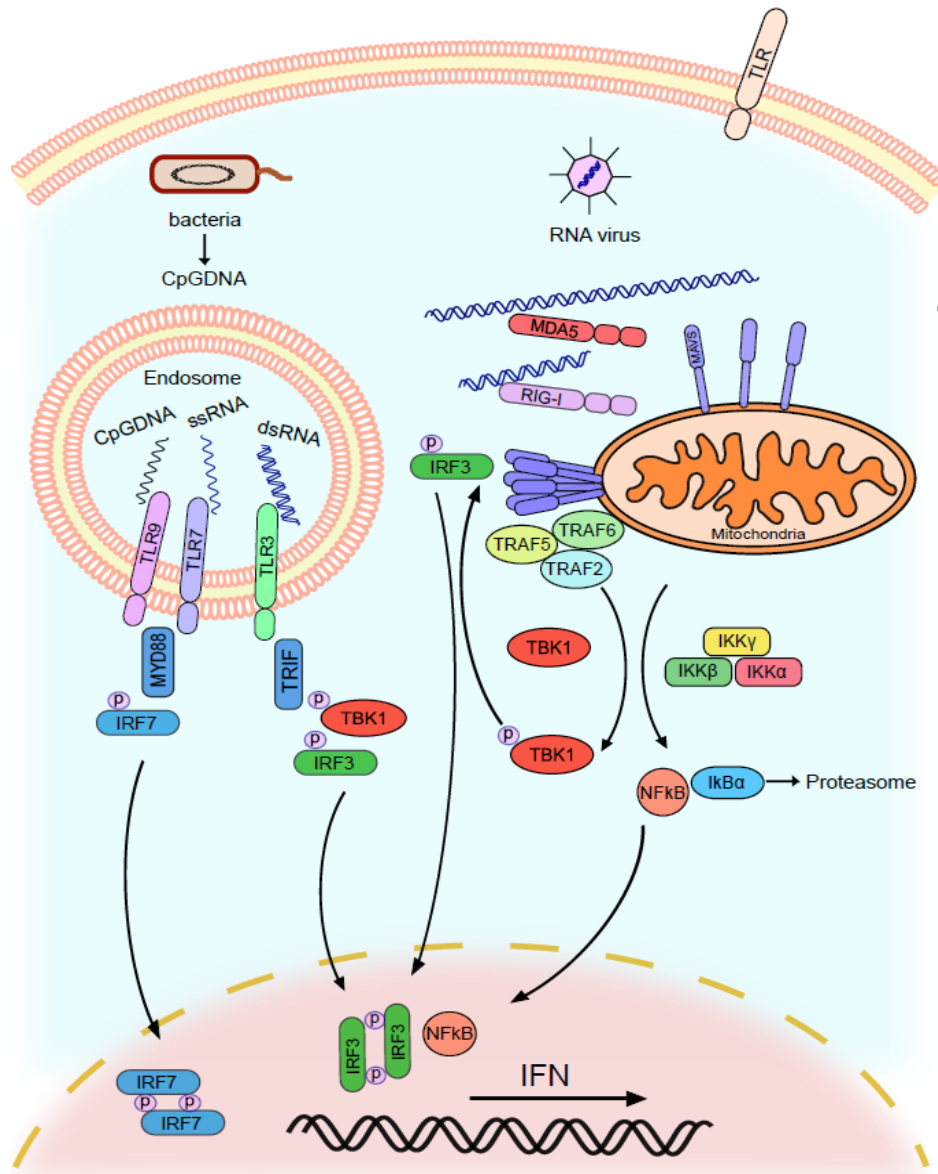


Figure 1. Nucleic acid sensing mediated by TLRs and RLRs. Different nucleic acids are detected by endosome membrane associated TLRs. TLRs signal through TRIF or Myd88, activate IRF3 or IRF7 and initiate type I IFN production. Cytosolic viral RNA is sensed by RLRs, including RIG-I and MDA-5. RLRs further transduce signal through MAVS, TRAF proteins, and finally activate IRF3 and NF- κ B, promoting Type I IFN transcription.

Upon activation, RIG-I forms a tetramer with four ubiquitin chains, leaving its CARD domains exposed (Zeng, Sun et al. 2010, Jiang, Kinch et al. 2012). Structural studies indicate the non-covalent binding of K63-ubiquitin chains (K63-Ub_n) to a tandem CARD (referred as 2CARD) of RIG-I induces its tetramer, which can be bound by three chains of K63-Ub₂. The helical tetramer of RIG-I resembles a 'lock-washer' model. Moreover, covalent ubiquitin conjugation of 2CARD further stabilizes the interaction between 2CARD and K63-Ub_n (Peisley, Wu et al. 2014). In comparison, the helicase domain and CTD of MDA5 assemble into helical filaments along the dsRNA, exposing CARD domains of MDA5 (Wu, Peisley et al. 2013). CARD domains of RIG-I and MDA5 sequentially interact and activate adaptor protein mitochondrial antiviral signaling (MAVS) on mitochondria (Seth, Sun et al. 2005).

MAVS contains an N-terminal CARD domain, a proline-rich region, and a C-terminal transmembrane (TM) domain (Kawai, Takahashi et al. 2005, Meylan, Curran et al. 2005, Seth, Sun et al. 2005, Xu, Wang et al. 2005). MAVS, upon activation, forms a prion-like structure, which is composed of detergent- and protease-resistant aggregates and is able to convert endogenous MAVS into the functional prion (Hou, Sun et al. 2011, Cai, Chen et al. 2014). Purified MAVS CARD also self-assembles into filaments. The MAVS CARD filament is a left-handed, single-stranded helix (Wu, Peisley et al. 2014). In RNA virus-infected cells, MAVS redistributes and changes into rod-shaped puncta on the membrane of mitochondria (Xu, He et al. 2014, Xu, He et al. 2015). Once MAVS is activated, it further recruits ubiquitin E3 ligase TRAF proteins (Liu, Chen et al. 2013). TRAF proteins including TRAF2, TRAF5 and TRAF6, function redundantly and activate a set of kinases, including the IKK kinase complex and TBK1. These kinases phosphorylate MAVS

at Ser442, recruiting transcription factor IRF3 to this phosphorylation site, which promotes TBK1 to phosphorylate IRF3 in close proximity (Liu, Cai et al. 2015). Phospho-IRF3 dimerizes and enters the nucleus. In parallel, IKK kinase complex phosphorylates the NF-kB inhibitor, I κ B α , leading to its degradation. After release from inhibition, NF-kB complex translocates into the nucleus and forms a transcription complex with IRF3, turning on the IFN response. Eventually, IFN acts in an autocrine and paracrine manner to induce expression of various antiviral genes.

Cytosolic RNA sensing pathways protect the host from RNA virus infection (Kato, Takeuchi et al. 2006). Cytosolic RNA sensors RIG-I and MDA5 show their preference in the detection of different strains of RNA viruses. RIG-I undertakes guard duty against a wide range of virus families, including Arenaviridae, Orthomyxoviridae, Flaviviridae, Rhabdoviridae, Paramyxoviridae, a bunyavirus and Ebola virus (Loo, Fornek et al. 2008). Conversely, MDA-5 mainly specializes in detection of picornaviruses, such as encephalomyocarditis virus (EMCV), Mengovirus and Theiler's virus (Loo, Fornek et al. 2008). IRF3 dimerization and IFN production in multiple cell types from *Mavs*^{-/-} mice, except in pDCs, are abolished during RNA virus infection (Sun, Sun et al. 2006). *Mavs*^{-/-} mice have remarkably decreased survival rate upon VSV challenge with high viral titer but low IFN production.

Due to its critical role, MAVS is targeted by pathogens such as HCV to suppress innate immunity. Viral serine protease NS3/4A from hepatitis c virus (HCV) cleaves MAVS at Cys-508, leading to dislodgement of N-terminal fragments from mitochondria and the silencing of MAVS signaling (Li, Sun et al. 2005, Meylan, Curran et al. 2005).

More importantly, dysregulation of the RNA sensing pathway is associated with autoimmune disease. The G821S mutant form of MDA5, which is constitutively active but non-responsive to RNA ligand, is associated with autoimmunity in mice (Funabiki, Kato et al. 2014). Similar to the G821S mutation, the A946T mutation has elevated Type I IFN signature and has been reported to be a risk variant for SLE. Genetic ablation of RNA sensing adaptor MAVS protects mice with G821S mutation from development of nephritis.

Patients with adenosine deaminase acting on RNA (ADAR) gene mutations have aberrant IFN expression. *Adar1*^{E861A/E861A} knock-in mice die embryonically due to hyper-inflammation (Liddicoat, Piskol et al. 2015). Interestingly, by knocking out MDA5, the survival of the mice with *Adar1*^{E861A/E861A} knock-in mutation is rescued. Long dsRNA stem loops within 3' untranslated regions of endogenous transcripts, which accumulate in *Adar1*^{E861A/E861A} cells, are further characterized as the substrates of ADAR1 in vivo.

Collectively, the RNA sensing pathway not only plays protective roles in anti-viral defense but also is involved in the progression of human autoimmune diseases.

Cytosolic DNA sensing pathway

DNA, as the genetic material for eukaryotes, is mainly confined to isolated compartments with membrane protection, such as the nucleus and mitochondria. In normal conditions, the cytosolic environment is free of DNA. DNA from microorganisms is exposed to the cytosol during infection and becomes a danger signal to induce innate immunity. Recent studies have shown that cytosolic DNA is sensed by the DNA sensor cyclic GMP-AMP synthase (cGAS), mounting the innate immune response (Fig 2) (Sun, Wu et al. 2013).

Sequence alignment reveals that cGAS contains a conserved nucleotidyltransferase (NTase) fold in the middle with a C-terminal male abnormal21 (Mab21) domain and an N-terminal unstructured region. Upon binding to DNA, cGAS synthesizes cyclic dinucleotide cyclic GMP-AMP (cGAMP) from ATP and GTP (Ablasser, Goldeck et al. 2013, Diner, Burdette et al. 2013, Wu, Sun et al. 2013). Structural studies have shown that cGAS harbors a bilobal scaffold which consists of α helices and β sheets (Gao, Ascano et al. 2013, Kranzusch, Lee et al. 2013). The binding of DNA is mediated by the interaction of the sugar-phosphate backbone of DNA and the positively charged surface of cGAS, which explains the sequence-independent binding of DNA. Structure analysis also indicates that cGAS forms a 2:2 complex with DNA, since mutations in the cGAS dimerization interface or DNA binding surface abrogate cGAMP production and DNA-induced IFN production (Li, Shu et al. 2013, Zhang, Wu et al. 2014). Upon association with DNA, the NTase catalytic pocket of cGAS undergoes dramatic conformational changes, which is accessible for ATP and GTP binding and subsequent cGAMP synthesis. The bond between 2'-OH of GTP and 5'-phosphate of ATP forms first, generating 5'-pppG(2',5')pA, which is further cyclized by the linkage between 3'-OH of adenosine and 5'-phosphate of guanosine. The second messenger-cGAMP is able to be transmitted through gap junction channels to neighboring cells, activating uninfected bystander cells during DNA virus infection (Ablasser, Schmid-Burgk et al. 2013).

cGAMP is a potent activator of downstream endoplasmic reticulum (ER) protein STING with a Kd around 4nM (Zhang, Shi et al. 2013). C-di-GMP, a signal transduction molecule found in a wide variety of bacteria, is known to activate STING and binds to

STING with a K_d of $1.21\mu M$. Other phosphodiester linkages of adenosine and guanosine, such as 2'-2' linkage, 3'-2' linkage, or 3'-3' linkage, largely reduce the binding affinity of

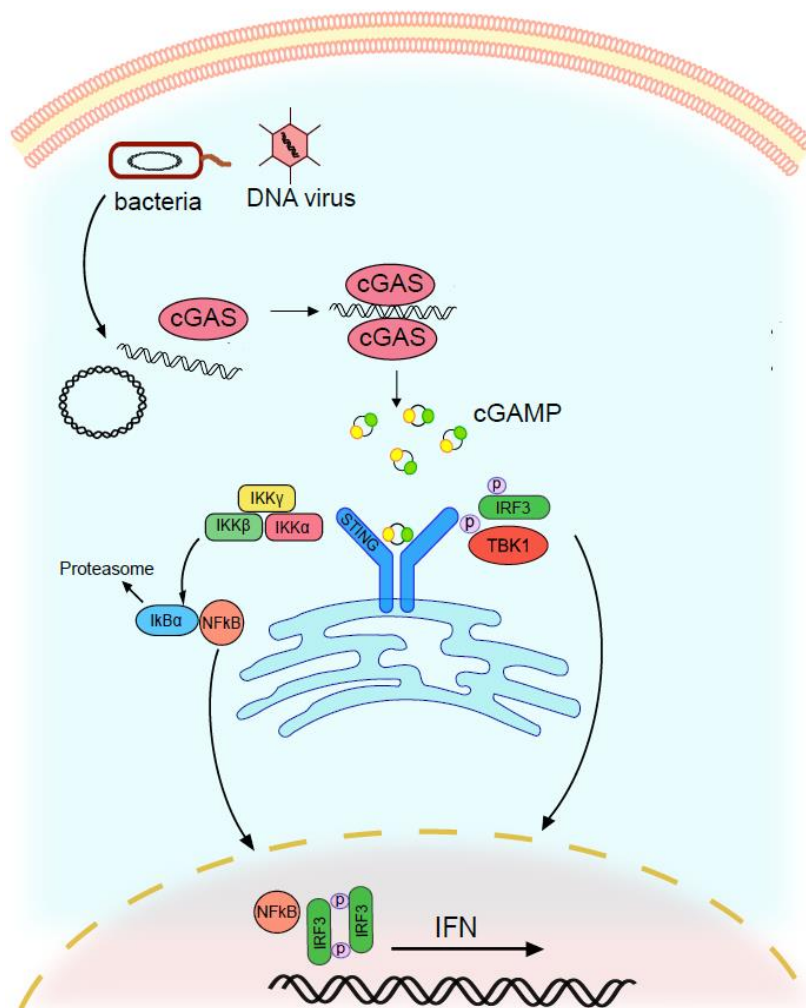


Figure 2. Cytosolic sensing of DNA by cGAS. Upon binding to cytosolic DNA derived from bacteria or DNA viruses, cGAS synthesizes cGAMP from ATP and GTP. cGAMP binds and activates STING on the ER. STING recruits kinases and transcription factors, initiating IFN production.

cGAMP to STING (Zhang, Shi et al. 2013). The STING mutation R231A uncouples the DNA/cGAMP sensing and c-di-GMP/c-di-AMP sensing pathways (Burdette, Monroe et al. 2011). Binding to cGAMP causes conformational changes in STING. Distinct from c-di-GMP binding, the binding pocket of two STING molecules with cGAMP is covered by a newly formed β sheet lid, with two arms of the STING dimer moving inward by about 20 \AA (Gao, Ascano et al. 2013, Zhang, Shi et al. 2013). Similar to MAVS, activated STING recruits TBK1, leading to TBK1 phosphorylation as well as subsequent phosphorylation of STING at Ser366 (Liu, Cai et al. 2015). Phosphorylated STING recruits IRF3, which is further phosphorylated and dimerized, resulting in transcription of Type I IFN.

The level of cGAMP is also tightly regulated. Ecto-nucleotide pyrophosphatase/phosphodiesterase 1(ENPP1) is a hydrolase in serum that degrades 2'3'-cGAMP. *Enpp1*^{-/-} MEF cells produce more IFN upon DNA virus challenge (Li, Yin et al. 2014).

The DNA sensing pathway is critical for immune defense against different pathogens. The cGAS-STING pathway restricts replication of DNA viruses such as HSV-1 in vivo. *cGas*^{-/-} and *Sting*^{-/-} mice are more susceptible to HSV-1 infection with a limited amount of type I IFN production (Ishikawa, Ma et al. 2009, Li, Wu et al. 2013). In the absence of protection by type I IFN, *cGas*^{-/-} and *Sting*^{-/-} mouse brains exhibit high viral load, whereas, wild-type mice have no detectable virus in their brains.

cGAS-STING pathway also stimulates autophagy in the face of bacterial infection, including Mycobacterium tuberculosis (Mtb). Mtb, a member of the Mycobacteriaceae family, primarily infects the mammalian respiratory system and causes most cases of tuberculosis. Mtb type VII secretion system ESX-1 translocates bacterial effector molecules

into host cytoplasm and is required for production of IFN (Stanley, Johndrow et al. 2007). Recognition of bacterial DNA by cGAS is crucial for Type I IFN induction in response to Mtb (Collins, Cai et al. 2015, Wassermann, Gulen et al. 2015, Watson, Bell et al. 2015). Meanwhile, Mtb DNA activates ubiquitin-mediated autophagy by p62 and nuclear dot protein 52 kDa (NDP52) through cGAS and STING (Watson, Manzanillo et al. 2012). Autophagy restrains Mtb bacterial load both in vitro and in vivo. Lyz-Cre-*Atg5*^{f/f} mice, which are defective in autophagy specifically in macrophages, are more susceptible to in vivo Mtb infection. *cGas*^{-/-} or cGAS knock-down cells have higher bacterial growth in comparison to control cells (Collins, Cai et al. 2015). The survival time of *cGas*^{-/-} mice significantly drops compared to wild-type mice when infected with Mtb in vivo (Collins, Cai et al. 2015).

Pathogens also hinder the immune response by targeting components in the DNA sensing pathway. *Shigella* IpaJ inhibits IFN by blocking STING translocation from the ER to ERGIC, which is important for downstream activation. And STING mutations that cause constitutive ER exit and ERGIC/Golgi accumulation have been found in patients with autoimmunity (Dobbs, Burnaevskiy et al. 2015).

DNase mutations and autoimmune diseases

Like most microbes, human cells also use DNA as genetic material, but the DNA is mainly restricted to the nucleus and mitochondria. However, unwanted DNA is generated during processes such as cell death, retroelement replication, and nucleus expulsion in erythropoiesis (Kawane, Fukuyama et al. 2001, Stetson, Ko et al. 2008). Since cGAS binds to DNA in a sequence-independent manner, aberrantly accumulated self-DNA in the cytosol

can possibly activate cGAS and cause autoimmune responses. DNases are a group of enzymes that degrade DNA. TREX1, known as DNaseIII, is cytosolic 3' DNA exonuclease (Mazur and Perrino 1999). Defect in *Trex1* leads to accumulation of cytosolic DNA, which potentially activates cGAS and initiates unnecessary autoimmune responses. In fact, *Trex1* mutations are associated with autoimmune disorders, such as Aicardi Goutieres syndrome (AGS) and SLE (Crow, Hayward et al. 2006, Lee-Kirsch, Gong et al. 2007). AGS patients develop early onset encephalopathy with intracranial calcification and cerebral atrophy, leading to intellectual disability (Aicardi and Goutieres 1984, Tolmie, Shillito et al. 1995). AGS patients also manifest dermal inflammation with high Type I IFN signatures. Mutations in other genes, such as Ribonuclease H2 (RNaseH2) enzyme complex (RNaseH2a, RNaseH2b, RNaseH2c), SAMHD1, ADAR1 and MDA5 also result in AGS (Crow, Leitch et al. 2006, Rice, Bond et al. 2009, Rice, Kasher et al. 2012, Rice, del Toro Duany et al. 2014).

Trex1^{-/-} mice develop multiple organ inflammation and have reduced lifespan (Morita, Stamp et al. 2004, Stetson, Ko et al. 2008, Gall, Treuting et al. 2012). Body weights of *Trex1^{-/-}* mice are lower than WT littermates. Organs such as skeletal muscle, tongue, skin, and the glandular stomach develop profound inflammation while other organs such as brain, colon, small intestine, pancreas, lung, and liver are not noticeably affected. Instead of mental disorders found in human AGS patients, *Trex1^{-/-}* mice suffer from severe myocarditis. In addition, anti-nuclear antibodies (ANA) and autoantibodies against heart antigens are detected in sera of *Trex1^{-/-}* mice.

TREX1 D18N mutant lacks the capacity to degrade DNA (Lehtinen, Harvey et al. 2008). Compared to *Trex1^{-/-}* mice, *TREX1^{D18N/D18N}* knock-in mice show less severe

autoimmune phenotypes, implying the DNase activity of TREX1 partially but not totally accounts for the autoimmunity phenotype (Grieves, Fye et al. 2015).

Interestingly, knocking-out IRF3, IFN receptor (IFNR) or STING rescues survival of *Trex1*^{-/-} mice, implying participation of the DNA sensing pathway in *Trex1*^{-/-} mice (Stetson, Ko et al. 2008, Gall, Treuting et al. 2012). Adoptive transfer experiments indicate non-hematopoietic cells produce IFN which acts on hematopoietic cells to promote autoimmunity. *Rag2*^{-/-}*Trex1*^{-/-} mice are also protected from mortality, which signifies the contribution of adaptive immunity in the autoimmune phenotype. Both T cells and B cells are involved in pathogenesis of *Trex1*^{-/-} mice since in the condition of *Ighm*^{-/-} (B cells deficient) or *Tcra*^{-/-}, *Trex1*^{-/-} mice are partially rescued from death.

IFN takes a part in the pathogenesis of *Trex1*^{-/-} mice. Nonetheless, elevated expression of ISGs in in vitro cultured *Trex1*^{-/-} cells is independent of IFN production (Hasan, Koch et al. 2013). Lysosomes abnormally accumulate in *Trex1*^{-/-} cells, insinuating other non-DNase-related functions of TREX1. In addition to its role in DNA degradation, TREX1 also regulates innate immunity through its C-terminus, which interacts with the oligosaccharyltransferase (OST) complex (Hasan, Fermaintt et al. 2015). Retinal vasculopathy with cerebral leukodystrophy (RVCL) patients express both normal and C-terminal truncated forms of TREX1. Truncated TREX1 is mislocalized but DNase active. RVCL cells and *Trex1-V235fs* cells have elevated free glycans and immune gene expression. In *Trex1-V235fs* knock-in mice, free glycan release causes the autoimmunity independent function of TREX1 to degrade DNA.

In comparison with TREX1, DNaseII is a lysosomal DNase, which is responsible for clearance of phagocytosed DNA derived from dead cells (Baker, Baron et al. 1998). During erythropoiesis, DNA, expelled from erythrocytes, is engulfed by macrophages (Kawane, Fukuyama et al. 2001). In the absence of DNaseII, accumulated undigested DNA stimulates macrophages to secrete IFN (Yoshida, Okabe et al. 2005). IFN induces cell death for unknown reasons and erythropoiesis is greatly impaired. *DnaseII*^{-/-} embryos are pale, smaller and embryonically lethal. Ablation of IFNR or STING prevents lethality of *DnaseII*^{-/-} embryos (Kawane, Ohtani et al. 2006, Ahn, Gutman et al. 2012). *Ifnar1*^{-/-}*DnaseII*^{-/-} mice develop polyarthritis due to overproduction of TNF- α . Treatment of anti-TNF antibody cures the mice of arthritis.

As recently shown, elevated ISGs in *Trex1*^{-/-} and *DnaseII*^{-/-} cells are rescued by knocking out cGAS (Ablasser, Hemmerling et al. 2014, Motani, Ito et al. 2015). However, whether genetic ablation of cGAS can rescue the autoimmune phenotypes in mice is still unknown.

AIM2 inflammasome-mediated DNA sensing

Cytosolic DNA not only triggers IFN response but also activates the inflammasome in myeloid cells. The inflammasome is a multiple protein complex that mediates inflammation by processing the proinflammatory cytokines IL-1 β and IL-18 and inducing a programmed cell death, known as pyroptosis (Schroder and Tschopp 2010). The inflammasome is activated by a variety of PAMPs and damage-associated molecular patterns (DAMPs). For example, anthrax lethal

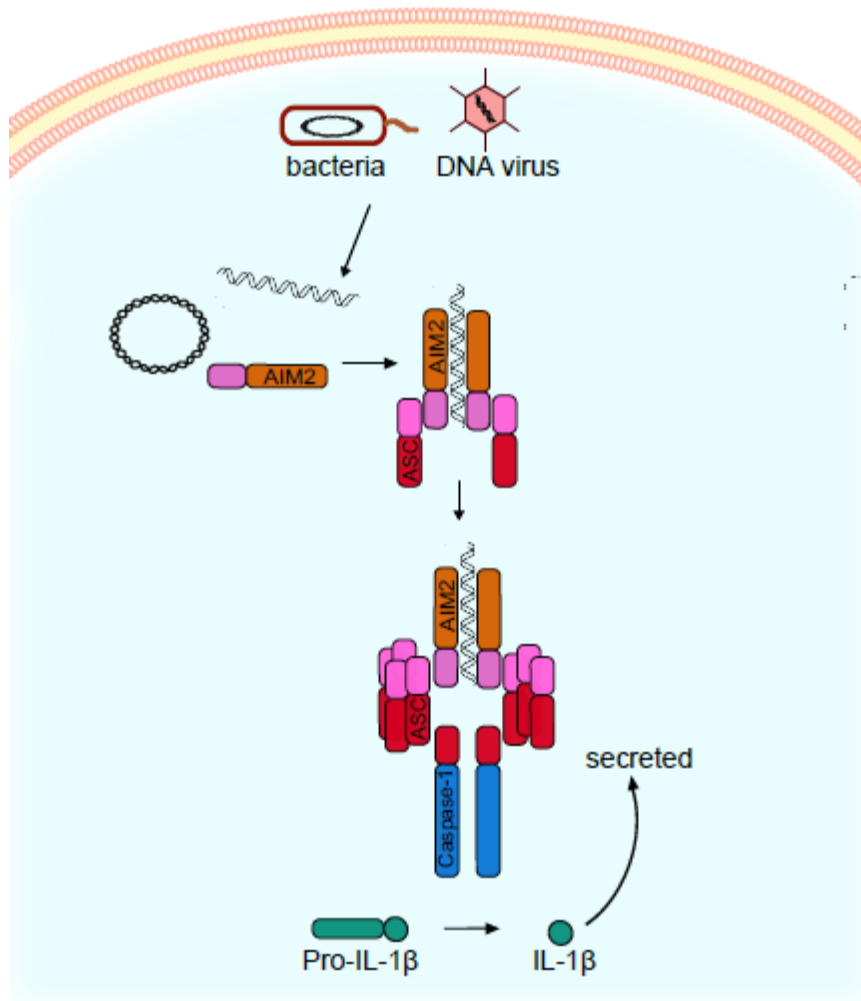


Figure 3. DNA-sensing mediated by AIM2 inflammasome. Cytosolic DNA in myeloid cells binds and activates AIM2, which recruits ASC. ASC forms a prion-like structure and activates caspase-1. Pro-IL1 β is cleaved into active form and secreted out of cells.

toxin activates the NLRP1 inflammasome, and bacterial flagellin activates the NLRC4 inflammasome (Zhao, Yang et al. 2011, Levinsohn, Newman et al. 2012). NLRP3 detects a broad range of PAMPs and DAMPs, such as nigericin, potassium efflux, extracellular ATP and reactive oxygen species (ROS) (Tschopp and Schroder 2010). Absent in melanoma 2 (AIM2) inflammasome is the sensor for dsDNA (Fig 3) (Fernandes-Alnemri, Yu et al. 2009).

The HIN200 domain of AIM2 binds to DNA, triggering AIM2 oligomerization. Upon activation, the N-terminal pyrin domain of AIM2 interacts with the pyrin domain of adaptor protein apoptosis-associated speck-like protein containing CARD (ASC) (Ishii, Coban et al. 2006). ASC forms prion-like filaments and activates caspase-1 through CARD-CARD interactions (Cai, Chen et al. 2014). Caspase-1 cleaves pro-IL-1 β or pro-IL-18 into mature IL-1 β or IL-18, which can be secreted out of cells (Sollberger, Strittmatter et al. 2014). IL-18 together with IL-12 induces cell-mediated immunity following infection (Tominaga, Yoshimoto et al. 2000). Natural killer (NK) cells and certain T cells release IFN γ , a Th1 cytokine, upon IL-18 stimulation. AIM2 is essential for inflammasome activation in response to bacteria such as Francisella tularensis (F.tularensis), or DNA viruses, such as vaccinia virus and MCMV (Fernandes-Alnemri, Yu et al. 2010, Rathinam, Jiang et al. 2010). *Aim2*^{-/-} mice suffer from a higher rate of mortality when infected with F.tularensis. IL-18 production and NK cell IFN- γ production during MCMV infection are also dependent on AIM2.

Collectively, AIM2 functions as an important sensor of DNA to activate the inflammasome during confrontation with bacterial and viral pathogens.

HIV and innate immunity

Human immunodeficiency virus (HIV), known to cause acquired immunodeficiency syndrome (AIDS), is one of the most serious health and development challenges around the world. There were 35 million people living with HIV in 2013. It is still the number one cause of death in Africa.

HIV belongs to the Lentivirus genus, part of the Retroviridae family. There are two subtypes of HIV: HIV-1 and HIV-2 (Gilbert, McKeague et al. 2003). HIV-1 is globally prevalent and has high infectivity and virulence. HIV-2 is mainly restricted to West Africa with lower virulence. The HIV genome consists of two copies of positive-sense single-stranded RNA which codes for the nine genes of the virus. The nine genes include *gag*, *pol*, *env*, *tat*, *rev*, *nef*, *vif*, *vpr*, *vpu* (or *vpx* in the case of HIV-2). *gag* encodes the Gag poly protein, which can be processed into matrix protein, capsid protein, spacer peptides, nucleocapsid protein and P6 protein. *pol* encodes for reverse transcriptase, integrase, and HIV protease. *env* encodes for envelope protein gp160 which is further cleaved into gp120 and gp40 (Chan, Fass et al. 1997). Trimers of gp120 and gp40 combine together, forming the envelope spikes, which mediate viral attachment and entry into cells. The other six genes play regulatory roles in HIV infection. For instance, Vif protein interacts and inhibits apolipoprotein B mRNA editing enzyme catalytic polypeptide-like 3G (APOBEC3G) (Stopak, de Noronha et al. 2003). APOBEC3G catalyzes the deamination of cytidine into uridine in ssDNA, resulting in extensive mutations in HIV cDNA, which efficiently terminates the viral life cycle. Vpu protein antagonizes the inhibitory effect of Tetherin, which causes retention of virions on cell surfaces and prevents HIV virion release (Neil, Zang et al. 2008). Nef protein excludes the incorporation of serine incorporator (SERINC) 5 or SERINC3 into the budding virions. SERINC5 and, to a lesser extent, SERINC3 disrupt HIV infectivity (Rosa, Chande et al. 2015, Usami, Wu et al. 2015).

In the HIV viral particles, both RNA genome and replication-related enzymes, such as reverse transcriptase, protease, and integrase, are enclosed by the capsid. The envelope,

which contains lipid bilayer taken from host cells and HIV envelope protein, surrounds and protects the viral nucleocapsid.

HIV infection abrogates adaptive immunity and causes AIDS by the depletion of CD4+ T cells. A normal range for CD4+ T cell count is about 600-1,500/mm³. With HIV progression, CD4+ T cell count drops to below 200/mm³. CD4+ T cells are the main cell type that HIV infects. HIV also infects macrophages and microglial cells through receptor CD4. Due to the capability to infiltrate into different kinds of tissues, macrophages contribute to the dissemination of HIV. Long-lived macrophages, which harbor the virus, constitute a viral reservoir that makes the virus hard to eliminate. HIV enters the cells through binding of envelope protein to CD4 as well as a chemokine coreceptor (CCR5 or CXCR4) (Coakley, Petropoulos et al. 2005). Based on the coreceptor, HIV can be divided into R5 tropic which solely uses CCR5, X4 tropic which uses CXCR4, and X4R5 tropic which uses both. HIV-1 BaL is an R5 tropic virus that efficiently infects macrophages, whereas HIV-1 IIIB is a pure X4 tropic strain that poorly replicates in macrophages (Kinter, Catanzaro et al. 1998).

Pseudotyped HIV, which is generated by lentiviral vector transfection, has been widely used in studies of HIV (He, Chen et al. 1997). The pNL4-3env-GFP plasmid provides the HIV backbone but contains a defective Env gene with frameshift and expresses GFP in place of *nef*. The other plasmid encodes VSV-glycoprotein (VSV-G) that substitutes for the function of Env. Pseudotype HIV is able to infect various cell types. Nonetheless, lacking Env, the pseudotyped virus cannot assemble into mature virion after infection.

There are several known factors that can interfere with HIV infection. IFNs play protective roles in acute HIV infection. In natural infection, DCs facilitate HIV infection of

co-cultured T-helper cells through *trans*-enhancement. However, Type I IFN suppresses *trans*-enhancement and protects T cells from infection. Also, many restriction factors of HIV are ISGs which are upregulated by IFN. IFN-induced myxovirus resistance 2 (MX2) accounts for the key component of IFN- α -mediated resistance to HIV-1 infection (Goujon, Moncorge et al. 2013, Kane, Yadav et al. 2013). MX2 blocks HIV infection at a late post-entry step, impeding accumulation of nuclear and integrated DNA.

TRIM5 is an HIV restriction factor which works in a species-specific manner. Rhesus monkey TRIM5alpha rather than human TRIM5alpha strongly restricts HIV replication by targeting HIV capsid for degradation (Stremlau, Owens et al. 2004). TRIM5 also catalyzes the synthesis of K63-Ub chains and further activates TAK1 kinase complex and downstream cytokine production (Pertel, Hausmann et al. 2011).

Notwithstanding intense study of anti-HIV factors, innate immune defense mechanisms against HIV are largely unknown since HIV was thought to trigger weak or no innate immune responses. Recent work has shown that by removal of host factors exploited by the virus, HIV can induce robust immune activation. For example, upon expression of Vpx protein, DCs make a large amount of IFN β during HIV-GFP infection (Manel, Hogstad et al. 2010). Vpx is found in HIV-2 or SIV, which is absent in HIV-1. Vpx has been shown to degrade SAMHD1 through DDB1–CUL4–DCAF E3 ligase complex (Goldstone, Ennis-Adeniran et al. 2011, Laguette, Sobhian et al. 2011). SAMHD1 is a cytosolic HIV restriction factor in myeloid lineage cells and resting CD4+ T cells (Baldauf, Pan et al. 2012, Descours, Cribier et al. 2012). SAMHD1 has dNTP hydrolase activity and RNase activity (Goldstone, Ennis-Adeniran et al. 2011, Ryoo, Choi et al. 2014). Depletion of dNTP by hydrolase activity

and degradation of viral RNA by RNase activity together strongly abrogates HIV reverse transcription. The function of SAMHD1 is also regulated by phosphorylation. Cyclin A2/CDK1 phosphorylates SAMHD1 at Thr592, which causes SAMHD1 to lose its restriction ability (Cribier, Descours et al. 2013). With SIV-VLP (Vpx) treatment or SAMHD1 knock-down, DCs are productively infected with pseudotyped HIV-GFP. As a result, DCs upregulate the costimulatory molecule CD86, indicating the maturation of DCs. Interestingly, the response relies on both IRF3 and interaction of cyclophilin A- capsid, since capsid binding mutant G89V abolishes HIV-induced immune response. However, the sensor was still enigmatic, so it was called the “cryptic sensor” for HIV.

Besides SAMHD1, TREX1 also takes part in alleviating innate immunity activated by HIV (Yan, Regalado-Magdos et al. 2010). *Trex1^{-/-}* MEF cells have increased reverse transcripts and produce IFN after infection with pseudotyped HIV. Moreover, the response is dependent on STING, TBK1, and IRF3, indicating accumulated HIV cDNA is responsible for triggering the immune response.

SIV

There are other species-specific retroviruses. Simian immunodeficiency viruses (SIVs) infect non-human primates. Some SIV subtypes, particularly SIV_{SM}, and SIV_{MAC} encode Vpx protein, which removes the restriction of SAMHD1 in myeloid cells.

Non-human primates are widely used as animal models that suitably emulate HIV pathogenesis. Unlike HIV-1 and HIV-2 which cause AIDS in humans, SIV infection of natural hosts is not pathogenic. For instance, SIV_{SM} does not cause simian AIDS in sooty

mangabeys regardless of high viral titer; nevertheless, the virus destroys the immune system of rhesus macaques. SIV infection of rhesus macaques of Asian origin is the most established model in AIDS-related research, whereas, for the non-pathogenic infection model, African natural hosts are extensively used.

MLV

Murine leukemia viruses (MLVs) that belong to the gammaretroviral genus are known to cause cancer in mice. MLVs include both exogenous and endogenous viruses. Friend murine leukemia virus (F-MLV) has been used in mouse models to study immune response against retroviruses (Browne and Littman 2009, Browne 2011). The virus is composed of a replication-defective spleen focus-forming virus (SFFV) and a replication-competent helper virus. In Balb/c mice, F-MLV promotes leukemia progression due to ineffective immune response. Conversely, C57BL/6 mice develop a CD8+T cell response and antibody production in the face of acute infection with F-MLV. Previous work has implied that DCs as well as the TLR pathway adaptor MyD88 are essential for immune clearance of F-MLV *in vivo*.

Goal of Current Research

In spite of tremendous research work on the immune response against HIV, whether HIV activates innate immunity remains unclear. And the PRR that is responsible for HIV detection needs to be identified and characterized. DNase mutations, which lead to abnormal

DNA accumulation, are associated with autoimmune diseases. Whether cGAS, the cytosolic DNA sensor, contributes to the pathogenesis of autoimmune diseases has not been explored.

CHAPTER TWO: cGAS is the sensor of retroviruses

Results

Immune detection of HIV-GFP in THP-1 cells

To clarify whether HIV triggers innate immunity, pseudotyped HIV was generated by transfecting HIV backbone vector and VSV-G expressing vector into 293T cells. Pseudotyped HIV was concentrated by PEG precipitation and titrated by detecting GFP after infection of THP-1 cells. HIV with MOI of 2 was used to infect THP-1 cells, a human monocyte cell line, which shares common features with human DCs. Upon infection, IRF3 dimerization was observed after 12hrs post-infection by native gel electrophoresis and western blotting (Fig 4A). Correspondingly, STAT1 was phosphorylated, indicating activation of the IFN pathway. And newly synthesized viral protein was detected at 16-hour time point by immunoblotting of GFP. Cells produced IFN and the chemokine CXCL10 along with the infection when measured by qRT-PCR (Fig 4B). Viral episomal DNA continued to increase after infection (Fig 4C). The IFN production was positively correlated with viral titer, and virus with MOI of 1 was enough to trigger pronounced IFN induction (Fig 4D).

Since the pseudotyped virus was made from DNA vector transfection, to rule out the possibility of DNA contamination, HIV was treated with DNase prior to the infection. As expected, DNase treatment did not affect IFN induction by HIV in THP-1 cells but largely blocked the response to DNA transfection (Fig 4E).

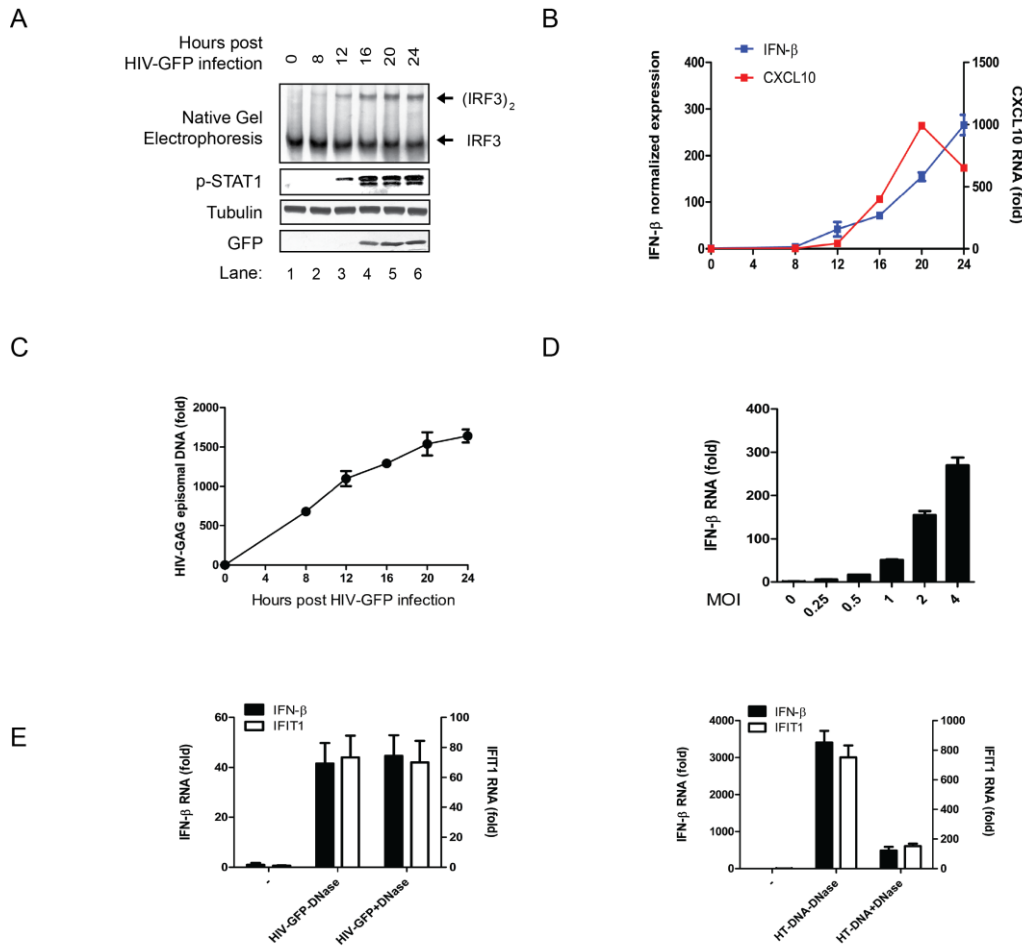


Figure 4. HIV-GFP virus induces innate immune responses in THP1 cells. (A) THP1 cells were infected with VSV-pseudotyped HIV-GFP virus at MOI = 2 for the indicated time, then cell extracts were analyzed by native gel electrophoresis or SDS-PAGE followed by immunoblotting with the indicated antibodies. (B) Similar to A, except that total RNA was isolated for qRT-PCR. (C) THP1 cells were infected with HIV-GFP for the indicated time, then episomal DNA was isolated to measure the viral GAG expression by qPCR. (D) THP1 cells were infected with HIV-GFP at the indicated MOI, then IFN β RNA levels were measured by qRT-PCR. (E) THP1 cells were infected with HIV-GFP virus (left) or transfected with DNA (right). HIV and DNA were pretreated with DNase I or mock treated. IFN β and IFIT1 RNA levels were measured by qRT-PCR.

THP-1 cells can be differentiated into macrophage-like cells by Phorbol myristate acetate (PMA). After PMA-differentiation, cells attached to the bottom of culture plates and were resistant to HIV infection. In the meantime, HIV-induced IFN production was

partially attenuated (Fig 5A-B). When treated with SIV-VLP, HIV infectivity increased together with elevated ISGs, suggesting the correlation between infectivity and innate immunity (Fig 5C-D).

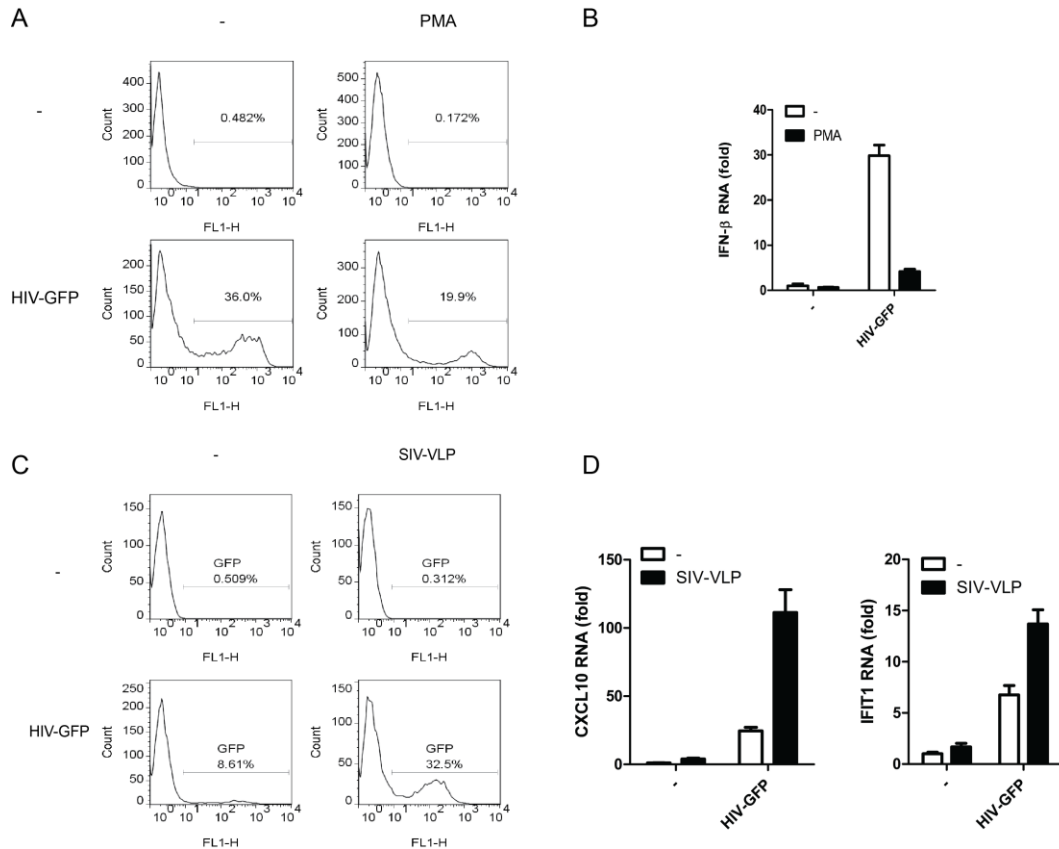


Figure 5. (A and B) THP-1 cells were treated with or without PMA for 24h, replaced with fresh medium for 12h and infected with HIV-GFP (MOI=0.5) for 21h. Cells were collected for FACS analysis (A) and IFN β RNA levels were measured by qRT-PCR (B). (C and D) THP-1 cells were treated with PMA, replaced with fresh medium for 12 hrs, pretreated with SIV-VLP for 12hrs and infected with HIV-GFP(MOI=0.5) for 20h. Cells were collected for FACS analysis (C) and ISG RNA levels were measured by qRT-PCR (D).

To make sure that the immune response is induced by HIV but not by other contaminations, THP-1 cells were treated with HIV-specific inhibitors, including two reverse transcriptase inhibitors, azidothymidine (AZT) and Nevirapine (NVP), and one integrase inhibitor, Raltegravir (RAL). All of the inhibitors potently suppressed protein

synthesis of HIV, however, only the two RT inhibitors, not the integrase inhibitor, abolished IRF3 dimerization as well as IFN production after HIV infection (Fig 6A-B).

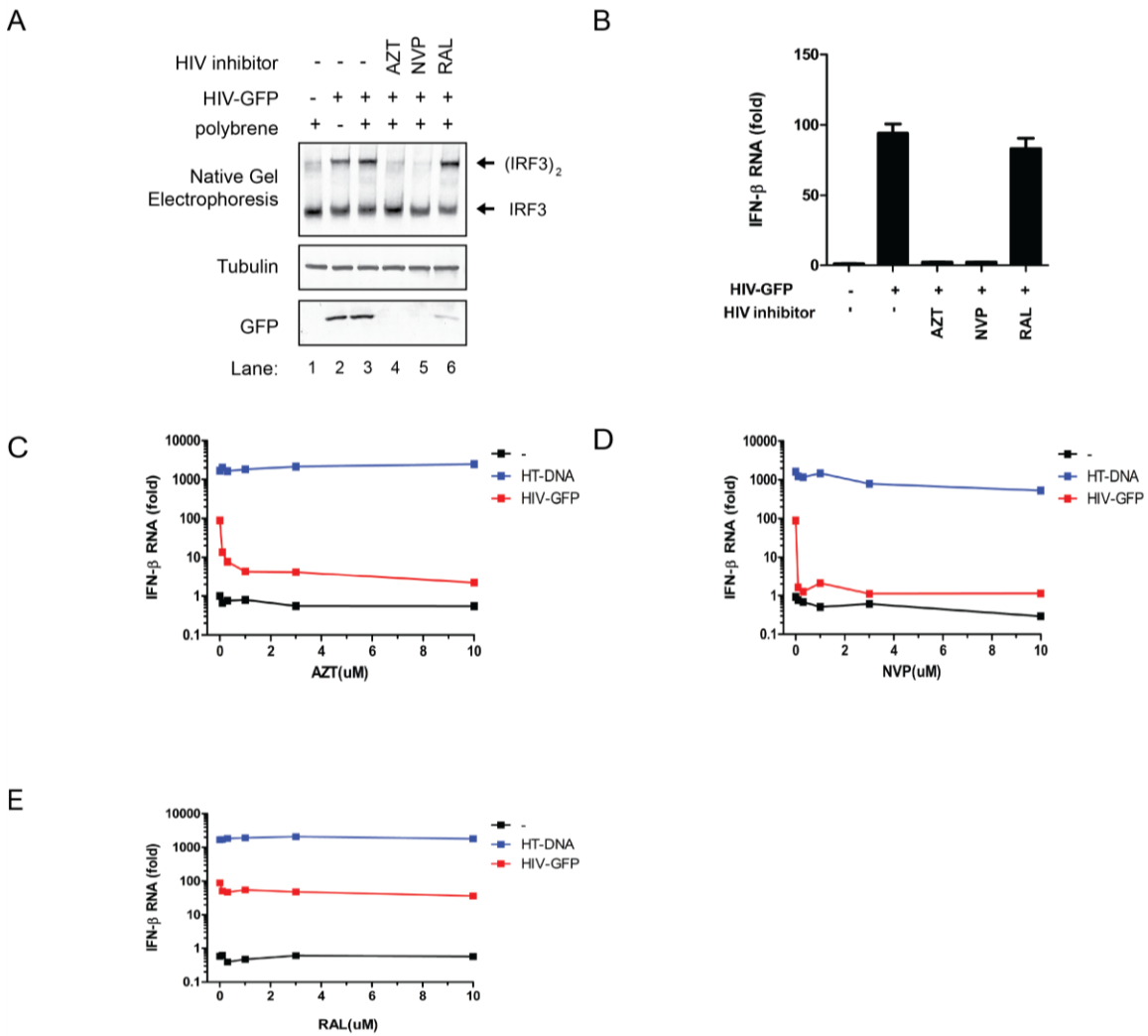


Figure 6. Innate immune responses against HIV depends on reverse transcription. (A and B) THP1 cells were treated with the HIV reverse transcriptase inhibitors (AZT at 5 μ M; NVP at 5 μ M) or integrase inhibitor (RAL at 10 μ M) for 30 min before infection with HIV-GFP. 24 h after infection, cell extracts were analyzed by native gel electrophoresis or SDS-PAGE followed by immunoblotting with indicated antibodies (A) and total RNA was isolated for qRT-PCR (B). (C-E) THP1 cells were treated with inhibitors of HIV reverse transcriptase (AZT and NVP) or integrase (RAL) at the indicated concentrations, then transfected with HT-DNA or infected with HIV-GFP. Total RNA was isolated to measure IFN β RNA levels by qRT-PCR.

Inhibitor titration experiments further showed that RT inhibitors blocked the HIV infection as well as IFN production at low concentration, leaving the DNA-induced IFN response unperturbed. In contrast, RAL did not overtly affect the HIV-induced IFN response (Fig 6C-E). These results demonstrated that the immune activation in THP1 was HIV specific and RT products were responsible for the induction of immune response. Given that HIV cDNA was generated during the RT process, the DNA sensing pathway was taken into consideration.

Involvement of cGAS-STING pathway in HIV sensing

By knocking down DNA sensing components cGAS and STING using shRNA, the induction of IFN and CXCL10 was almost completely abrogated when cells were infected with HIV-GFP (Fig 7A-B). And knocking down either cGAS or STING abolished IRF3 dimerization, suggesting the participation of cGAS and STING in HIV sensing (Fig 7C-D). Furthermore, disruption of cGAS only affected DNA but not cGAMP-induced IFN production (Fig 7E).

Previous work has discovered that in *Trex1^{-/-}* MEF, Type I IFN can be activated by HIV-GFP. To test whether cGAS is involved in HIV recognition in *Trex1^{-/-}* cells, cGAS and STING were knocked down in *Trex1^{-/-}* cells by shRNA (Fig 8A-B). The potent inhibition of IFN and CXCL10 induction by sh-cGAS or sh-STING proved that the response to HIV in *Trex1^{-/-}* cells was dependent on cGAS and STING. In comparison, cytokines induced by polyinosine-polycytidine (poly (I:C)), a synthetic activator for RNA

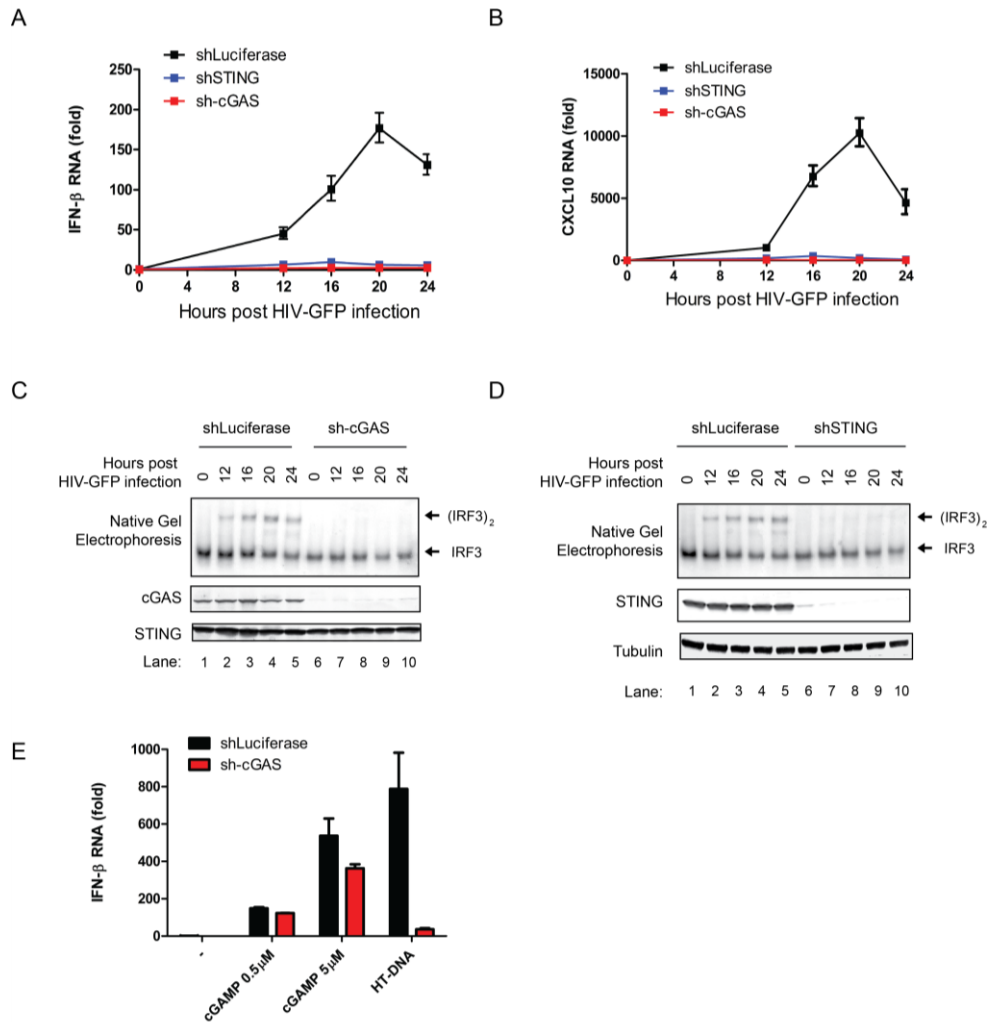


Figure 7. HIV-GFP virus induces innate immune response through the cGAS-STING pathway (A-D)
 THP1 cells stably expressing an shRNA against human cGAS, STING or luciferase (control) were infected with HIV-GFP for the indicated time followed by measurement of IFN β (A) and CXCL10 (B) RNA by qRT-PCR and immunoblotting with the indicated antibodies (C and D). (E) THP1 cells expressing an shRNA against cGAS or luciferase were stimulated with cGAMP or HT-DNA, then IFN β RNA levels were measured by qRT-PCR.

sensing, were not suppressed by the disruption of cGAS or STING. Thus shRNAs against cGAS or STING did not target downstream components shared by DNA and RNA sensing pathways (Fig 8C-D).

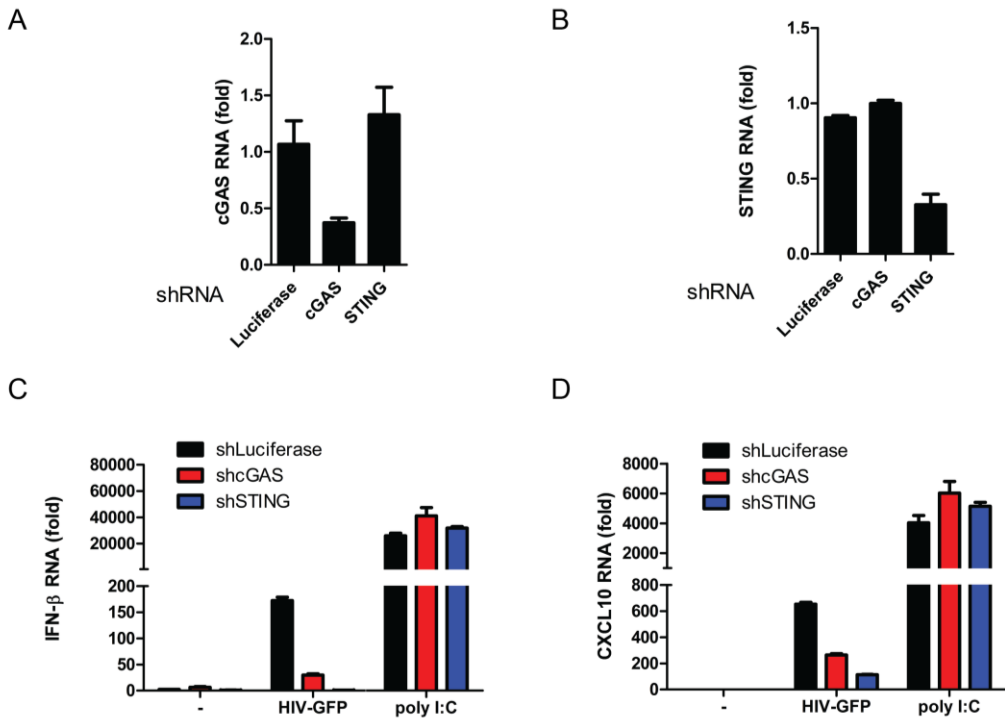


Figure 8. HIV-GFP virus induces innate immune responses in TREX1-deficient MEF cells. *Trex1^{-/-}* MEF cells stably expressing shRNA against mouse cGAS, STING or luciferase were analyzed for the knockdown efficiency by qRT-PCR (**A and B**). These cells were infected with HIV-GFP (MOI=2) for 20 hr or transfected with poly(I:C) for 6 hr, then total RNA was isolated to measure the expression of IFN β (**C**) or CXCL10 (**D**) by qRT-PCR. N.D: non-detectable.

To exclude the possibility of off-target effects of RNAi, cGAS knockout cells were generated by a technology called Transcription activator-like effector nuclease (TALEN) in a mouse fibroblast cell line, L929 cells. *cGas^{-/-}* L929 cells were not responsive to DNA transfection but responded normally to RNA virus infection (data not shown). When control L929 cells were infected with HIV-GFP, there was no IRF3 dimer detected. Interestingly, further knocking down TREX1 rendered cells responsive to HIV infection with detectable IRF3 dimer and cytokine production. Albeit, IRF3 dimer was abolished in *cGas^{-/-}* cells with HIV infection, providing the genetic evidence that GAS

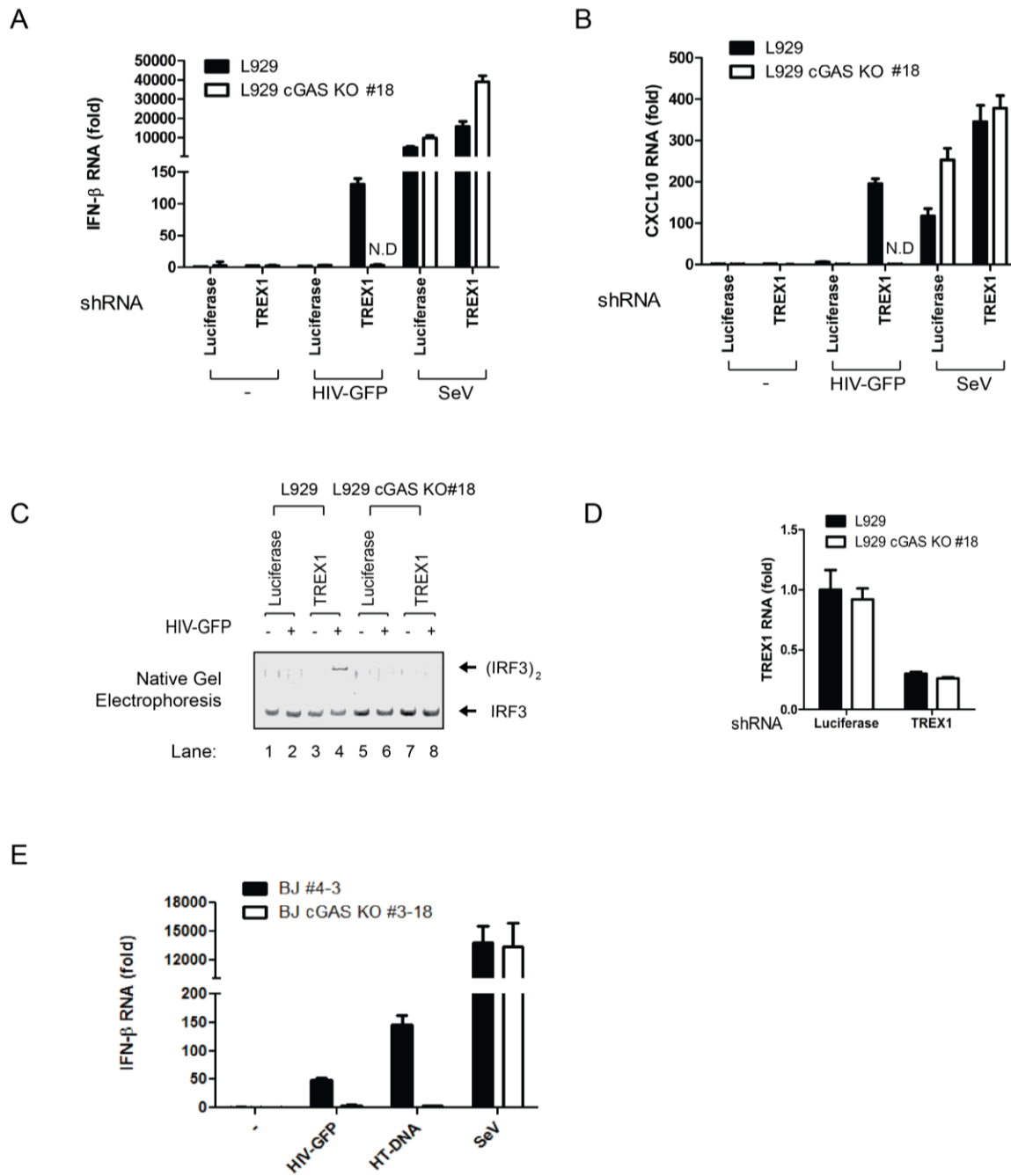


Figure 9. cGAS is essential for innate immune responses triggered by DNA transfection and HIV infection. (A-B) L929 cGAS KO clone#18 and parental L929 cells were stably transfected with shRNA vectors targeting TREX1 or luciferase (as a control). These cells were infected with HIV-GFP for 20 h or SeV for 12 h, then the RNA levels of IFN β (A) and CXCL10 (B) were measured by qRT-PCR. (C)

Similar to (**A** and **B**) except that cell lysates were analyzed by native gel electrophoresis followed by immunoblotting with an IRF3 antibody. N.D: non-detectable. (**D**) TREX1 knock-down efficiency was measured by qRT-PCR. (**E**) BJ cGAS KO clone#3-18 and wild type control #4-3 were infected with HIV-GFP for 20 h, RNA levels of IFN β were measured by qRT-PCR.

was the sensor for HIV (Fig 9C). Meanwhile, when measured by qRT-PCR, HIV-GFP triggered production of IFN and CXCL10 in TREX1 knockdown cells. If cGAS was further knocked out, the induction of cytokines totally disappeared. In comparison, immune responses to SeV, an RNA virus, were comparable between cGAS competent and cGAS deficient cells, suggesting the specific role of cGAS in sensing HIV (Fig 9A-D).

In another human fibroblast cell line, BJ cells, cGAS was targeted for frameshift mutations by TALEN. Induction of IFN by HIV-GFP was apparent in WT BJ cells. And consistent with results from L929 cells, ablation of cGAS in BJ cells only diminished IFN production in HIV-GFP or DNA treated cells but not SeV infected cells (Fig 9E).

RT products from HIV activate cGAS to produce cGAMP

Upon binding to DNA, cGAS synthesizes cGAMP which functions as a second messenger. To substantiate the activation of cGAS, HIV-infected cells were subjected to measurement of cGAMP. Dr. Josh Sun developed an in vitro assay to detect cGAMP indirectly (Sun, Wu et al. 2013, Wu, Sun et al. 2013). Cells were lysed and boiled to denature the proteins. In the presence of benzonase, the supernatant of the extract was delivered into recipient THP-1 cells which were permeabilized by bacterial toxin Perfringolysin O (PFO). This allowed cGAMP to enter the cell and activate IRF3. If the extract contained cGAMP, IRF3 would show the dimer form in Western blotting. By utilizing this in vitro assay, 293T cells and THP-1 cells were tested for cGAMP production.

THP-1 cells but not 293T cells produced cGAMP upon HIV infection, in agreement with IRF3 dimerization and STAT1 phosphorylation (Figure 10A-B). 293T cells do not

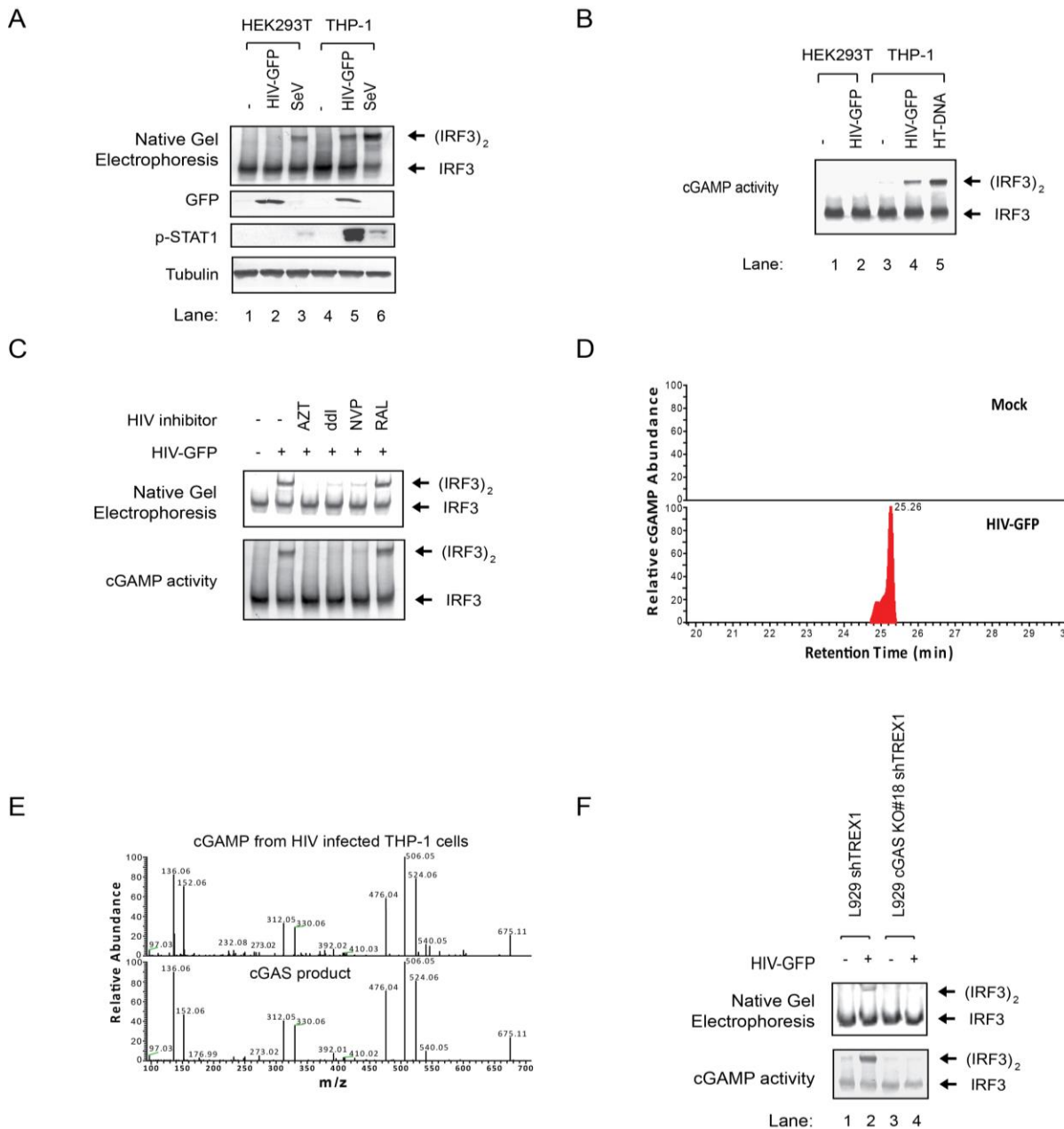


Figure 10. HIV-GFP retroviral DNA induces cGAMP activity in THP1 cells. (A) HEK293T or THP1 cells were infected with HIV-GFP or Sendai virus, then cell lysates were prepared for immunoblotting with the indicated antibodies. (B) HEK293T or THP1 cells were infected with HIV-GFP for 24 h, then cell

extracts were treated at 95°C for 5 min to prepare cGAMP-containing supernatant, the activity of which was measured by its delivery into PFO-permeabilized THP1 cells followed by IRF3 dimerization assay. HT-DNA was transfected into THP1 cells to generate cGAMP as a positive control. (C) THP1 cells were treated with inhibitors of HIV reverse transcriptase (AZT, DDI and NVP) or integrase (RAL) before infection with HIV-GFP for 24h. Cell extracts were prepared for native gel electrophoresis to detect endogenous IRF3 dimer (top panel). Aliquots of the cell extracts were measured for cGAMP activity in the supernatant by delivering the supernatant into PFO-permeabilized THP1 cells followed by IRF3 dimerization assay (bottom panel). (D) The heat-resistant supernatants from THP-1 cells without (mock) or with HIV-GFP infection were fractionated by HPLC using a C18 column, and the abundance of cGAMP was quantitated by mass spectrometry using SRM. (E) Comparison of the MS/MS spectra of cGAMP isolated from HIV-infected THP-1 cells and that synthesized in vitro by recombinant human cGAS protein. Higher-energy collision dissociation (HCD) was used to fragment the precursor ion ($[M+H]^+=675.107$) and normalized collision energy was set at 25. (F) L929 cGAS KO clone #18 and the parental cells, both stably expressing an shRNA against TREX1, were infected with HIV-GFP for 22 h. Endogenous IRF3 activation and cGAMP production in the cells were measured as described in (A).

express cGAS or STING, thus HIV could not elicit the immune response in these cells. As a control, SeV infection triggered IRF3 dimer in both cell lines.

To further address whether RT products contribute to cGAS activity, THP-1 cells were treated with HIV inhibitors before administration of the virus. Corresponding to the endogenous IRF3 dimer result, RT inhibitors but not the integrase inhibitor blocked cGAMP activity after HIV infection (Figure 10C). In order to confirm the production of cGAMP, cell lysates were fractionated by C18 column followed by mass spectrometry for detection of cGAMP. cGAMP peak only existed in HIV-infected but not in the mock-infected THP-1 cells. The spectrum of cGAMP from HIV-infected sample was the same as the cGAS in-vitro product-2'3'cGAMP (Figure 10D-E). In response to HIV, L929-shTREX1 cells also produced cGAMP, whereas cells with cGAS dysfunction did not produce cGAMP, validating that cGAS was necessary for cGAMP production during HIV infection (Figure 10F).

To demonstrate that RT products directly activate cGAS, the cytosolic fraction of HIV-infected 293 cells was inoculated with recombinant cGAS protein, and the reaction

was further applied to cGAMP activity assay. Cytosol of HIV-infected 293T cells activated cGAS to produce cGAMP. The induction of cGAMP could be inhibited by the pretreatment of HIV RT inhibitors which prevented accumulation of RT products (Figure 11A-C).

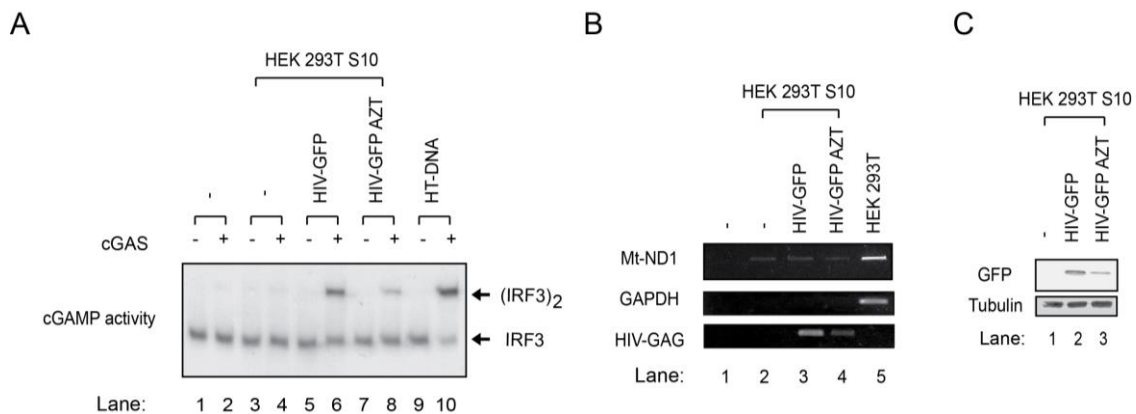


Figure 11. HIV retroviral DNA induces cGAMP activity in vitro (A) HEK293T cells were pretreated with the RT inhibitor AZT (5 μ M, 30 min) or mock treated before infection with HIV-GFP (MOI = 4) for 20 h. Cytosolic extracts were incubated with purified human cGAS protein to produce cGAMP, whose activity to stimulate IRF3 was measured after its delivery into THP1 cells. (B) DNA in the cytosolic extracts shown in (A) were extracted and amplified by PCR using specific primers of the indicated genes and then analyzed by agarose gel electrophoresis. In lane 5, total DNA in HEK293T cells was used as the template for PCR. MTND1: mitochondrial NADH dehydrogenase subunit 1. GAPDH: glyceraldehyde 3-phosphate dehydrogenase. In lane 2-4, only trace amounts of the mitochondrial DNA (MTND1) and nuclear DNA (GAPDH) are detected in the cytosolic extracts. (C) Proteins in the cytosolic extracts shown in (A) were immunoblotted with the indicated antibodies.

RT products from HIV activate cGAS to produce cGAMP in primary human cells

DCs can be efficiently infected with HIV-GFP and secrete a large amount of IFN when pretreated with SIV-VLP (Vpx). We wanted to find out whether the immune response in DCs also relies on cGAS. In collaboration with Dr. Nan Yan's group, cGAMP

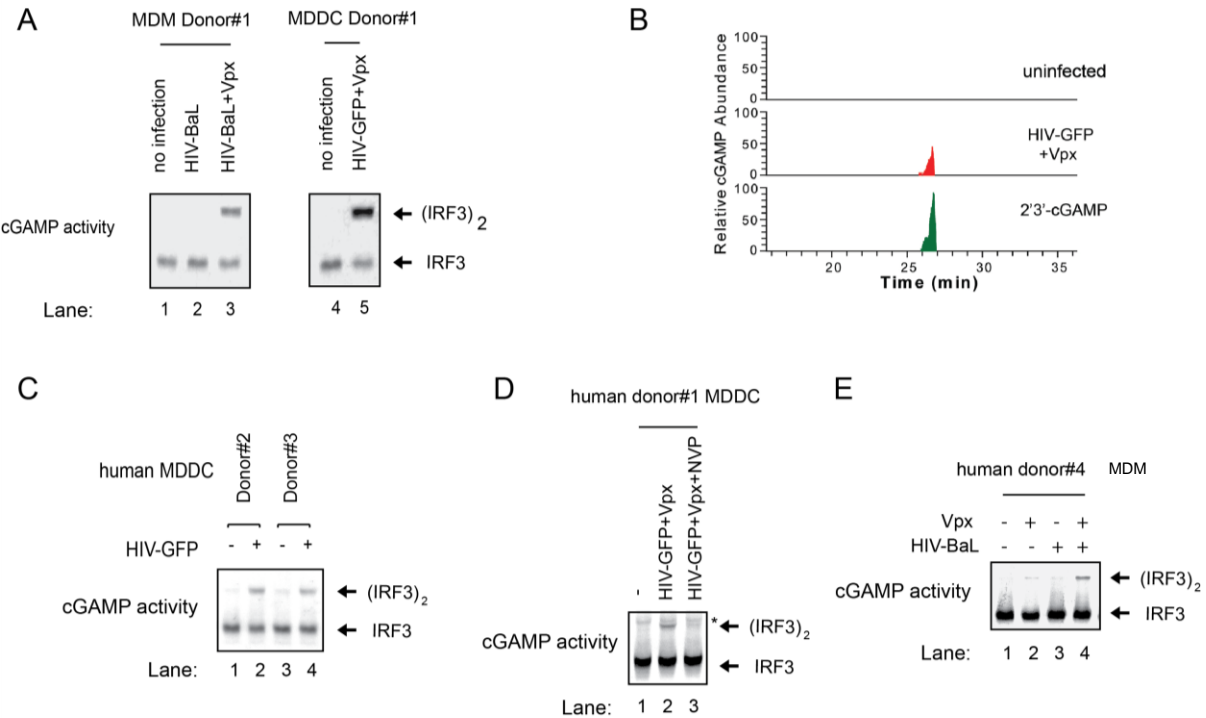


Figure 12. HIV-induced cGAMP production in human primary cells. (A and B) Monocyte-derived macrophages (MDMs) or dendritic cells (MDDCs) from a human donor were either untreated or treated with Vpx –VLP for 24 h before infection with HIV. MDMs were infected with HIV-BaL for 3 days, whereas MDDCs were infected with HIV-GFP for 1 day. The cGAMP activity (A) in these cells were measured as described in figure10. cGAMP abundance in MDDCs was measured by mass spectrometry (B). (C) MDDCs were pretreated with Vpx-VLP for 1 day before infection with HIV-GFP for 2 days. (D) similar to (C), except MDDCs were treated with NVP. (E) MDMs from human donor #4 were pretreated with Vpx-VLP or not for 1 day before infection with HIV-BaL for 3 days. The cGAMP activity in these cells was measured.

activity was measured in DCs after SIV-VLP and HIV-GFP infection (Figure 12A). As expected, cGAMP was produced in DCs after HIV infection, which was further confirmed by mass spectrometry (Figure 12B). These results were reproduced from different donors (Figure 12C). Furthermore, RT inhibitor NVP strongly suppressed cGAMP production in DCs (Figure 12D).

Previously only pseudotyped virus was proven to be immune stimulatory. In order to test whether wild-type HIV can also activate innate immunity, the wild-type strain, HIV-1 BaL, was utilized to infect human primary macrophages. It usually takes a long time to establish HIV infection during natural processes in macrophages. And there is usually no IFN response to HIV. When SAMHD1 was depleted by SIV-VLP, macrophages could be efficiently infected and rendered capable of synthesizing cGAMP in response to HIV. This result was also repeated in another donor (Figure 12A; E).

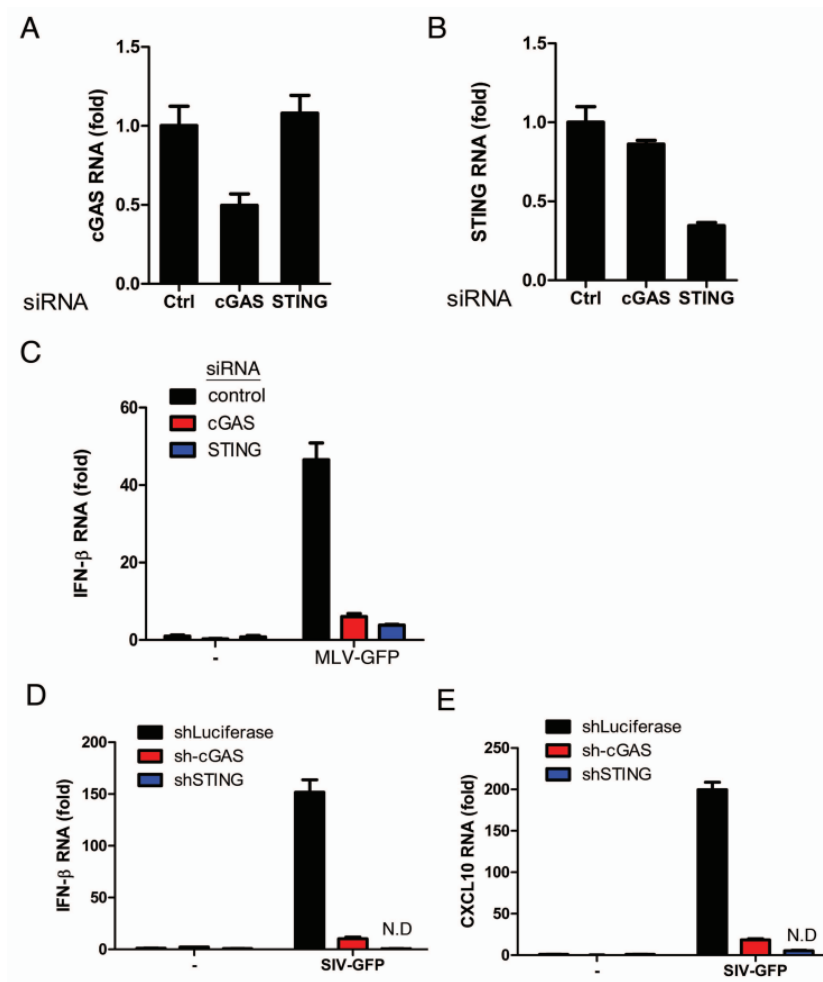


Figure 13. cGAS and STING mediate IFN β induction by MLV. (A-C) $Trex1^{-/-}$ MEF cells were transfected with indicated siRNA to knock down endogenous cGAS or STING as verified by qRT-PCR (A and B). These cells were infected with MLV-GFP (MOI = 2) for 20 h, then IFN β RNA levels were measured by qRT-PCR (C). (D and E) $Trex1^{-/-}$ MEF cells stably expressing shRNA against mouse cGAS, STING or luciferase were infected with SIV-GFP (MOI = 1) for 20 h. RNA levels of IFN β (D) and CXCL10 (E) were measured by qRT-PCR. ND: not detectable.

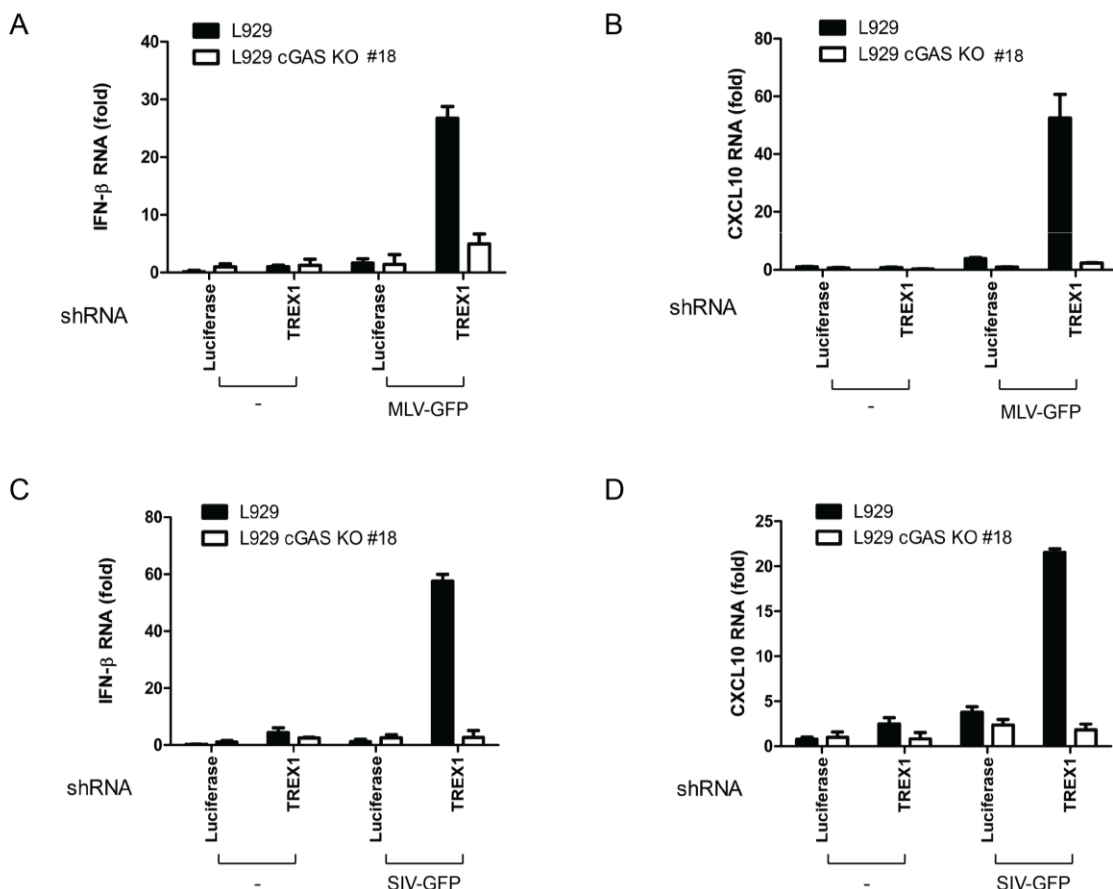


Figure 14. MLV and SIV activate innate immune responses through cGAS (A and B) L929 cGAS KO clone#18 and the parental L929 cells stably expressing shRNA against TREX1 or luciferase (control) were infected with MLV-GFP (MOI=2) for 20 h, followed by measurement of IFN β (A) and CXCL10 (B) RNA by qRT-PCR. (C and D) Similar to (A and B), except that cells were infected with SIV-GFP (MOI=1.5) for 20 h.

cGAS senses other retroviruses

To corroborate that detection of RT products by cGAS is a general mechanism of innate immune sensing of retroviruses, pseudotyped SIV and MLV were used to infect *Trex1^{-/-}* MEF. Similar to HIV infection, SIV-GFP and MLV-GFP activated IFN production, which was impeded by knocking down cGAS or STING by siRNA or shRNA (Figure 13A-E). Pseudotyped SIV and MLV were also administered to L929 cells. On condition that TREX1 was knocked down by shRNA, cells produced IFN and CXCL10 during infection. Consistently, the cytokine induction was abolished in *cGas^{-/-}* cells. This demonstrated that the retroviral DNA activated innate immunity signaling through DNA sensor cGAS (Figure 14A-D).

Conclusions and discussion

In the current study, the pseudotyped virus was utilized to study the mechanism of innate immune responses to HIV. HIV-GFP induces IRF3 dimerization and IFN production in various cell lines. RT products, which are usually restricted by host factors including SAMHD1 and TREX1, are essential for activation of the DNA sensor cGAS. cGAS subsequently synthesizes cGAMP, which transduces the signal through STING and activates innate immunity. This is also a general mechanism of innate immune detection of wild-type HIV as well as other retroviruses (Fig 15).

HIV and innate immune evasion

The induction of IFN by HIV-GFP is much lower when compared to DNA transfection or SeV infection (Fig 4E;9A). One reason may be because the HIV RNA

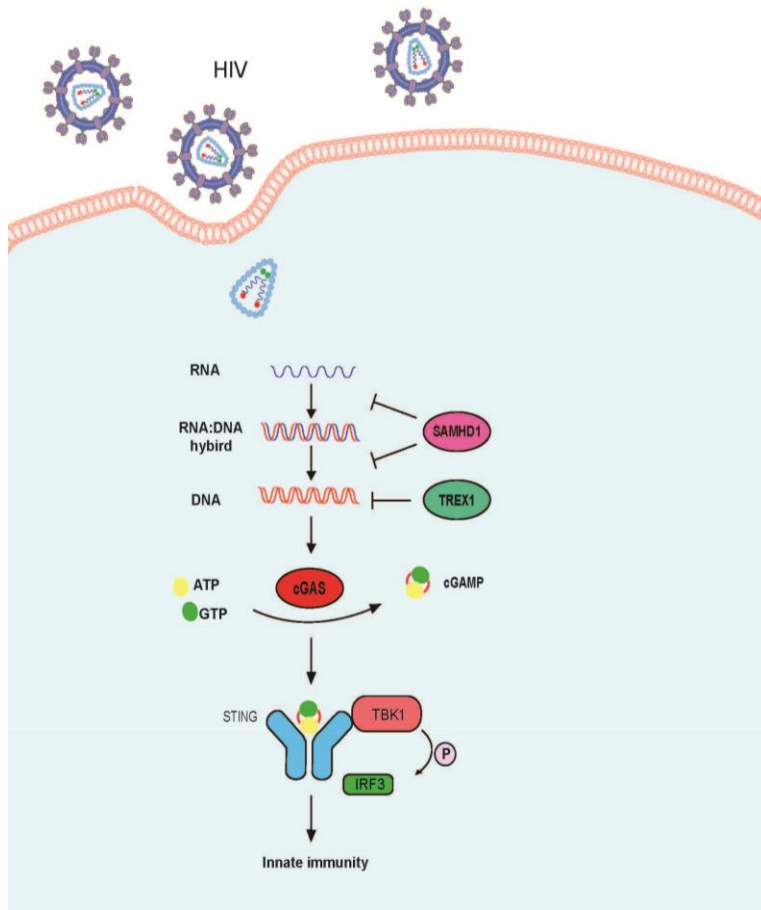


Figure 15. HIV sensing by cGAS. After HIV infection, the reverse transcripts are recognized by cGAS. cGAS produces cGAMP, which triggers downstream innate immunity. In natural infection, there is not much HIV DNA accumulation due to the functions of SAMHD1 and TREX1.

genome is reversed transcribed into DNA, which is not amplified, and probably cannot efficiently generate DNA as abundantly as DNA transfection. Also, RT products are

partially protected by capsid protein and are not exposed to cytosol directly. Furthermore, the detection of HIV is often inhibited by exploitation of host factors, such as SAMHD1 and TREX1. It is also possible there are other host factors assisting HIV to evade immune recognition.

Among those host restrictive factors, SAMHD1 mainly functions in myeloid lineage cells-DCs and macrophages. Although THP-1 cells express SAMHD1, HIV-GFP can productively infect THP-1 cells. According to previously published work, phosphorylation of SAMHD1 at threonine 592 strongly suppresses SAMHD1 function, and in THP-1 cells SAMHD1 is highly phosphorylated at Thr 592. PMA treatment reduces phosphorylation of SAMHD1 at Thr 592. Therefore, HIV was restrained in PMA differentiated THP-1 cells (Fig 5). We also observed that IFN production decreased correspondingly in PMA-treated THP-1 cells. The infection efficiency correlates with IFN response to HIV in THP-1 cells.

Another host factor, TREX1, helps to clear HIV cDNA in the cytoplasm. In MEF cells or L929 cells, HIV does not elicit strong immunity because of the powerful DNA clearance ability of TREX1 in these cells. When TREX1 is eliminated, viral cDNA accumulates and stimulates innate immunity. Compared to MEF or L929 cells, THP-1 or BJ cells have profound innate immune responses to HIV, indicating TREX1 is not so “effective” in suppressing the immune responses in these cells. It is likely that further knocking down TREX1 in these cells will facilitate IFN production induced by HIV.

The HIV capsid - cyclophilin A interaction can affect HIV-induced IFN production. Wild-type HIV is known to be immunologically silent when macrophages are infected.

Nonetheless, HIV capsid mutant N74D, which has reduced affinity to cofactor cleavage and polyadenylation specificity factor subunit 6 (CPSF6), or capsid mutant P90A, which lacks cyclophilin A binding ability, cannot replicate in macrophages due to induction of IFN (Rasaiyaah, Tan et al. 2013). Another paper published in *Immunity* also reveals that the capsid mutant which enhances cyclophilin A binding allows for innate sensing (Lahaye, Satoh et al. 2013). The mechanism is not clear, but HIV capsid - host factor binding possibly influences HIV cDNA leakage into the cytosol. Evolutionarily, binding affinities between HIV capsid and host factors are maintained in a delicate balance, through which HIV replicates in host cells and avoids innate immunity.

Additional factors for cGAS-mediated HIV sensing

According to a recent publication, PQBP1 participates in cGAS-mediated HIV sensing, but not in DNA sensing in general (Wang, Moore et al. 2013). It has further been shown that PQBP1 binds to both HIV viral cDNA and cGAS. Why PQBP1 is necessary for innate immune activation is not clear, but it is possible that PQBP1 somehow promotes exposure of viral DNA to the cytosol or that cGAS requires PQBP1 to bind to the special structure of HIV cDNA.

It has been recently shown that HIV ssDNA has a Y-form structure, which has short base-paired DNA stretches with unpaired DNA nucleotides flanking, and it is highly stimulatory (Herzner, Hagmann et al. 2015). Since dsDNA is also generated during reverse transcription, the structure of the main form of DNA sensed by cGAS still needs to be explored.

cGAMP and HIV vaccine adjuvant

Since we identified cGAMP as the second messenger for retroviral sensing, and cGAMP has a potent adjuvant effect to induce a CD8+ T cell response as well as an antibody response, cGAMP can be potentially used as an HIV vaccine adjuvant (Li, Wu et al. 2013). The dead or attenuated virus has been successfully used in vaccine design. Inactivated HIV has been tested to load onto DCs as a vaccine for immunization (Garcia, Climent et al. 2013). However, since dead HIV does not stimulate strong innate immunity, the vaccine only shows limited effect. To improve vaccine efficacy, cGAMP can be combined with inactivated HIV to prime DCs. Inactivated HIV provides the antigen that can be presented by MHC, and cGAMP stimulation mimics the protective innate immunity triggered by actively replicating HIV.

Moreover, HIV particles can incorporate cGAMP during virion maturation and deliver it into newly infected cells (Bridgeman, Maelfait et al. 2015, Gentili, Kowal et al. 2015). Modified Vaccinia Ankara (MVA) virus and MCMV also packages cGAMP inside of virions and transmits cGAMP into neighboring cells. These findings give us hints about the delivery of cGAMP in vivo.

Retroviruses and innate immune sensing

HIV-2 is a less virulent strain compared with HIV-1, but the reason for this difference is not clear. One major difference between HIV-1 and HIV-2 is that HIV-2 expresses Vpx protein that allows HIV-2 to replicate in myeloid lineage cells.

Pseudotyped HIV-2 is known to induce innate immunity in DCs (Lahaye, Satoh et al. 2013). Wild-type HIV-2 possibly can productively infect macrophages, and should also activate IFN since viral cDNA is the stimulator. In comparing HIV-1 and HIV-2, there seem to be correlations between innate immune activation and effective adaptive immune protection during HIV progression. However, whether cGAS mediated innate immunity plays a role in the adaptive immune response against HIV remains to be discovered.

Human T cell leukemia virus type 1 (HTLV-1), another human retrovirus that causes T cell lymphoma, is restricted in a SAMHD1-dependent manner in myeloid lineage cells. Viral reverse transcription intermediates (RTI), but not productive reverse transcripts, trigger STING-IRF3 dependent apoptosis (Sze, Belgnaoui et al. 2013). This process could signal through cGAS, which has not been investigated yet.

MLV, which lacks expression of the viral glycosylated-Gag protein (MLV^{gGag}), has a destabilized capsid and induces higher levels of IFN β RNA in macrophages (Stavrou, Blouch et al. 2015). Both APOBEC3 and STING restrict viral replication in mice. This provides evidence that the DNA sensing pathway controls retroviral infection *in vivo*.

Adaptive immune cells and retroviral sensing

T cells

Although HIV primarily infects CD4+ T cells, it is unclear whether the cGAS-STING pathway in T cells is activated during HIV infection. It is known that activated CD4+ T cells are productively infected by HIV, whereas resting CD4+ T cells are highly resistant to HIV infection, which is also known as abortive infection. Dr. Warner

Greene's group has shown that abortive infection in tonsillar T cells not only triggers inflammatory cell death but also activates IFN production in T cells (Doitsh, Cavrois et al. 2010). However, whether CD4 T cells have a functional cGAS-STING pathway and whether cGAS is involved in IFN production in this context remain to be investigated.

Retroviral sensing in B cells

cGAS was reported to directly contribute to activation of B cells and IgM production (Zeng, Hu et al. 2014). T cell-independent type 2 (TI-2) antigens, such as 4-hydroxy-3-nitrophenylacetyl-Ficoll (NP-Ficoll) induce B cells to secrete IgM in a cGAS- and MAVS- dependent manner. It has been further shown that NP-Ficoll induces upregulation of endogenous retrovirus (ERV) RNAs in antigen-specific mouse B cells. ERV RNA and reverse transcribed DNA stimulate the MAVS pathway and cGAS pathway, respectively, promoting antigen-specific IgM production.

Other innate immune sensors and HIV sensing

Besides cGAS, other putative sensors such as IFI16, DDX41, DAI, and DNA-PK were proposed to be the detector for cytosolic DNA. However, my work provides the first piece of genetic evidence that cGAS is responsible for retroviral detection.

IFI16 has been reported to be the sensor for HIV in quiescent "bystander" CD4 T cells to induce pyroptosis accompanied by the release of IL-1 β (Monroe, Yang et al. 2014). Additionally, by knocking down IFI16, IFN induction by HIV is abolished in CD4+ T cells. Another paper also points out that IFI16 is pivotal for HIV-induced IFN

production (Jakobsen, Bak et al. 2013). Although IFI16 binds strongly to transfected DNA and knocking down of IFI16 blocks DNA-induced IFN production, there is still no genetic evidence as to whether IFI16 is the direct sensor for DNA or HIV. Also, it is controversial whether IFI16 activates the inflammasome pathway. Nonetheless, IFI16 seems involved in HIV pathogenesis and it has been reported that SNP rs1417806 in *IFI16* is associated with CD4+ T-cell counts during HIV progression (Nissen, Hojen et al. 2014). The true role of IFI16 in DNA sensing or HIV sensing need be fully clarified in future work.

The HIV RNA genome could potentially be recognized by RNA sensors. HIV RNA has been reported to be sensed by TLR7 in pDCs to produce IFN after endocytosis. Whereas HIV-1 gp120 specifically inhibits TLR9-mediated activation, TLR9 in pDCs stays inactive upon HIV infection. Nonetheless, pDCs are not the primary target for HIV, and HIV can only be sensed after endocytosis, which greatly reduces the detection efficiency of pDCs. In fibroblasts or THP-1 cells, RT inhibitors thoroughly block IFN production, indicating no participation of the RNA sensing pathway in IFN production (Fig 6). This is probably because the HIV genome is protected by capsids, which separate HIV RNA from the cytosolic RNA sensors.

Future plan

In the future, the main focus will be on the identification of new regulators in the HIV sensing pathway. Since PQBP1 is an essential modulator, we can perform a PQBP1 knock-out by clustered regularly interspaced short palindromic repeats (CRISPR) in

THP-1 cells. If the *PQBP1*^{-/-} cells are not responsive to HIV, we can further rescue the response with recombinant protein. We can then study potential interaction partners by immunoprecipitation (IP). In addition, lenti-CRISPR screening can be used to identify new components in the HIV sensing pathway as well.

Materials and methods

Cells, Antibodies, Nucleotides, Chemical inhibitors and General methods

L929 and Human Embryonic Kidney (HEK293T) were cultured in DMEM (Sigma) supplemented with 10% calf serum and antibiotics. TREX1 knock out (TREX1^{-/-}) primary mouse embryonic fibroblasts (MEF) were provided by Dr. Nan Yan (UT Southwestern) and cultured in DMEM supplemented with 20% fetal bovine serum and antibiotics. THP-1 cells were cultured in RPMI containing 10% fetal bovine serum, antibiotics, nonessential amino acids, and 50 µM of β-mercaptoethanol.

The rabbit polyclonal antibodies against STING were generated and affinity purified as described previously (Tanaka and Chen 2012). Antibodies against human and murine IRF3 were obtained from Santa Cruz Biotechnology and Invitrogen, respectively. GFP antibody was obtained from Covance. Antibodies against tubulin and h-cGAS were obtained from Sigma. P-STAT1 (Tyr701) antibody was from cell signaling.

Cyclic GMP-AMP (cGAMP) was synthesized by Cyclic GMP-AMP Synthase (cGAS) in vitro and purified as previously described (Sun, Wu et al. 2013). Polybrene, poly(I:C) and herring testis (HT)-DNA were from Sigma. Poly(I:C) and HT-DNA were

transfected with LipofectamineTM 2000 (Invitrogen). HIV reverse transcriptase inhibitors azidothymidine (AZT) nevirapine (NVP), didanosine (ddI) and integrase inhibitor raltegravir(RAL) were from Selleckchem.

The lentiviral shRNA vector for knocking down target genes and the generation of stable cell lines were described previously(Tanaka and Chen 2012). The same vector and method were employed to establish L929/shLuciferase, L929/shTREX1, L929/shDNaseII(-a), L929/shDNaseII-b, TREX1-/-MEF/shLuciferase, TREX1-/-MEF/sh-cGAS, TREX1-/-MEF/shSTING, THP-1/shSTING(-a), THP-1/shSTING-b, THP-1/shcGAS using the following target sequences (only sense strand sequence is shown):

Luciferase: AACTTACGCTGAGTACTTCGA; TREX1:
GATCACAGGTCTGAGCAAA; m-cGAS: GGATTGAGCTACAAGAATA; mSTING:
CGAAATAACTGCCGCCTCA; hSTING-a: GCACCTGTGTCCTGGAGTA; hSTING-b:
CCTCATCAGTCCAATGGAA; h-cGAS: GGAAGGAAATGGTTCCAA
shSTING corresponds to shSTING-a; siRNA oligos were purchased from Sigma and the sense strand sequences targeting the following mouse genes were:

Control: GCCUAGAUCCUGUGCUUUAdTdT;
m-cGAS: GGAUUGAGCUACAAGAAUAdTdT;
mSTING: CGAAAUAACUGCCGCCUCAdTdT

siRNA oligos were transfected with LipofectamineTM 2000 (Invitrogen).

The procedures for native gel electrophoresis for detection of IRF3 dimerization, SDS-polyacrylamide gel electrophoresis (SDS-PAGE), and Western blotting have been

described previously (Seth, Sun et al. 2005). Reverse transcription and real-time PCR reactions were carried out. Briefly, iScript cDNA synthesis kit and iQ SYBR Green Supermix (Bio-Rad) were used according to manufacturer's instructions. Quantitative real time PCR was performed on an Applied Biosystem Vi7 with the following primers:

Gene	forward	reverse
GAPDH	ATGACATCAAGAAGGTGGTG	CATACCAGGAATGAGCTTG
CXCL10	TGGCATTCAAGGAGTACCTC	TTGTAGCAATGATCTAACACG
IFN-β	AGGACAGGATGAACCTTGAC	TGATAGACATTAGCCAGGAG
STING	ACTGTGGGTGCCTGATAAC	TGGCAAACAAAGTCTGCAAG
cGAS	GGGAGCCCTGCTGTAACACTCTTAT	CCTTGCATGCTGGGTACAAGGT
MTND1	ATGGCCAACCTCCTACTCCT	GCGGTGATGTAGAGGGTGAT
RPL19	AAATCGCCAATGCCAACTC	TCTTCCTATGCCCATATGC
mDNAaseII	TGCTCTGGAGCCTATCAGGT	GGGTTTCCAGTCTTCACCA
mIFN-β	TCCGAGCAGAGATCTCAGGAA	TGCAACCACCACTCATTCTGAG
mSTING	AAATAACTGCCGCCTCATTG	TGGGAGAGGCTGATCCATAC
mCXCL10	GCCGTCATTTCTGCCTCA	CGTCCTTGCAGAGAGGATC
mTREX1	CACATGCTGCCACAGCTACT	GGCCAGGAAGAGTCCATACA
mcGAS	ACCGGACAAGCTAAAGAAGGTGCT	GCAGCAGGCCTCCACAACTTAT
HIV-GAG	GGCAAGAGTTTGGCTGAAG	CACATTCCAACAGCCCTT
HIV-LTR	GGAACCCACTGCTTAAGCCTCAA	TGTCGGCGCCACTGCTAGAGA

Table 1. list of qRT-PCR primers

Viruses and infection

The HIV-GFP plasmid (pNL4-3/Env-) was provided by D. Gabuzda. 24 hours after transfection of HIV-GFP and VSVG, HEK 293T cell media was replaced with fresh media. Viral supernatants were harvested and filtered through a 0.45uM in three batches every 12 hours at 24-48 hours after replacement of media. Viral supernatants were concentrated by PEG8000 precipitation. Viral supernatants with a final concentration of 5% PEG8000, 0.15M NaCl were incubated at 4°C overnight and centrifuged at 2000g for

20min. Pellets were resuspended in fresh medium as virus stock. HIV-GFP was titered on L929 cells (for mouse cell experiments) and on HEK 293T cells (for human cell experiments) by flow cytometry analysis of GFP+ cells 24 hrs after infection. For infection, 10 µg/mL polybrene was added.

For experiments measuring HIV episomal DNA, viral stocks were pretreated with Turbo DNase by following the protocol (TURBO DNA-free™ Kit, Life Technologies). Episomal DNA was purified by PureLink Quick Plasmid Miniprep Kit (Invitrogen) and quantified by qRT-PCR. Mitochondrial NADH dehydrogenase subunit 1 (MTND1) gene was used as internal control. Sendai virus (Cantell strain, Charles River Laboratories) was used at a final concentration of 50 hemagglutinating units/ml.

In vitro Assay for cGAMP activity

As previously described (Wu, Sun et al. 2013), cells were infected with HIV-GFP or transfected with DNA and then homogenized by douncing in hypotonic buffer [10mM Tris-HCl, pH7.4, 10mM KCl, 1.5mM MgCl₂]. The homogenate was centrifuged at 100,000 rpm for 5 min, and then the supernatant was heated at 95°C for 5 min and centrifuged again at 12,000 rpm for 5 min to remove denatured proteins. The heat-resistant supernatant was mixed with 106 THP-1 or Raw264.7 cells in an 8µl reaction containing 2 mM ATP, 1 U/µl Benzonase and 1.5 ng/µl PFO. The mixture was incubated at 30°C for 1.5 hr. Cells in the reaction were lysed by adding 0.2% NP40 and subjected to native gel electrophoresis. IRF3 dimerization was detected by immunoblotting with an IRF3 antibody.

Stimulation of cGAS activity by HIV DNA

In the presence of DNA, cGAS converts ATP and GTP into cGAMP and pyrophosphate. The latter can be further hydrolysed to phosphate by a pyrophosphatase. Activity of cGAS stimulated by DNA was assessed by measurement of phosphate release in the presence of Yeast Inorganic Pyrophosphate (YIPP). Specifically, serial dilutions of double-stranded or single-stranded DNAs from HIV GAG gene sequence were added to a 10 μ l reaction mixture containing 20mM Tris-Cl, pH7.5, 5mM NaCl, 2mM CoCl₂, 0.2mg/ml BSA, 0.1Unit/ μ l of YIPP, 1mM ATP, 1mM GTP, and 0.1 μ M of SUMO-tagged hu-cGAS(aa147-522). The mixture was incubated at 37°C for 20 min, and stopped by heating at 95°C for 3 min. Pi release was measured using malachite green method as described (Lanzetta, Alvarez et al. 1979). Briefly, 90 μ l of water, 43 μ l of reagent A (28mM ammonium molybdate in 2M H₂SO₄), and 32 μ l of reagent B (0.76mM malachite green, 0.35% polyvinyl alcohol) were added sequentially to the 10 μ l reaction above. After incubation for 10 min at room temperature, absorbance at 630nm was read on a plate reader. Concentrations of phosphate were calculated from a standard curve using serial dilutions of KH₂PO₄.

CHAPTER THREE: cGAS initiates autoimmunity caused by self-DNA

Results

In addition to retroviral DNA, cGAS senses DNA derived from other pathogens. Self-DNA in the cytosol can also activate cGAS, since cGAS has no observed sequence preference for its DNA ligands. In a mouse autoimmune disease model caused by self-DNA accumulation, *Trex1*^{-/-} mice die within a few months after birth. While several lines of evidence have implicated involvement of the DNA sensing pathway in the pathogenesis of *Trex1*^{-/-} mice, the role of cGAS remains to be investigated in detail.

cGAS is accountable for the inflammatory diseases and death of *Trex1*^{-/-} mice

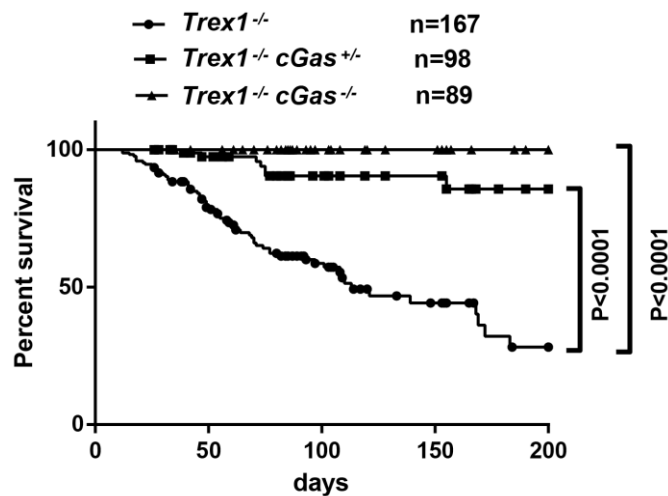


Figure 16. cGAS deletion rescues the lethality of *Trex1*^{-/-} mice. Survival curves of *Trex1*^{-/-}, *Trex1*^{-/-} *cGas*^{+/-}, and *Trex1*^{-/-} *cGas*^{-/-} mice are shown for comparison. All mice were on a C57BL/6 background. Statistical analysis was performed with a Mantel-Cox test.

To determine whether activation of cGAS is responsible for the reduced survival of *Trex1*^{-/-} mice, as well as the severe inflammation in multiple organs, especially myocarditis in the heart, *Trex1*^{-/-} mice were crossed with *cGas*^{-/-} mice, generating *Trex1*^{-/-} *cGas*^{-/-} mice and *Trex1*^{-/-} *cGas*^{+/-} mice. Although 61% (65/167) of *Trex1*^{-/-} mice died within 200 days after birth, all *Trex1*^{-/-} *cGas*^{-/-} mice were (89/89) viable within this period. Even removal of just one allele of *cGas* in *Trex1*^{-/-} mice allowed 93% (91/98) of the mice to survive (Figure 16).

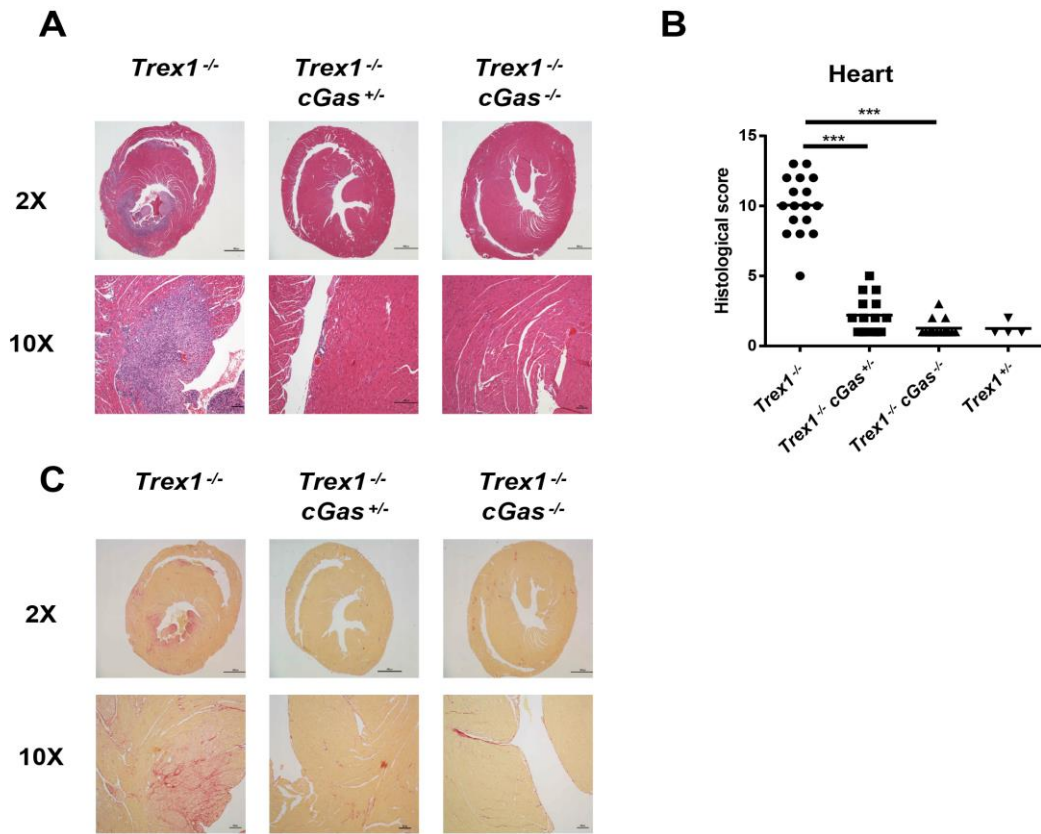


Figure 17. cGAS mediates myocarditis in *Trex1*^{-/-} mice. (A and C) Representative H&E-stained (A) and Picro-Sirius Red (PSR; to measure fibrosis)-stained (C) heart sections from 12-wk-old *Trex1*^{-/-}, *Trex1*^{-/-} *cGas*^{+/-}, and *Trex1*^{-/-} *cGas*^{-/-} mice. Blue-stained cells indicate infiltrating leukocytes in the heart. (B) Blinded histological analysis of the hearts of 12-wk-old *Trex1*^{-/-}, *Trex1*^{-/-} *cGas*^{+/-}, and *Trex1*^{-/-} *cGas*^{-/-}

mice as well as *Trex1*^{+/−} mice. Histological scores were calculated as described in *Materials and Methods*. Statistical analysis was performed with a two-tailed, unpaired Student's *t* test. ****P* < 0.001.

H&E staining of the heart showed massive infiltration of lymphocytes in *Trex1*^{−/−}

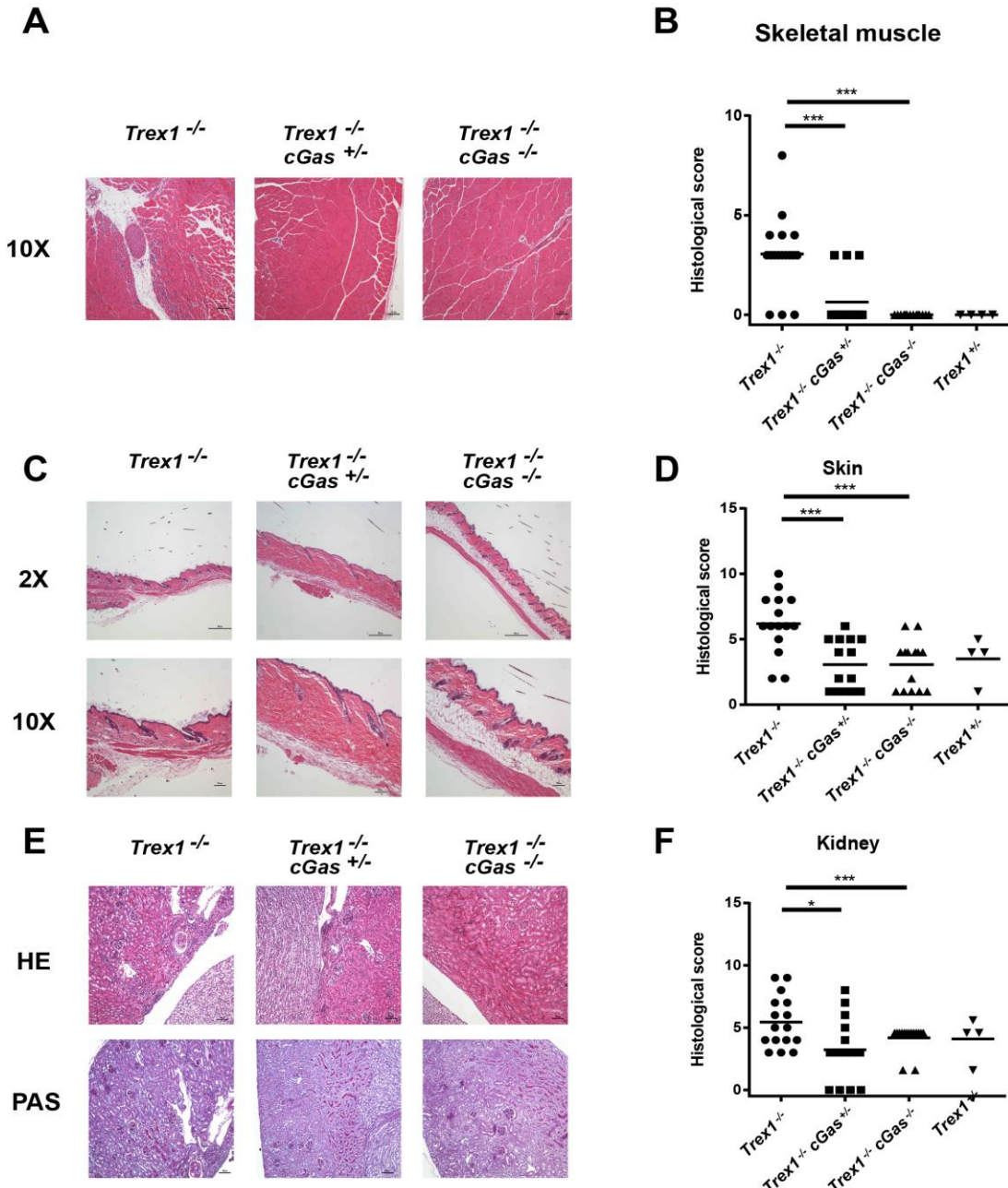


Figure 18. cGAS is responsible for the pathology and splenomegaly of *Trex1*^{−/−} mice. Representative H&E-stained skeletal muscle (A) sections from 12-wk-old *Trex1*^{−/−}, *Trex1*^{−/−}*cGas*^{+/-}, and *Trex1*^{−/−}*cGas*^{−/−}

mice. Blue-stained cells indicate leukocytes that infiltrate the heart. (B) Blinded analysis of the indicated tissues of 12-wk-old *Trex1^{-/-}*, *Trex1^{-/-}cGas^{+/+}*, and *Trex1^{-/-}cGas^{-/-}* mice as well as *Trex1^{+/+}* mice. (C) Representative H&E-stained skin sections. (D) Blinded analysis of the skin tissues represented in (C). (E) Representative H&E-stained (*Upper*; $\times 10$) and Periodic Acid Schiff (PAS; to detect glycogen) stained (*Lower*; $\times 10$) kidney sections. (F) Blinded analysis of the kidney tissues represented in (E).

mice and Picosirius red staining indicated severe fibrosis in heart tissues. In contrast, *Trex1^{-/-}cGas^{-/-}* mice were free of inflammation, and even *Trex1^{-/-}cGas^{+/+}* mice rarely showed any signs of inflammation. Histological scores of hearts also reflected this observation, in that histological scores of *Trex1^{-/-}cGas^{-/-}* mice were dramatically lower than those of *Trex1^{-/-}* counterparts, but largely comparable to *Trex1^{+/+}* mice.

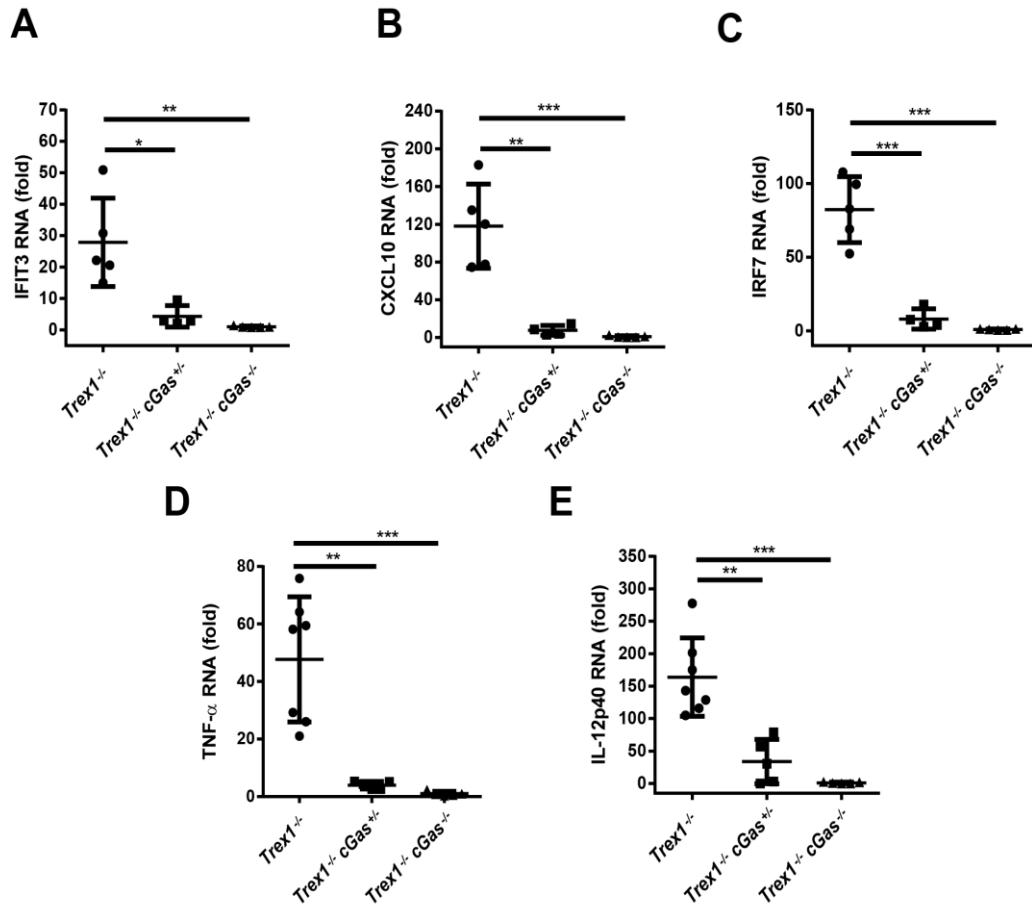


Figure 19. cGAS is essential for the expression of ISGs and inflammatory cytokines in *Trex1^{-/-}* mice. (A–E) qRT-PCR analysis of indicated ISGs (A–C), TNF- α (D), and IL12p40 (E) in hearts from 12-wk-old mice of indicated genotypes. Fold changes are relative to *Trex1^{-/-}cGas^{-/-}* mice. Error bars represent SD. * P < 0.05; ** P < 0.01; *** P < 0.001.

Consistent with heart, inflammation in skeletal muscle, skin and kidney were largely eliminated in both *Trex1^{-/-}cGas^{+/+}* mice and *Trex1^{-/-}cGas^{-/-}* mice. Due to the

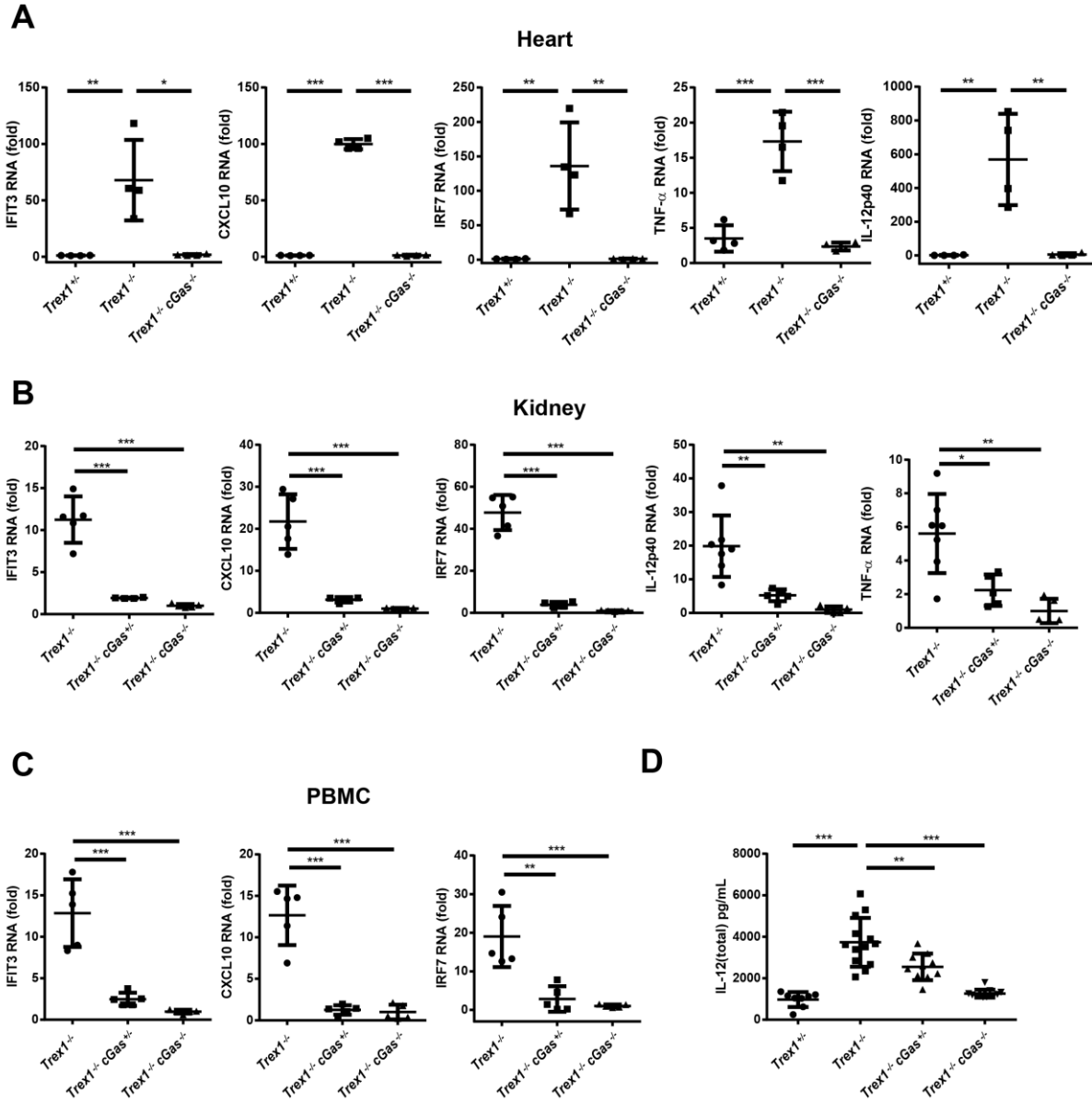


Figure 20. cGAS is essential for ISG expression in *Trex1^{-/-}* mice. (A) qRT-PCR analysis of indicated ISGs, TNF- α , and IL12p40 in hearts from 12-wk-old mice of indicated genotypes. Fold changes are relative to *Trex1^{+/+}* mice. (B) qRT-PCR analysis of indicated ISGs, TNF- α , and IL12p40 in kidneys from 12-wk-old mice. Fold changes are relative to *Trex1^{-/-cGas^{-/-}}* mice. (C) qRT-PCR analysis of indicated ISGs in PBMCs from 5-wk-old mice. Fold changes are relative to *Trex1^{-/-cGas^{-/-}}* mice. (D) Measurement of IL-12 (total) in the plasma of 12-wk-old mice. Error bars represent SD. *P < 0.05; **P < 0.01; ***P < 0.001.

C57BL/6 background of the mice, *Trex1^{+/+}* control as well as *Trex1^{-/-cGas^{-/-}}* mice spontaneously developed the basal levels of inflammation in skin and kidney (Fig 18 A-F). Overall, genetic ablation of cGAS protected mice from autoinflammation in multiple organs caused by *Trex1* deficiency.

cGAS abrogates the expression of interferon-stimulated genes and inflammatory cytokines in *Trex1^{-/-}* mice

To further characterize the rescue effect, ISG expression in affected organs was analyzed by qRT-PCR in 12-week old *Trex1^{-/-}* and *Trex1^{+/+}* mice. Hearts from *Trex1^{-/-}* mice had raised levels of ISGs, including IFIT3, CXCL10, and IRF7. Elevation of ISGs was largely abrogated in *Trex1^{-/-cGas^{+/+}}* mice and completely diminished in *Trex1^{-/-cGas^{-/-}}* mice (Fig 19A-C). Similarly, proinflammatory cytokines, TNF α and IL-12, were upregulated in *Trex1^{-/-}* mice in a cGAS dependent manner (Fig 19 D-E). Similar results were obtained in kidneys and peripheral blood monocytes (Fig 20A-C). Serum IL-12 p40 measured by ELISA also showed consistent results (Fig 20D). Altogether, the upregulation of ISGs and cytokines in *Trex1^{-/-}* mice relied on cGAS.

To check what kinds of cell types display increased level of ISGs, bone marrow dendritic cells, macrophages, and embryonic fibroblasts were cultured in vitro. Because all

of these cell types have a functional DNA sensing pathway, they inevitably showed elevated levels of ISGs in the *Trex1^{-/-}* background. The high ISGs were moderately reduced when only one cGAS allele was removed and totally diminished when both alleles were knocked out (Fig 21A-C).

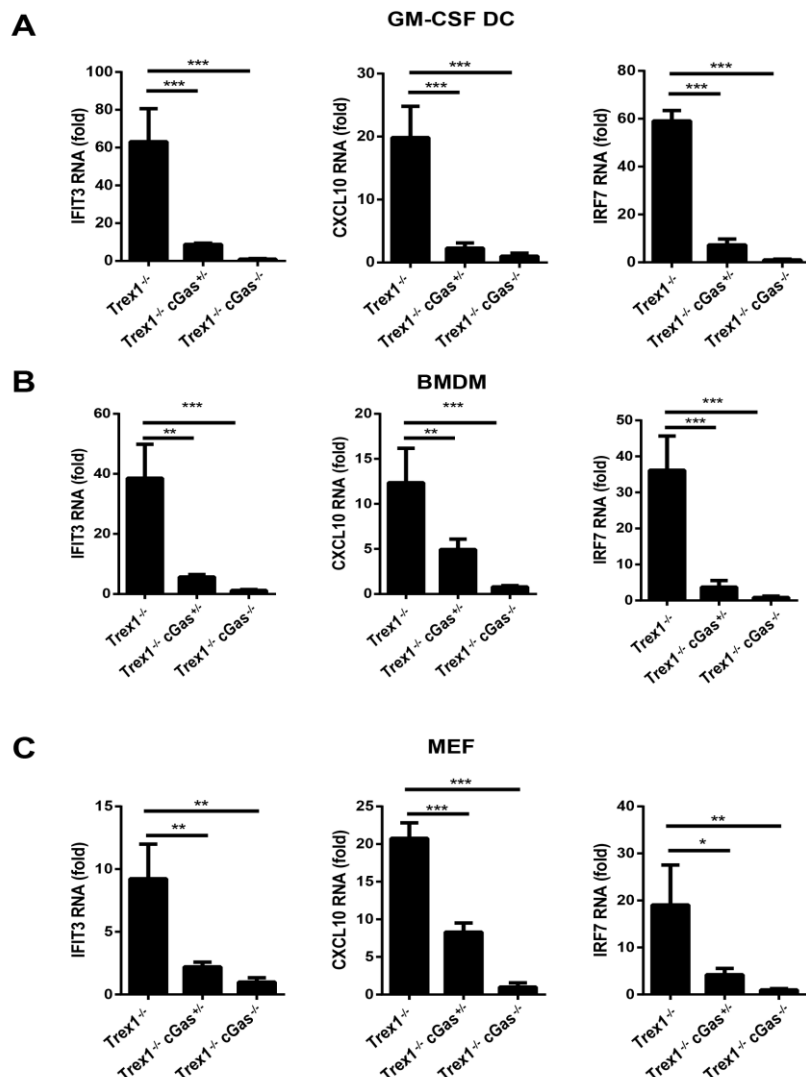


Figure 21. cGAS is required for ISG induction in different cell types from *Trex1^{-/-}* mice. GM-CSF-derived BMDCs (A), BMDMs (B), and mouse embryonic fibroblasts (MEF; C) from indicated genotypes

were analyzed by qRT-PCR for expression of ISGs. Fold changes are relative to *Trex1^{-/-}cGas^{-/-}* mice. Error bars represent SD of triplicate assays. **P* < 0.05; ***P* < 0.01; ****P* < 0.001.

cGAS is essential for cGAMP accumulation in *Trex1^{-/-}* mice

Next, cGAMP levels in mouse hearts of different genotypes were quantified by a mass spectrometry-based assay developed in the Chen laboratory. Absolute quantification was enabled by spiking in ¹³C₁₀¹⁵N₅-labeled cGAMP as an internal standard. While wild-type hearts did not have detectable levels of cGAMP, in *Trex1^{-/-}* mice, robust production of cGAMP was detected. Modest levels of cGAMP were present in *Trex1^{-/-}cGas^{+/+}* hearts and *Trex1^{-/-}cGas^{-/-}* mice did not produce any detectable cGAMP in hearts (Fig 22A-B).

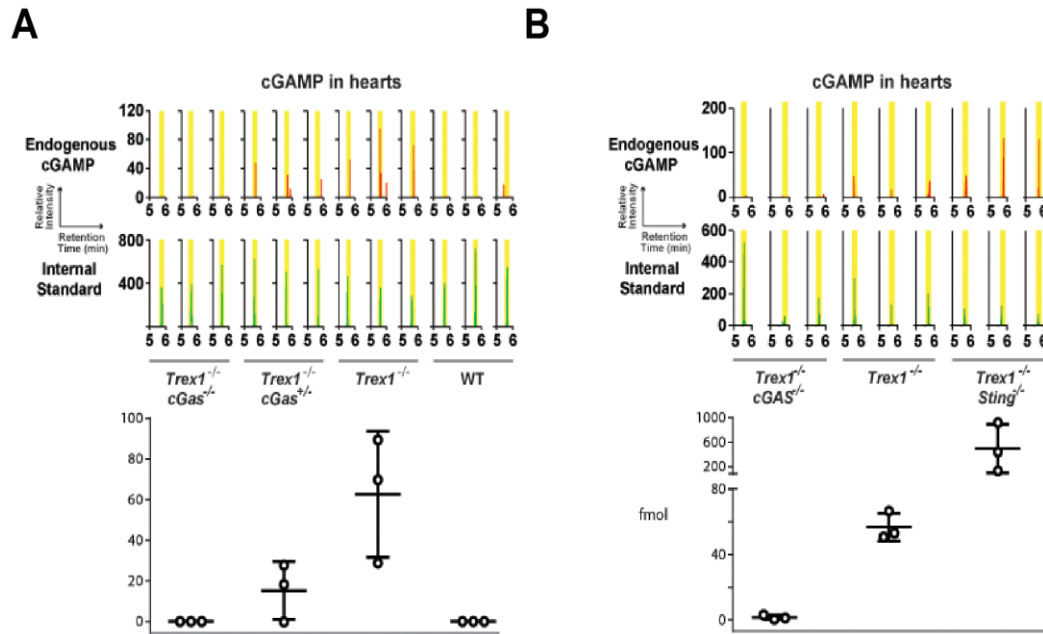


Figure 22. cGAMP levels in mouse hearts of indicated genotypes were quantified by LC-MS. (A and B) Upper shows zoomed chromatograms displaying relative intensities of endogenous cGAMP (red) and internal standard (green). Lower shows the calculated amounts of cGAMP (fmol) in each sample. Error bars represent SEM.

Interestingly, the cGAMP levels in *Trex1^{-/-}Sting^{-/-}* mice were significantly higher than those in *Trex1^{-/-}* mice, indicating STING might be involved in cGAMP clearance. Since *Trex1^{-/-}*

Sting^{-/-} mice were also healthy, high levels of cGAMP did not impose any adverse effect on the fitness of the animals.

***Trex1*^{-/-} mice have elevated autoantibody production and T cell activation in a cGAS dependent manner**

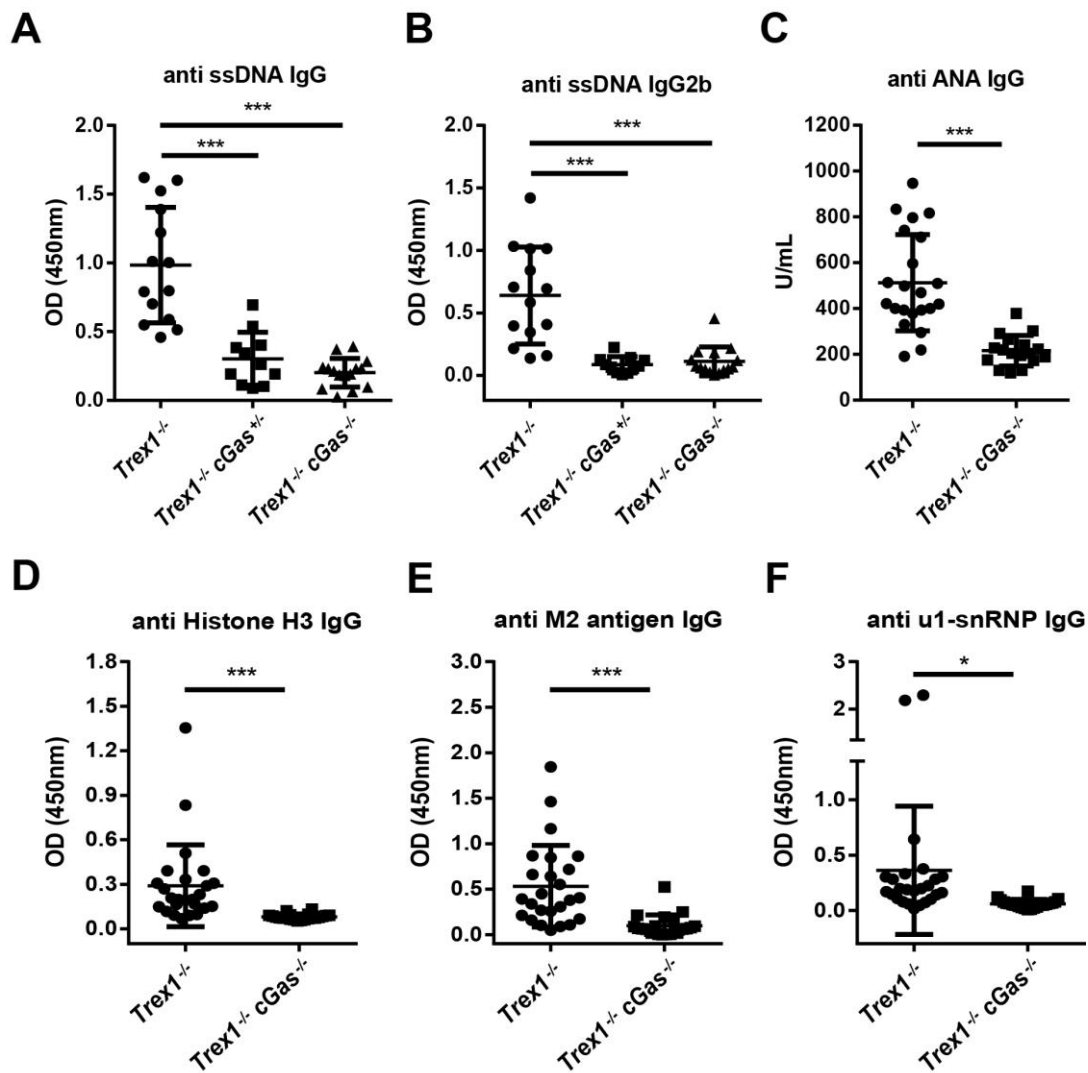


Figure 23. cGAS deletion mitigates autoantibodies in *Trex1*^{-/-} mice. (A–F) Detection of autoantibodies, including ssDNA IgG (A), ssDNA IgG2b subtype (B), ANA IgG (C), Histone H3 IgG (D), M2 antigen IgG (E), and u1-snRNP (F) in the sera of 12-wk-old mice of indicated genotypes.

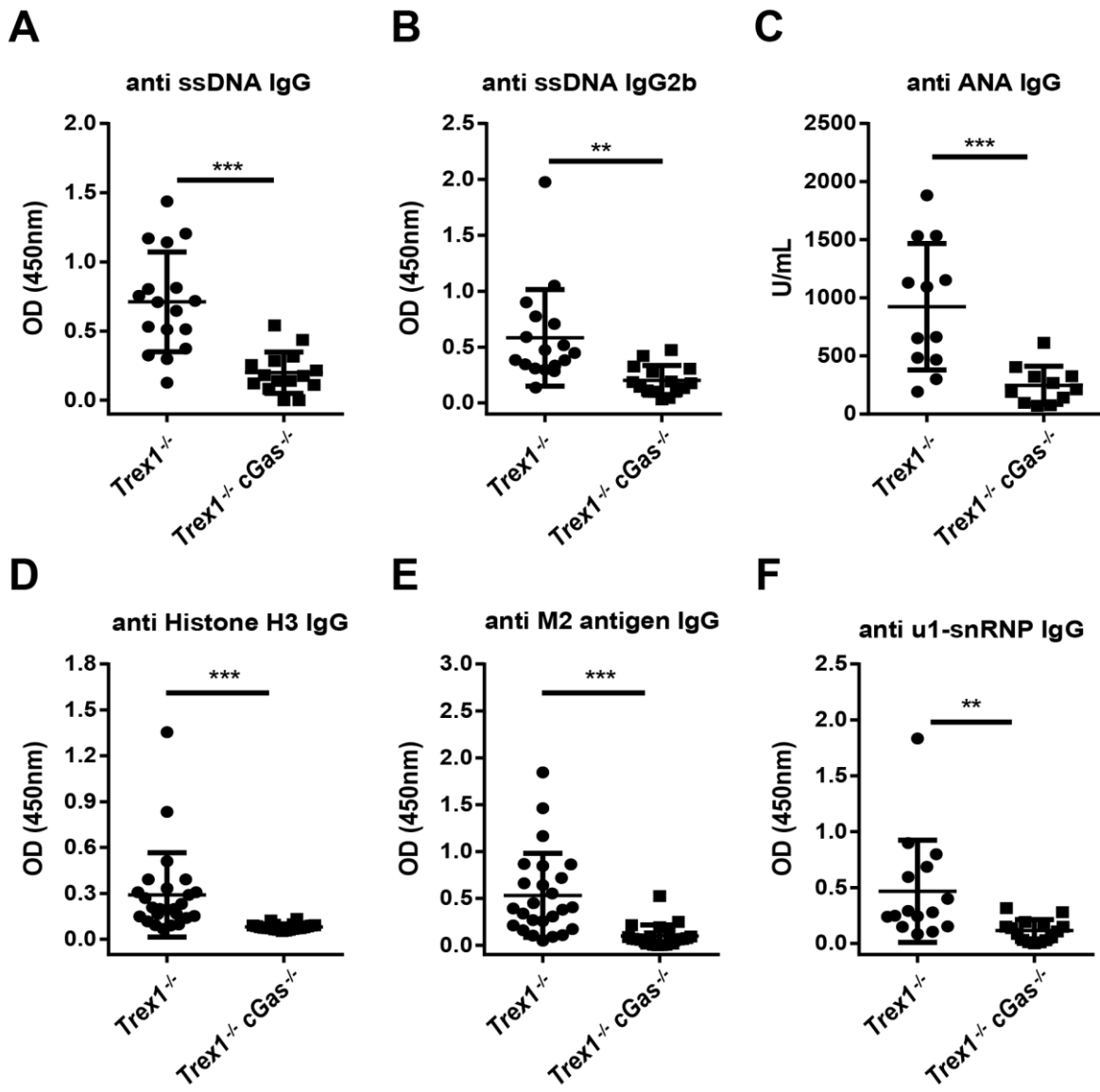


Figure 24. cGAS deletion mitigates autoantibodies in older *Trex1^{-/-}* mice. (A–F) Detection of autoantibodies, including ssDNA IgG (A), ssDNA IgG2b subtype (B), ANA IgG (C), Histone H3 IgG (D), M2 antigen IgG (E), and u1-snRNP (F) in the sera of 5-mo-old mice of indicated genotypes.

ELISA assays showed that *Trex1^{-/-}* mice at 12-weeks of age developed autoantibodies against ssDNA, nuclear antigens (ANA), and other self-antigens, such as histone H3, M2, and the U1 subunit of small nuclear ribonucleoprotein (U1-snRNP) (Fig 23A-F).

Remarkably, all of these auto-antibodies were significantly reduced when cGAS was genetically blunted. Mice of 5 months old recapitulated these observations (Fig 24A-F). One of the major isotypes of the anti-ssDNA antibody was IgG2b, which was correlated with Th1 response (Fig 22B;23B).

Because *Trex1* deficiency leads to overactive adaptive immunity, which might affect the development of immune organs, spleens of *Trex1*^{-/-} mice and *Trex1*^{-/-}*cGas*^{-/-} mice

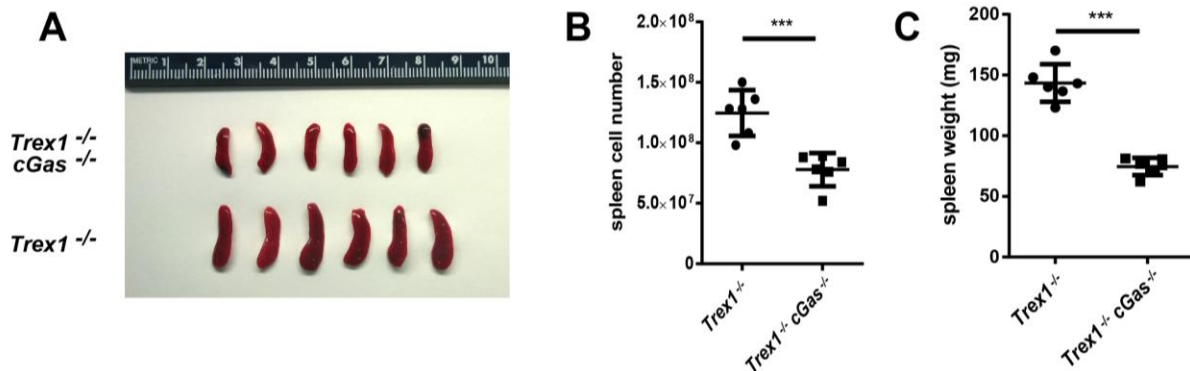


Figure 25. Knocking out cGAS rescues splenomegaly in *Trex1*^{-/-} mice. (A) Spleens from 12-wk-old *Trex1*^{-/-} and *Trex1*^{-/-}*cGas*^{-/-} mice. (B and C) Spleen cell numbers (B) and spleen weights (C) were measured from 12-wk-old *Trex1*^{-/-} and *Trex1*^{-/-}*cGas*^{-/-} mice. Statistical analysis was performed with a two-tailed, unpaired Student's *t* test. **P* < 0.05; ****P* < 0.001.

were examined. *Trex1*^{-/-} mice obviously developed splenomegaly in that their spleens were on average twice the size of *Trex1*^{+/-} or *Trex1*^{-/-}*cGas*^{-/-} spleens (Fig 25A-C). And *Trex1*^{-/-} mice also had more splenocytes, indicating the systematic inflammation. But *Trex1*^{-/-} and *Trex1*^{-/-}*cGas*^{-/-} spleens had comparable ratios of CD4+ T cells, CD8+ T cells and B cells (data not shown).

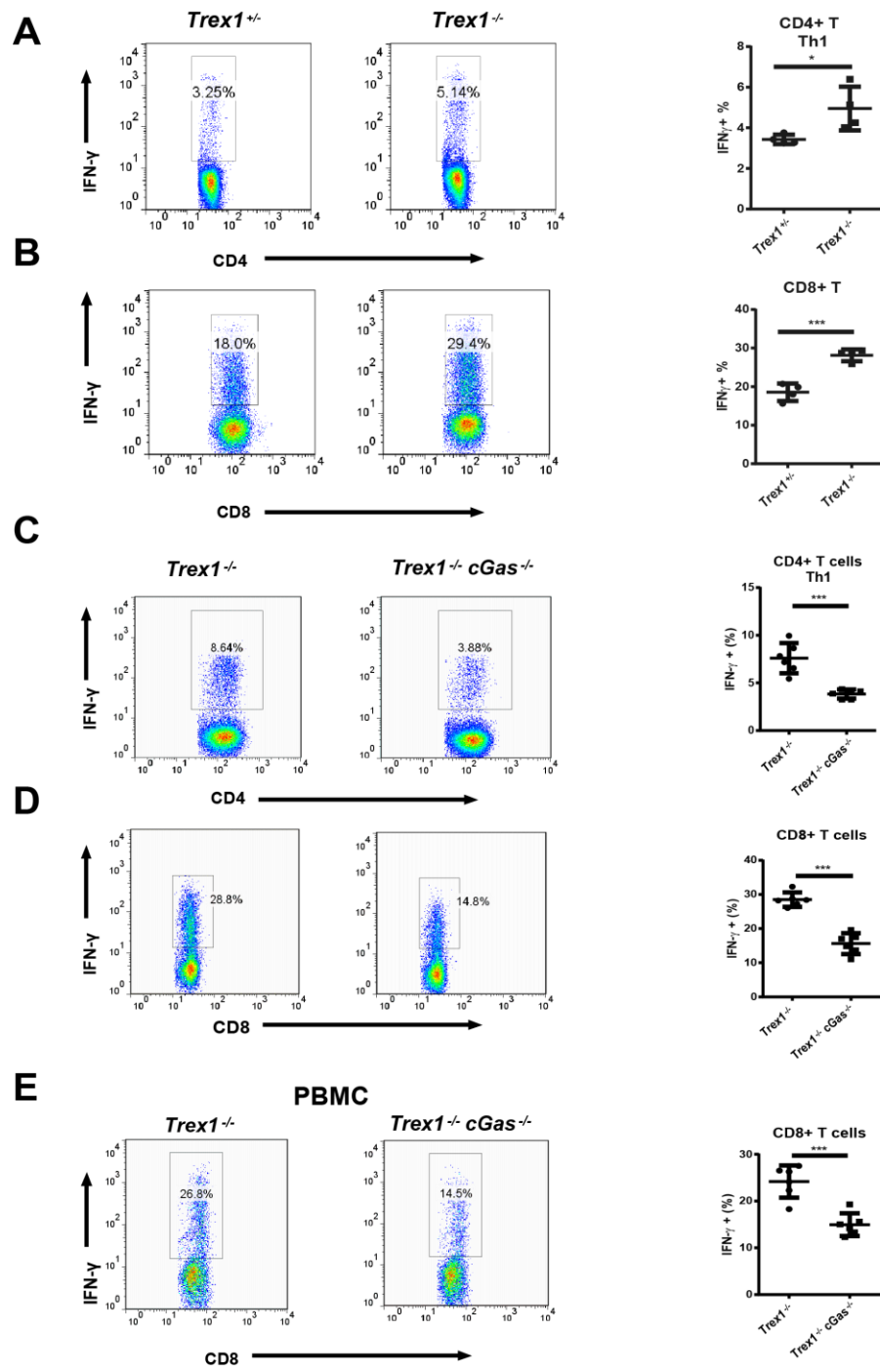


Figure 26. cGAS is required for the generation of hyperreactive T cells in *Trex1*^{-/-} mice. (A–D) Flow-cytometric analysis of intracellular IFN- γ in response to PMA plus ionomycin in splenic CD4+ T cells or CD8+ T cells from 12-wk-old mice of indicated genotypes. (E) Similar to (D), except that CD8 T cells in PBMC were analyzed. Error bars represent SD. * $P < 0.05$; *** $P < 0.001$.

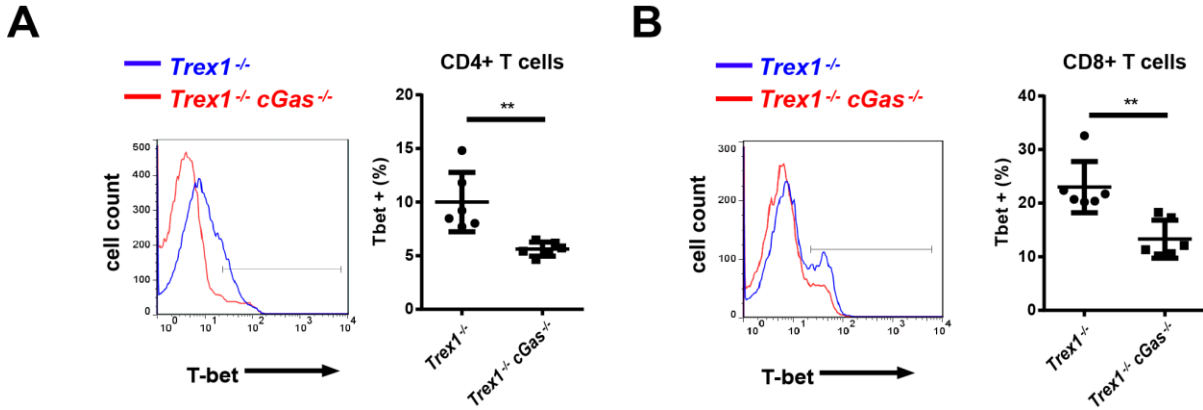


Figure 27. cGAS is essential for the differentiation of Th1 cells in *Trex1*^{-/-} mice. (A and B) Flow-cytometric analysis of T-bet in splenic CD4 (A) and CD8 (B) T cells from 12-wk-old mice. Error bars represent SD. ** $P < 0.01$.

We then tried to investigate the subsets of T cells in spleens. In response to PMA and ionomycin stimulation, the CD4+ and CD8+ T cells from *Trex1*^{-/-} spleens had higher expression of IFN γ than that of *Trex1*^{+/-} cells, which was also dependent on cGAS (Fig 26 A-E). This result indicated a hyperactive Th1 response in spleens of *Trex1*^{-/-} mice. When I stained the Th1 specific transcription factor T-bet in the CD4+ and CD8+ T cells, *Trex1*^{-/-} cells expressed higher levels of T-bet in comparison to *Trex1*^{-/-}*cGas*^{-/-} cells (Fig 27 A-B). Also, we assessed the Th1 response in hearts by quantifying gene expression via qRT-PCR. The results showed that elevated levels of IFN γ and T-bet were only detected in *Trex1*^{-/-} mice but not in *Trex1*^{+/-} or *Trex1*^{-/-}*cGas*^{-/-} mice (Fig 28A-D).

Autoreactive splenic T cells in *Trex1*^{-/-} mice upregulated expression of activation marker-CD69 on CD4+ and CD8+ T cells and memory marker-Ly6c on CD8+ T cells (Fig 29C-E). Deletion of *cGas* in *Trex1*^{-/-} mice dramatically decreased the number of activated T cells (Fig 30C-E). Memory CD4+ and CD8+ T cells (CD44^{hi}/CD62L^{lo}) increased in *Trex1*^{-/-}

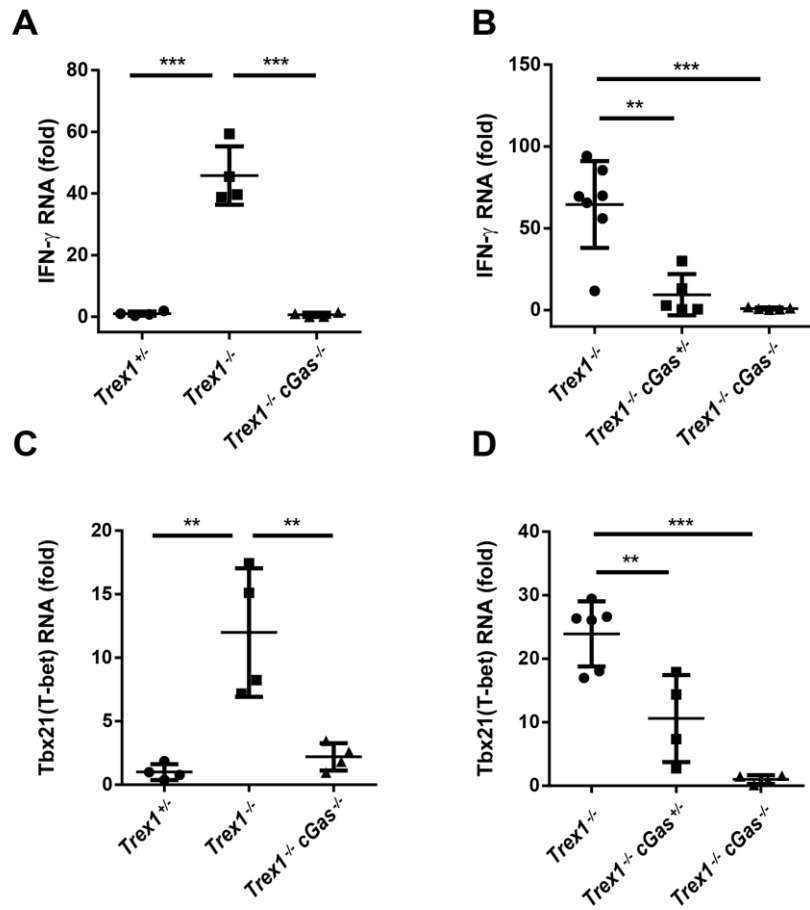


Figure 28. cGAS is essential for infiltration of autoreactive immune cells in the hearts of *Trex1*^{-/-} mice. qRT-PCR analysis of IFN- γ (A and B) or T-bet (C and D) RNA in hearts from 12-wk-old mice of indicated genotypes is shown. Fold changes are relative to *Trex1*^{+/+} (A and C) or *Trex1*^{-/-} cGas^{-/-} (B and D). Error bars represent SD. **P < 0.01; ***P < 0.001.

mice, while naïve T cells (CD44^{lo}/CD62L^{hi}) decreased compared to *Trex1*^{+/+} mice (Fig 29A-B). As expected, memory and naïve cell percentages in *Trex1*^{-/-} cGas^{-/-} mice were similar to *Trex1*^{+/+} mice (Fig 30A-B). These results demonstrated that overactive adaptive immunity in *Trex1*^{-/-} mice depended on cGAS.

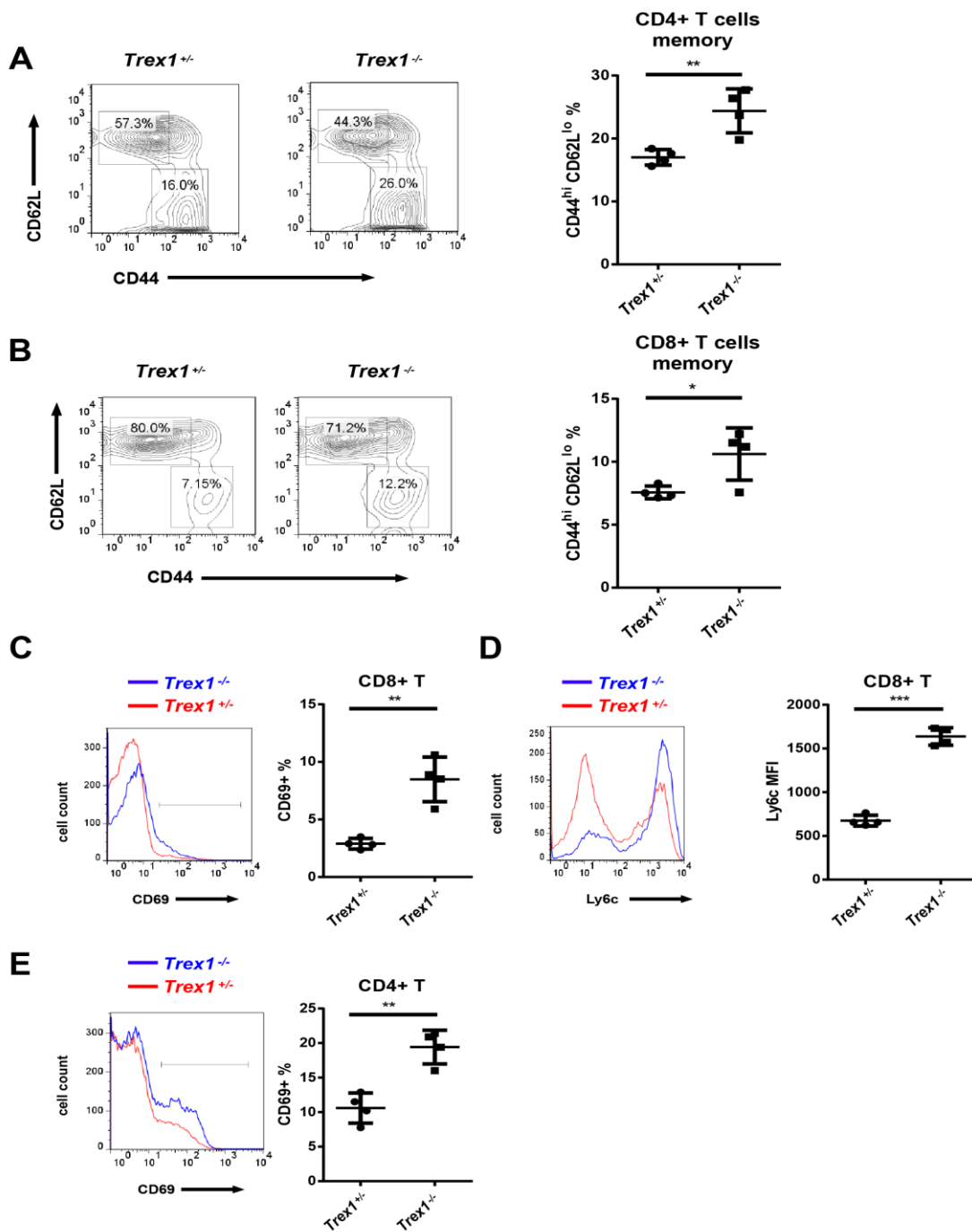


Figure 29. *Trex1^{−/−}* mice have higher percentages of activated and memory T cells. (A and B) Flow-cytometric analysis of surface expression of CD62L and CD44 in splenic CD4+ T cells (A) and CD8+ T cells (B) from 12-wk-old *Trex1^{+/−}* and *Trex1^{−/−}* mice. (C–E) Flow-cytometric analysis of CD69 (C) and Ly6c (D) in splenic CD8+ T cells and CD69 (E) in splenic CD4+ T cells from 12-wk-old mice. Error bars represent SD. *P < 0.05; **P < 0.01; ***P < 0.001.

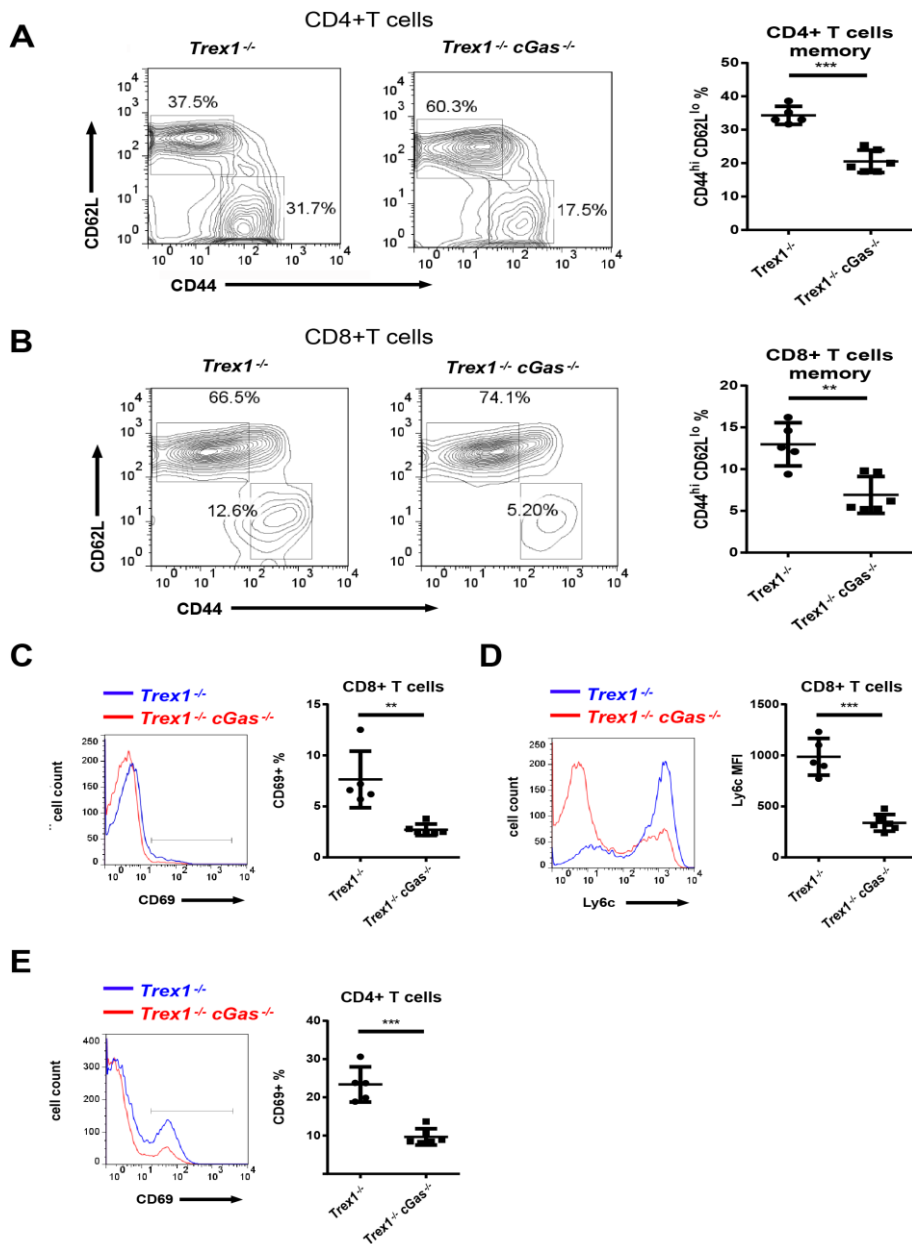


Figure 30. cGAS is responsible for higher percentages of activated and memory T cells in *Trex1*^{-/-} mice. (A and B) Representative flow-cytometric analysis of CD62L and CD44 expression in splenic CD4+ (A) and CD8+ T cells (B) from 12-wk-old mice of indicated genotypes. (C–E) Flow-cytometric analysis of expression of CD69 (C) and Ly6c (D) in splenic CD8+ T cells and CD69 (E) in splenic CD4+ T cells. Error bars represent SD. ** $P < 0.01$; *** $P < 0.001$.

cGAS activation leads to autoimmune lethality in *DNaseII*^{-/-} mice

To assess the role of cGAS in *DNaseII*^{-/-} mice, another autoimmune disease model, *DNaseII*^{-/-}*cGas*^{-/-} were generated by crossing *DNaseII*^{+/+} mice with *cGas*^{-/-} mice. Unlike *DNaseII*^{-/-} mice, *DNaseII*^{-/-}*cGas*^{-/-} mice were born viable. *DNaseII*^{-/-}*cGas*^{-/-} mice were

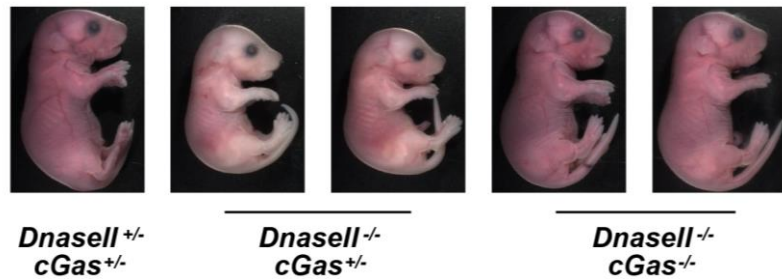


Figure 31. cGAS is responsible for embryonic lethality in *DNaseII*^{-/-} mice. Representative E17.5 embryos of indicated genotypes.

further crossed with *DNaseII*^{+/+}*cGas*^{+/-} mice and the embryos were collected and assessed. *DNaseII*^{-/-}*cGas*^{+/-} embryos resembled *DNaseII*^{-/-} embryos, in that they were pale and smaller than their wild-type littermates. Conversely, *DNaseII*^{-/-}*cGas*^{-/-} mice developed normally and survived after birth. Therefore, one allele of cGAS was sufficient to induce lethality in *DNaseII*^{-/-} mice, while the ablation of both alleles was necessary to rescue the lethality (Fig 31).

Fetal livers and limbs were analyzed for ISG expression. *DNaseII*^{-/-}*cGas*^{+/-} embryos had enhanced ISG levels compared to *DNaseII*^{-/-}*cGas*^{+/-} control. ISG levels were drastically reduced in *DNaseII*^{-/-}*cGas*^{-/-} embryos (Fig 32;33A). Interestingly, CXCL10 levels only partially decreased, possibly because in *DNaseII*^{-/-} fetal livers some other pathways might mediate the induction of CXCL10. ISGs measured in MEFs also led to a

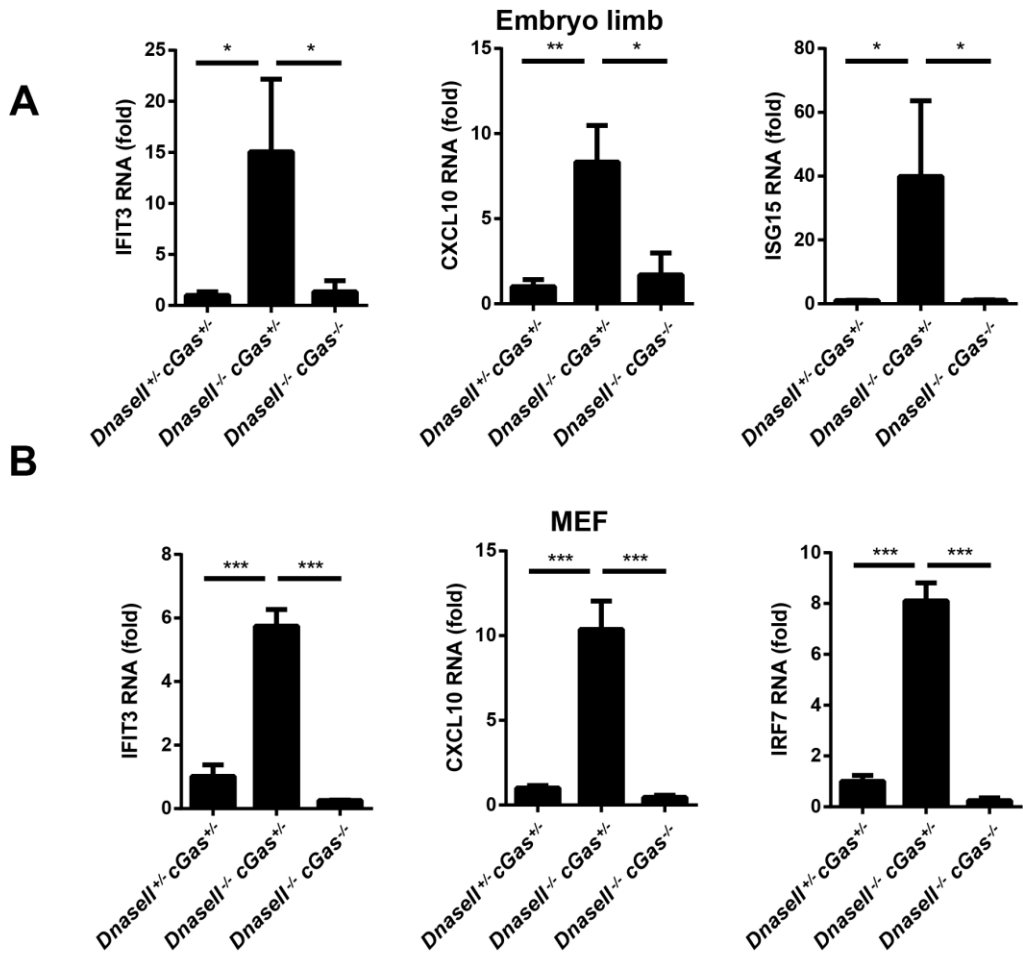


Figure 32. cGAS promotes ISG increase in *DNaseII*^{-/-} cells. (A and B) qRT-PCR analysis of indicated ISGs in E15.5 embryo limbs (A) and embryonic fibroblasts (B). Error bars represent SD * $P < 0.05$; ** $P < 0.01$; *** $P < 0.001$.

similar conclusion (Fig 32B). Again we applied quantitative mass spectrometry to measure cGAMP levels in fetal livers. cGAMP was detected in *DNaseII*^{-/-} *cGas*^{+/+} fetal livers but not in that of *DNaseII*^{-/-} *cGas*^{-/-} livers, illustrating that cGAS was critical for cGAMP accumulation in these fetal livers (Fig 33B).

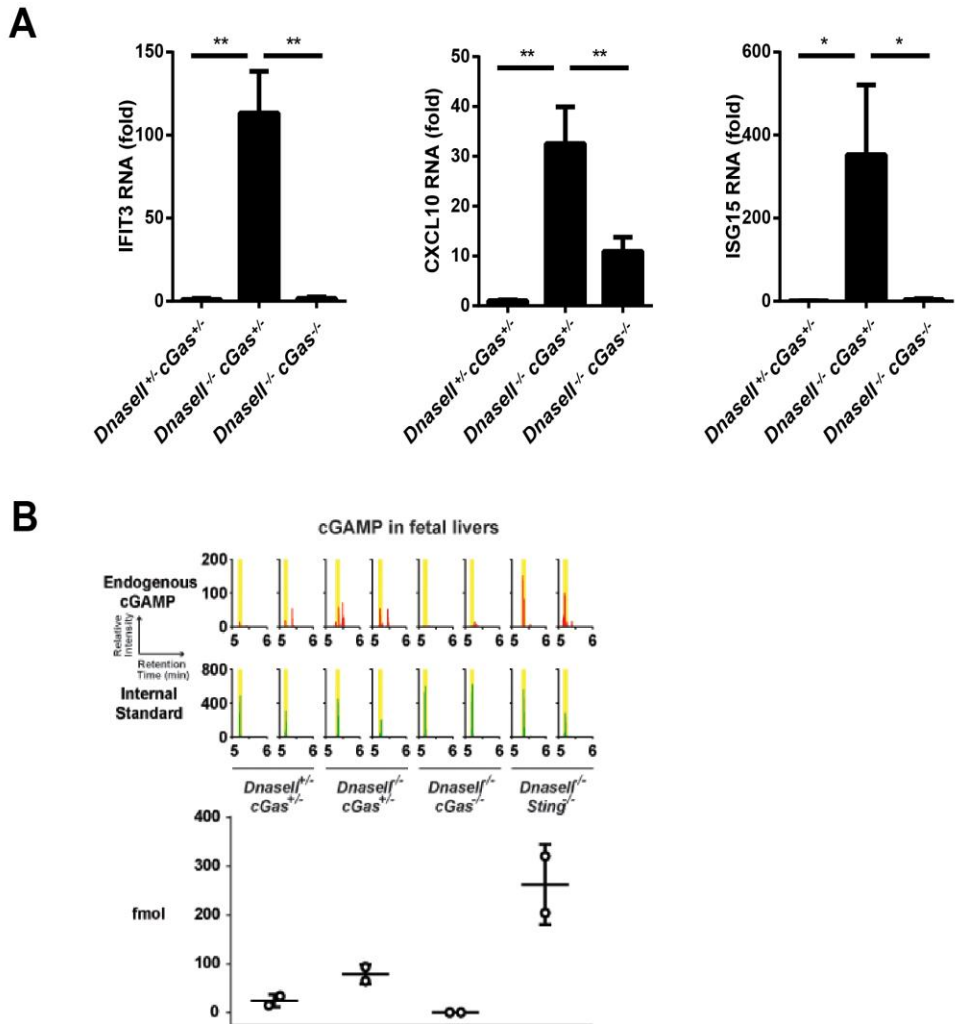


Figure 33. cGAS is essential for ISG up-regulation and cGAMP production in fetal livers of *DnaseII*^{−/−} mice. (A) qRT-PCR analysis of indicated ISGs in fetal liver from E15.5 mouse embryos of indicated genotypes ($n = 3$). (B) cGAMP levels in mouse fetal livers of indicated genotypes were quantified by LC-MS. *Upper* shows zoomed chromatograms displaying relative intensities of endogenous cGAMP (red) and internal standard (green). *Lower* shows the calculated amounts of cGAMP in each sample. Error bars represent SD (A) or SEM (B). * $P < 0.05$; ** $P < 0.01$.

cGAS activity causes polyarthritis and autoantibody production in *DnaseII*^{−/−} *IfnrI*^{−/−} mice

As previously reported, *DnaseII*^{−/−} *IfnrI*^{−/−} mice showed polyarthritis due to the overt production of TNF α . In contrast, *DnaseII*^{−/−} *cGas*^{−/−} mice didn't develop obvious

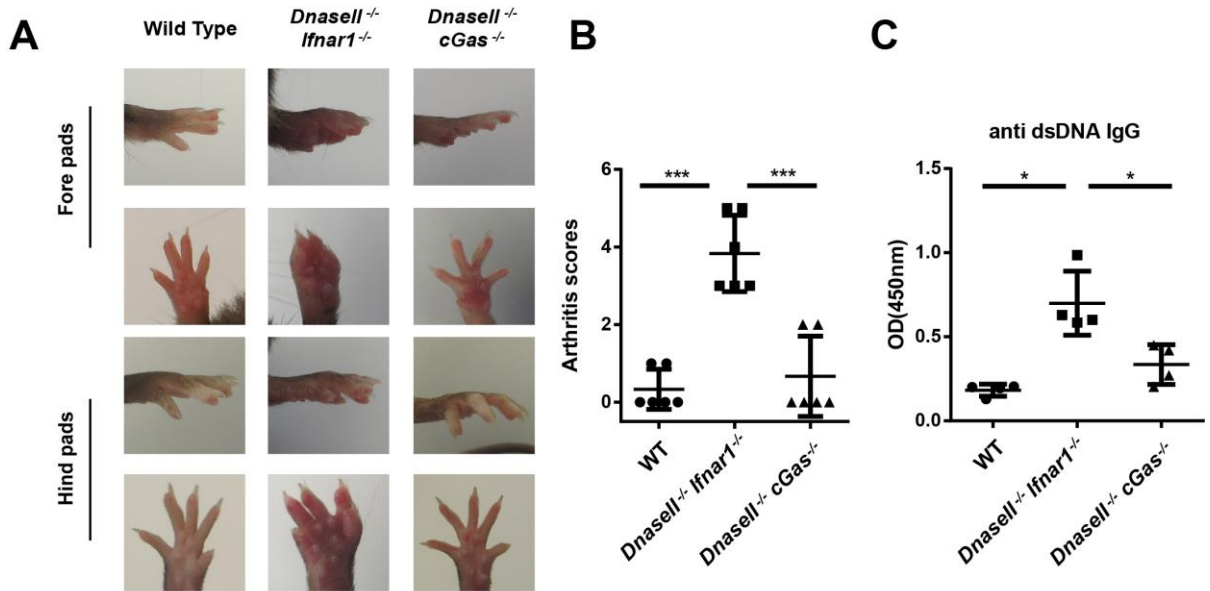


Figure 34. cGAS activation causes polyarthritis in *DNaseII^{-/-}Ifnar1^{-/-}* mice. (A and B) Representative foot pad pictures (A) and arthritis scores (B) of 7-mo-old WT, *DNaseII^{-/-}Ifnar1^{-/-}*, and *DNaseII^{-/-}cGAS^{-/-}* mice. Arthritis scores were calculated as described in *Materials and Methods*. (C) Detection of serum autoantibodies against dsDNA. Statistical analysis was performed with a two-tailed, unpaired Student's *t* test. Error bars represent SD. **P* < 0.05; ****P* < 0.001.

polyarthritis symptoms, which was further confirmed by histological scoring (Fig 34A-B).

This result implied that the overt TNF production in *DNaseII^{-/-}Ifnr1^{-/-}* mice was caused by cGAS. *DNaseII^{-/-}Ifnr1^{-/-}* sera also contained high levels of anti-dsDNA antibodies, but autoantibodies in *DNaseII^{-/-}cGas^{-/-}* were greatly reduced (Fig 34C).

Identification of accumulated cytosolic DNA in *Trex1^{-/-}* cells

To further identify the source of accumulated DNA in the cytosol, we performed the isolation of cGAS, in hopes of capturing cGAS-DNA complexes from cells. 293T cells were utilized because of the absence of TREX1 and the likelihood of the presence of a high concentration of cytosolic DNA. Cells were reconstituted with Flag-tagged cGAS

due to lack of cGAS expression in 293T cells. To test whether immunoprecipitation (IP) with cGAS can pull down interacting DNA, cells were transfected with the p-shuttle vector. Protein and DNA interactions were crosslinked by formaldehyde before lysis. cGAS was pulled down, and DNA from eluate was purified and examined by qRT-PCR. cGAS IP, but not Protein A/G Resin beads IP, pulled down more p-shuttle compared to 293T-PTY cells, suggesting cGAS binds to transfected DNA (Fig 35A-B). This assay can be further utilized to purify and identify accumulated cytosolic DNA in 293T cells.

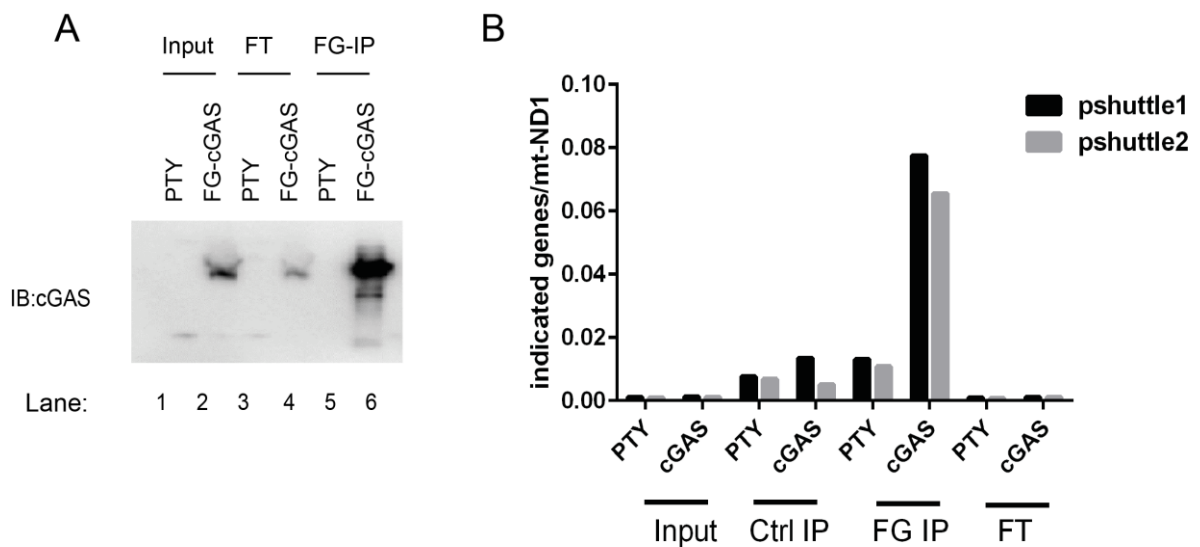


Figure 35. cGAS-IP pulls down interacting DNA. (A and B) 293T cells stably expressing Flag-tagged cGAS or empty PTY vector were transfected with p-shuttle. Cells were fixed, lysed and IP for Flag. The eluate was blotted by the cGAS antibody (A). DNA from eluates was purified and quantified by qRT-PCR (B).

Conclusions and discussion

TREX1 is a DNase that resides in the cytoplasm where it functions to clear mislocalized cytosolic DNA. The loss-of-function defect of *Trex1* leads to self-DNA accumulation in the cytosol, which activates the DNA sensor cGAS. Activated cGAS produces cGAMP and subsequently turns on signaling cascades that induce the production of ISGs as well as proinflammatory cytokines. Overactive innate immunity further promotes the development of the Th1 response and autoantibody production, and ultimately results in autoimmunity. Another DNase, DNaseII is a lysosomal DNase. In *DNaseII* null mice, DNA accumulation in phagocytes also initiates IFN production through cGAS and leads to embryonic lethality. If the IFN pathway is blocked in *DNaseII*^{-/-} *Ifnar1*^{-/-} mice, mice survive through the stages of embryo development but develop polyarthritis in adulthood, which is dependent on cGAS-mediated TNF production. (Fig 36)

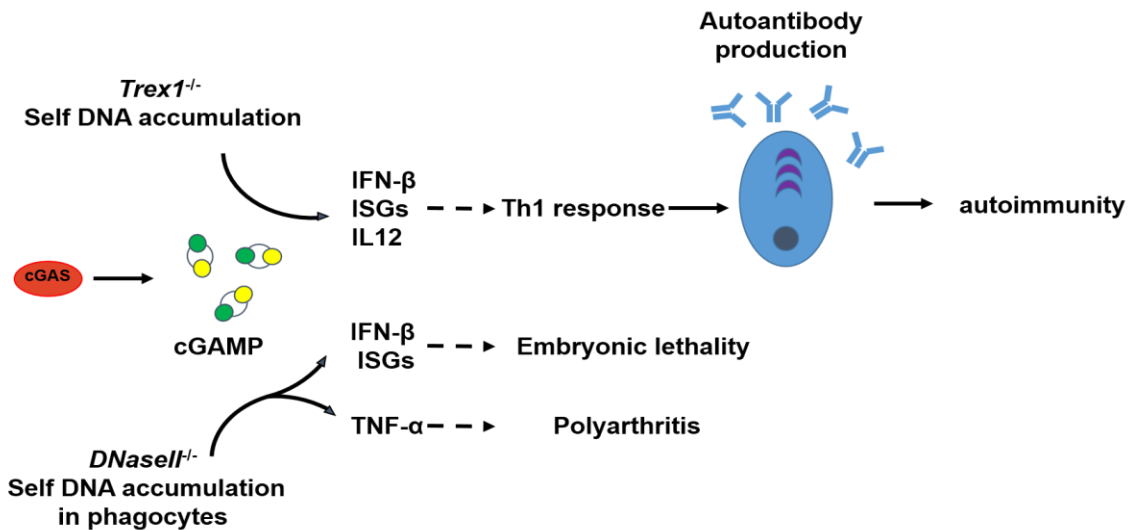


Figure 36. cGAS initiates autoimmunity in mice. In *Trex1^{-/-}* mice, cytosolic DNA accumulates and activates cGAS, leading to IFN or inflammatory cytokine production. The overactive innate immunity exacerbates Th1 response. Autoantibodies are produced and involved in the pathogenesis of autoimmunity. cGAS in *DNaseII^{-/-}* macrophages of fetal liver senses undigested DNA and generates cGAMP that is responsible for the subsequent production of IFN, leading to embryonic lethality. Undigested DNA in *DNaseII^{-/-}Ifnr1^{-/-}* mice provokes cGAS and induces TNF- α dependent polyarthritis.

Autoimmunity in *Trex1^{-/-}* mice

We observed an overactive Th1 response in *Trex1^{-/-}* mice. How this Th1 response is developed after IFN production is unknown. *Trex1^{-/-}* mice produced high levels of both IL12 and IFN. The former is known to be essential for the development and maintenance of Th1 differentiation. IFN production may also be involved since in DNA vaccination, IFNAR deficient mice have a compromised Th1 response. (Tudor, Riffault et al. 2001).

A paper published in *Cell* reveals that endogenous retroelements are responsible for autoimmunity in *Trex1^{-/-}* mice (Stetson, Ko et al. 2008). However, it remains unsolved why the treatment with a reverse transcriptase inhibitor, AZT, fails to rescue *Trex1^{-/-}* mice from lethality. It is possible that AZT cannot sufficiently inhibit diverse reverse transcriptases in mice, or that there are alternative sources of DNA other than retroelements. To address this dilemma, we attempted to purify accumulated DNA from 293T cytosol because 293T cells lack the expression of TREX1 (Fig 35). When overexpressed, recombinant cGAS theoretically can bind and be crosslinked with the cytosolic DNA. Cytosolic DNA can further be purified and sequenced. In the future, we can also IP endogenous cGAS in *Trex1^{-/-}Sting^{-/-}* MEF cells and WT MEF cells. Since STING may contribute to DNA clearance through autophagy, there will be more DNA present in *Trex1^{-/-}Sting^{-/-}* cytosol, which makes it easier to identify.

In *TREX1-V235fs* knock-in mice, although TREX1 functions normally in digesting DNA, the mice still show signs of autoimmune disease. This phenotype can be explained by glycan accumulation which does not signal through cGAS (Hasan, Fermaintt et al. 2015). We have shown that cGAS knock-out completely rescues ISG levels and autoinflammation in several organs of *Trex1^{-/-}* mice, but whether or not other specific organs show inflammation will still need to be investigated.

Autoimmunity in *DnaseII^{-/-}cGas^{-/-}* mice

In addition to the cGAS-STING pathway, AIM2, a DNA sensor in the inflammasome pathway, is also involved in arthritis development. Dysfunction of AIM2 partially rescues arthritis (Baum, Sharma et al. 2015). AIM2 seems to detect DNA to activate the inflammasome pathway that is required for the processing of pro-IL1 β or pro-IL-18 into mature IL-1 β or IL-18, which can further enhance the inflammatory response induced by TNF.

DnaseII^{-/-Ifnr1^{-/-}}, *DnaseII^{-/-cGas^{-/-}}* and *DnaseII^{-/-Sting^{-/-}}* mice all develop splenomegaly. A recent publication has shown that knocking out UNC93B1 in mice rescues the splenomegaly phenotype, indicating the activation of UNC93B1-dependent TLR pathway in *DnaseII^{-/-Ifnr1^{-/-}}* mice (Pawaria, Moody et al. 2015).

Based on a recent report, most of the autoantibody production in *DnaseII^{-/-Ifnr1^{-/-}}* mice depends on TLR pathways but not the cGAS-STING pathway (Baum, Sharma et al. 2015). Although we determined that anti-dsDNA production partly depends on cGAS, we have yet to test production of other types of autoantibodies.

Haploinsufficiency of cGAS and autoimmune diseases

Haploinsufficiency of cGAS largely rescues survival of *Trex1^{-/-}* mice, while the rescue of *DNaseII^{-/-}* mice requires defects in both *cGas* alleles. It is not entirely clear why, but it is possibly due to the different functions of DNases in different cell types. TREX1, a cytosolic DNase, digests DNA in the cytosol in various cell types. The source of cytosolic DNA that serves as the ligand of cGAS is still unclear. As a matter of fact, DNA, as the genetic material, usually stays in nucleus and mitochondria. Cytosolically localized DNA could be randomly leaked DNA. In contrast, DNaseII is a lysosomal DNase, which mainly functions in phagocytes. Phagocytes engulf dead cells which contain large amounts of DNA from nuclei. In *DNaseII^{-/-}* cells, uncleared DNA potentially enters the cytosol and activates the DNA sensor cGAS. It is possible that the amount of DNA in *DNaseII^{-/-}* phagocytes is much more than *Trex1^{-/-}* cells. So even in *DNaseII^{-/-} cGas^{+/-}* cells, DNA can still stimulate potent IFN production.

STING and cGAMP clearance

Trex1^{-/-} Sting^{-/-} mice have increased cGAMP production compared with that of *Trex1^{-/-}* mice, suggesting a STING-dependent cGAMP clearance pathway. Similarly, *DNaseII^{-/-} Sting^{-/-}* livers have much higher cGAMP levels than that of *DNaseII^{-/-} cGas^{+/-}*. This statement must be interpreted with caution. In this setting, *DNaseII^{-/-} cGas^{+/-}* control is not included, thus, it is possible that cGAS haploinsufficiency may produce less

cGAMP, or that STING may play a regulatory role in cGAMP clearance in *DNaseII*^{-/-}.

This issue should be clarified in the future work.

Future plan

Similar to AGS patients, some SLE patients have a high IFN signature and ANA antibody production. It has been proven that some SLE patients have TREX1 mutations. Therefore, those SLE patients may have cGAMP production in PBMCs due to TREX1 abnormality. In the future, we can potentially measure the cGAMP levels in PBMCs isolated from SLE patients. If cGAMP production is confirmed, a cGAS inhibitor can be used to treat autoimmune diseases like SLE and AGS. We can further test the inhibitor in *DNaseII*^{-/-}*Ifnrl1*^{-/-} mice and *Trex1*^{-/-} mice. A good inhibitor of cGAS will rescue the autoimmune phenotypes in these mice.

Also, we will attempt to rescue *Trex1*^{-/-} mice with cGAS conditional knock-out in specific cell types. We hypothesize that cGAS in DCs may play an important role in the pathogenesis of autoimmunity in *Trex1*^{-/-} mice. In order test this hypothesis, we will use the Cre-Lox system by crossing *cGas*^{flx/flx} mice with Cre mice driven by a CD11c-promoter. To rule out the involvement of other cell types such as macrophages, we will also employ this strategy to generate the relevant conditional *cGas* mutant strains.

We will continue to identify the source of DNA mainly through IP of cGAS-DNA complexes, especially under the condition of more DNA accumulated in the cytosol. We will also use an in vitro assay to deliver the *Trex1*^{-/-} cytosol into PFO-permeabilized THP-1 cells since it was previously shown that accumulated DNA in *Trex1*^{-/-} cells is 60-65bp

(Yang, Lindahl et al. 2007). By establishing a biochemical assay, we can then purify the DNA which can be sequenced.

Materials and methods

Mice

Trex1^{-/-} mice were from Dr. Deborah Barnes (Cancer Research UK) and Dr. Nan Yan (UT Southwestern), and *DNaseII^{-/-}* mice were from Dr. Shigekazu Nagata (Kyoto University). *cGas^{-/-}* mice were generated in our lab as previously described (Li, Wu et al. 2013). All mice used in this study were on C57/B6 background. The mice were bred and maintained under specific pathogen-free conditions in the animal care facility of the University of Texas Southwestern Medical Center at Dallas according to experimental protocols approved by the Institutional Animal Care and Use Committee.

Pathology

Tissues were fixed in 4% paraformaldehyde, paraffin embedded, cut into 5 μ m sections, and stained with hematoxylin and eosin. Heart tissues were stained with picrosirius red, and kidney samples were stained with Periodic acid–Schiff. Inflammation and fibrosis were evaluated based on degree of severity. The sum of individual scores was used to obtain a total tissue histological score. Specific information about the scoring criteria for each tissue was previously described (Gall, Treuting et al. 2012). Clinical

assessment of foot pads for arthritis was described in previous study (Kawane, Ohtani et al. 2006).

Quantitative RT-PCR

Reverse transcription and real-time PCR reactions were carried out using iScript cDNA synthesis kit and iQ SYBR Green Supermix (Bio-Rad). qRT-PCR was performed on an Applied Biosystems Vii7 using the following primers:

Rpl19	AAATCGCCAATGCCAACTC	TCTTCCCTATGCCCATATGC
Cxcl10	GCCGTCATTTCTGCCTCA	CGTCCTTGCAGAGAGGGATC
Ifng	CTTGAGCTCTCCTCATGGCTGTTCTG	TGACGCTTATGTTGCTGATGGCCTG
Tnf	CACAGAAAGCATGATCCGCGACGT	CGGCAGAGAGGAGGTTGACTTTCT
Tbx21	TCAGGACTAGGCGAAGGAGA	TAGTGGCACCTTCCAATT
Ifit3	TGGCCTACATAAAGCACCTAGATGG	CGCAAACCTTGGCAAACCTTGCT
Irf7	ATGCACAGATCTCAAGGCCTGGC	GTGCTGTGGAGTGCACAGCGGAAGT
Il10	CTATGCTGCCTGCTCTTACTG	AACCCAAGTAACCCTAAAGTC
Il12p40	GTTCAACATCAAGAGCAGTAGCA	CTGCAGACAGAGACGCCATT
Isg15	GGAACGAAAGGGCCACAGCA	CCTCCATGGGCCTTCCCTCGA

Table 2. list of qRT-PCR primers

Cells

Embryonic fibroblasts from genotype indicated mice were prepared from day 15.5 embryos and cultured in DMEM supplemented with 10% FBS.

Bone marrow cells were collected from femurs and tibiae of mice. To obtain BMDM, about 10 million bone marrow cells were cultured in DMEM containing 10% FBS, antibiotics and conditioned media from L929 cell culture. After 7 days, mature macrophages were harvested and cultured in 12-well plates for experiments. To obtain dendritic cells, bone marrow cells were cultured in RPMI 1640 containing 10% FBS, 10

mM HEPES (pH 7.4), 50 µM β-mercaptoethanol, 10 ng/ml murine GM-CSF (peproTech). After 7 days, cells were collected and used as GM-CSF-induced BMDCs.

ELISA

Serum anti-ssDNA IgG levels were quantified by sandwich ELISA. Briefly, 96-well ELISA plates (Greiner Bio One) were coated with 1ug/mL calf thymus ssDNA (Sigma-Aldrich) overnight at 4°C. After blocking of the plates with 10% FBS, test sera were added at 1:100 dilution. HRP-conjugated goat anti-mouse IgG (Santa Cruz) was added at a dilution of 1:10000. The reaction was developed with TMB substrate (Thermo Scientific), and the OD at 450 nm was determined. Serum IgG subclasses were quantified as described, except that the samples were reacted with goat Ab specific for IgG2b (Southern Biotech) at 1:10000 dilution. For anti-histone, anti-M2 antigen, anti-dsDNA and anti-u1-snRNP assays, ELISA plates were coated overnight with 1ug/mL histones H3 (Sigma), 0.5ug/mL M2 antigen (Diarect), 1ug/mL calf thymus DNA (Sigma-Aldrich) and 0.5ug/mL u1-snRNP (Diarect) respectively. ANA IgG levels were determined by Anti-ANA bioassay ELISA kit (US Biological Life Sciences) according to manufacturer's instruction.

Plasma IL-12 was measured using the mouse TH1/TH2 9-Plex Ultra-sensitive Kit (Meso Scale Discovery) according to the manufacturer's instructions.

Flow cytometry

For surface staining, cells were washed in ice-cold FACS buffer (2% BSA in PBS), and then incubated with indicated antibody for 15 min and washed with FACS buffer. For intracellular IFN- γ staining, splenocytes or PBMCs were stimulated with 50 ng/ml phorbol myristate acetate (PMA) and 1 μ M ionomycin in the presence of 1 μ g/ml brefeldin A for 4.5 hr, followed by surface staining (CD3, CD4 and CD8), fixed with 2% paraformaldehyde, permeabilized with 0.1% saponin, and stained for IFN- γ . For transcription factor staining, cells were stained by surface antibody, followed intracellular staining for anti-T-bet (Biolegend). The stained cells were analyzed with FACSCalibur flow cytometer (BD Biosciences). Data were analyzed with FlowJo software. CD4-APC, CD4-FITC, CD3-Percp, IFN- γ -PE antibodies were purchased from Biolegend; CD62L-PE, Ly6c-APC, CD8-FITC, CD69-PE antibodies were purchased from eBioscience; CD44-APC, CD8-APC antibodies were purchased from BD Bioscience.

cGAMP extraction and quantification

Fresh organs were snap frozen in liquid nitrogen, minced immediately with dissecting scissors in cold 80% methanol with 2% acetic acid (HAc), and stored in -80°C before further processing. On the day of analysis, the frozen samples were thawed on ice, and $^{13}\text{C}_{10}^{15}\text{N}_5$ -labeled cGAMP (+15 a.m.u.) internal standard was supplemented. Samples were then homogenized with a tissue tearor (Biospec Products, Bartlesville, OK) for 30 sec, and cleared by centrifugation (10,000 g) for 10 min. The pellets were further extracted in 20% methanol and 2% HAc for two more rounds, and all the cleared extracts

were combined. From these extracts, cGAMP was enriched by solid phase extraction (SPE) using HyperSep Aminopropyl SPE Columns (Thermo Scientific). Briefly, the columns were first activated by methanol and washed twice with 2% HAc; after drawing through the extracts, columns were washed twice with 2% HAc, once with 80% methanol, and finally eluted with 4% ammonium hydroxide in 80% methanol. The eluents were spin vacuumed to dryness, reconstituted in LC/MS-grade water, cleared by centrifugation, and transferred to autosampler vials for MS analyses.

MS analyses were performed as previously described (Angela et al. Cell Host & Microbe. 2015). Briefly, the SPE eluents were separated on an Xbridge Amide column (3.5 µm, 3.5 mm ID × 100 mm L, Waters) on a Dionex Ultimate 3000 Rapid Separation Liquid Chromatography system (Thermo Scientific). Mobile phase A was 20 mM ammonium bicarbonate with 20 mM ammonium hydroxide in water, and mobile phase B was acetonitrile. The separation ran at a flow of 400 µL/min for the first 14.5 min and 800 µL/min for the remaining 8.5 min, through the following gradient: 0 min 85% B, 3 min 85% B, 10 min 2% B, 14 min 2% B, 14.5 min 85% B and 23 min 85% B.

The LC eluent was ionized by an Ion Max NG heated electrospray source, with a spray voltage of +3750 V, an ion transfer tube temperature of 342°C, a vaporizing temperature of 292°C, and the sheath, auxiliary and sweep gas at 45, 17 and 1 arbitrary units, respectively. The spray was analyzed online on a TSQ Quantiva triple quadrupole mass spectrometer (Thermo Scientific), which performed continuous MRM scans with a

dwell time of 50 ms, Q1 and Q3 resolutions of 0.7 FWHM and the CID gas of 1.5 units.

cGAMP and the internal standard were monitored by the positive mode with four transitions respectively (cGAMP: 675-136, 675-152, 675-476, 675-524 and the internal standard: 691-146, 691-152, 691-491, 691-539). Raw MS Data was converted to the mzXML format with ReAdW, and read into MATLAB for noise reduction and data processing. Absolute quantities of endogenous cGAMP were calculated with the light:heavy ratios and the molar quantity of supplemented internal standard.

Identification of accumulated cytosolic DNA in *Trex1^{-/-}* cells

293T cells with GFP expression or Flag-cGAS expression were transfected with 0.5ug/mL p-shuttle vector for 5 hrs. Protein and DNA interactions were crosslinked by 1% formaldehyde at 37 °C for 15 min before lysis. cGAS was pulled down by protein A/G beads and cGAS antibody in the presence of 0.2% SDS, and DNA from eluate was purified and examined by qRT-PCR.

Statistics

Statistical analysis of mouse survival was performed using Mantel-Cox test. Other statistical analyses were performed with a two-tailed, unpaired Student's t test.

References

- Ablasser, A., M. Goldeck, T. Cavlar, T. Deimling, G. Witte, I. Rohl, K. P. Hopfner, J. Ludwig and V. Hornung (2013). "cGAS produces a 2'-5'-linked cyclic dinucleotide second messenger that activates STING." *Nature* **498**(7454): 380-384.
- Ablasser, A., I. Hemmerling, J. L. Schmid-Burgk, R. Behrendt, A. Roers and V. Hornung (2014). "TREX1 deficiency triggers cell-autonomous immunity in a cGAS-dependent manner." *J Immunol* **192**(12): 5993-5997.
- Ablasser, A., J. L. Schmid-Burgk, I. Hemmerling, G. L. Horvath, T. Schmidt, E. Latz and V. Hornung (2013). "Cell intrinsic immunity spreads to bystander cells via the intercellular transfer of cGAMP." *Nature* **503**(7477): 530-534.
- Ahmed, M., L. M. Mitchell, S. Puckett, K. L. Brzoza-Lewis, D. S. Lyles and E. M. Hiltbold (2009). "Vesicular stomatitis virus M protein mutant stimulates maturation of Toll-like receptor 7 (TLR7)-positive dendritic cells through TLR-dependent and -independent mechanisms." *J Virol* **83**(7): 2962-2975.
- Ahn, J., D. Gutman, S. Saijo and G. N. Barber (2012). "STING manifests self DNA-dependent inflammatory disease." *Proc Natl Acad Sci U S A* **109**(47): 19386-19391.
- Aicardi, J. and F. Goutieres (1984). "A progressive familial encephalopathy in infancy with calcifications of the basal ganglia and chronic cerebrospinal fluid lymphocytosis." *Ann Neurol* **15**(1): 49-54.
- Akira, S. and K. Takeda (2004). "Toll-like receptor signalling." *Nat Rev Immunol* **4**(7): 499-511.
- Akira, S., S. Uematsu and O. Takeuchi (2006). "Pathogen recognition and innate immunity." *Cell* **124**(4): 783-801.
- Baker, K. P., W. F. Baron, W. J. Henzel and S. A. Spencer (1998). "Molecular cloning and characterization of human and murine DNase II." *Gene* **215**(2): 281-289.
- Baldauf, H. M., X. Pan, E. Erikson, S. Schmidt, W. Daddacha, M. Burggraf, K. Schenkova, I. Ambiel, G. Wabnitz, T. Gramberg, S. Panitz, E. Flory, N. R. Landau, S. Sertel, F. Rutsch, F. Lasitschka, B. Kim, R. Konig, O. T. Fackler and O. T. Keppler (2012). "SAMHD1 restricts HIV-1 infection in resting CD4(+) T cells." *Nat Med* **18**(11): 1682-1687.
- Bauer, S., C. J. Kirschning, H. Hacker, V. Redecke, S. Hausmann, S. Akira, H. Wagner and G. B. Lipford (2001). "Human TLR9 confers responsiveness to bacterial DNA via species-specific CpG motif recognition." *Proc Natl Acad Sci U S A* **98**(16): 9237-9242.
- Baum, R., S. Sharma, S. Carpenter, Q. Z. Li, P. Bustos, K. A. Fitzgerald, A. Marshak-Rothstein and E. M. Gravallese (2015). "Cutting edge: AIM2 and endosomal TLRs differentially regulate arthritis and autoantibody production in DNase II-deficient mice." *J Immunol* **194**(3): 873-877.

- Boule, M. W., C. Broughton, F. Mackay, S. Akira, A. Marshak-Rothstein and I. R. Rifkin (2004). "Toll-like receptor 9-dependent and -independent dendritic cell activation by chromatin-immunoglobulin G complexes." *J Exp Med* **199**(12): 1631-1640.
- Bridgeman, A., J. Maelfait, T. Davenne, T. Partridge, Y. Peng, A. Mayer, T. Dong, V. Kaever, P. Borrow and J. Rehwinkel (2015). "Viruses transfer the antiviral second messenger cGAMP between cells." *Science* **349**(6253): 1228-1232.
- Browne, E. P. (2011). "Toll-like receptor 7 controls the anti-retroviral germinal center response." *PLoS Pathog* **7**(10): e1002293.
- Browne, E. P. and D. R. Littman (2009). "Myd88 is required for an antibody response to retroviral infection." *PLoS Pathog* **5**(2): e1000298.
- Burdette, D. L., K. M. Monroe, K. Sotelo-Troha, J. S. Iwig, B. Eckert, M. Hyodo, Y. Hayakawa and R. E. Vance (2011). "STING is a direct innate immune sensor of cyclic di-GMP." *Nature* **478**(7370): 515-518.
- Cai, X., J. Chen, H. Xu, S. Liu, Q. X. Jiang, R. Halfmann and Z. J. Chen (2014). "Prion-like polymerization underlies signal transduction in antiviral immune defense and inflammasome activation." *Cell* **156**(6): 1207-1222.
- Chan, D. C., D. Fass, J. M. Berger and P. S. Kim (1997). "Core structure of gp41 from the HIV envelope glycoprotein." *Cell* **89**(2): 263-273.
- Chiu, Y. H., J. B. Macmillan and Z. J. Chen (2009). "RNA polymerase III detects cytosolic DNA and induces type I interferons through the RIG-I pathway." *Cell* **138**(3): 576-591.
- Christensen, S. R., M. Kashgarian, L. Alexopoulou, R. A. Flavell, S. Akira and M. J. Shlomchik (2005). "Toll-like receptor 9 controls anti-DNA autoantibody production in murine lupus." *J Exp Med* **202**(2): 321-331.
- Christensen, S. R., J. Shupe, K. Nickerson, M. Kashgarian, R. A. Flavell and M. J. Shlomchik (2006). "Toll-like receptor 7 and TLR9 dictate autoantibody specificity and have opposing inflammatory and regulatory roles in a murine model of lupus." *Immunity* **25**(3): 417-428.
- Coakley, E., C. J. Petropoulos and J. M. Whitcomb (2005). "Assessing chemokine co-receptor usage in HIV." *Curr Opin Infect Dis* **18**(1): 9-15.
- Collins, A. C., H. Cai, T. Li, L. H. Franco, X. D. Li, V. R. Nair, C. R. Scharn, C. E. Stamm, B. Levine, Z. J. Chen and M. U. Shiloh (2015). "Cyclic GMP-AMP Synthase Is an Innate Immune DNA Sensor for Mycobacterium tuberculosis." *Cell Host Microbe* **17**(6): 820-828.
- Cribier, A., B. Descours, A. L. Valadao, N. Laguette and M. Benkirane (2013). "Phosphorylation of SAMHD1 by cyclin A2/CDK1 regulates its restriction activity toward HIV-1." *Cell Rep* **3**(4): 1036-1043.
- Crow, Y. J., B. E. Hayward, R. Parmar, P. Robins, A. Leitch, M. Ali, D. N. Black, H. van Bokhoven, H. G. Brunner, B. C. Hamel, P. C. Corry, F. M. Cowan, S. G. Frants, J. Klepper, J. H. Livingston, S. A. Lynch, R. F. Massey, J. F. Meritet, J. L. Michaud, G.

- Ponsot, T. Voit, P. Lebon, D. T. Bonthon, A. P. Jackson, D. E. Barnes and T. Lindahl (2006). "Mutations in the gene encoding the 3'-5' DNA exonuclease TREX1 cause Aicardi-Goutieres syndrome at the AGS1 locus." *Nat Genet* **38**(8): 917-920.
- Crow, Y. J., A. Leitch, B. E. Hayward, A. Garner, R. Parmar, E. Griffith, M. Ali, C. Semple, J. Aicardi, R. Babul-Hirji, C. Baumann, P. Baxter, E. Bertini, K. E. Chandler, D. Chitayat, D. Cau, C. Dery, E. Fazzi, C. Goizet, M. D. King, J. Klepper, D. Lacombe, G. Lanzi, H. Lyall, M. L. Martinez-Frias, M. Mathieu, C. McKeown, A. Monier, Y. Oade, O. W. Quarrell, C. D. Rittey, R. C. Rogers, A. Sanchis, J. B. Stephenson, U. Tacke, M. Till, J. L. Tolmie, P. Tomlin, T. Voit, B. Weschke, C. G. Woods, P. Lebon, D. T. Bonthon, C. P. Ponting and A. P. Jackson (2006). "Mutations in genes encoding ribonuclease H2 subunits cause Aicardi-Goutieres syndrome and mimic congenital viral brain infection." *Nat Genet* **38**(8): 910-916.
- Descours, B., A. Cribier, C. Chable-Bessia, D. Ayinde, G. Rice, Y. Crow, A. Yatim, O. Schwartz, N. Laguette and M. Benkirane (2012). "SAMHD1 restricts HIV-1 reverse transcription in quiescent CD4(+) T-cells." *Retrovirology* **9**: 87.
- Diebold, S. S., T. Kaisho, H. Hemmi, S. Akira and C. Reis e Sousa (2004). "Innate antiviral responses by means of TLR7-mediated recognition of single-stranded RNA." *Science* **303**(5663): 1529-1531.
- Diner, E. J., D. L. Burdette, S. C. Wilson, K. M. Monroe, C. A. Kellenberger, M. Hyodo, Y. Hayakawa, M. C. Hammond and R. E. Vance (2013). "The innate immune DNA sensor cGAS produces a noncanonical cyclic dinucleotide that activates human STING." *Cell Rep* **3**(5): 1355-1361.
- Dobbs, N., N. Burnaevskiy, D. Chen, V. K. Gonugunta, N. M. Alto and N. Yan (2015). "STING Activation by Translocation from the ER Is Associated with Infection and Autoinflammatory Disease." *Cell Host Microbe* **18**(2): 157-168.
- Doitsh, G., M. Cavrois, K. G. Lassen, O. Zepeda, Z. Yang, M. L. Santiago, A. M. Hebbeler and W. C. Greene (2010). "Abortive HIV infection mediates CD4 T cell depletion and inflammation in human lymphoid tissue." *Cell* **143**(5): 789-801.
- Ehlers, M., H. Fukuyama, T. L. McGaha, A. Aderem and J. V. Ravetch (2006). "TLR9/MyD88 signaling is required for class switching to pathogenic IgG2a and 2b autoantibodies in SLE." *J Exp Med* **203**(3): 553-561.
- Fernandes-Alnemri, T., J. W. Yu, P. Datta, J. Wu and E. S. Alnemri (2009). "AIM2 activates the inflammasome and cell death in response to cytoplasmic DNA." *Nature* **458**(7237): 509-513.
- Fernandes-Alnemri, T., J. W. Yu, C. Juliana, L. Solorzano, S. Kang, J. Wu, P. Datta, M. McCormick, L. Huang, E. McDermott, L. Eisenlohr, C. P. Landel and E. S. Alnemri (2010). "The AIM2 inflammasome is critical for innate immunity to Francisella tularensis." *Nat Immunol* **11**(5): 385-393.
- Funabiki, M., H. Kato, Y. Miyachi, H. Toki, H. Motegi, M. Inoue, O. Minowa, A. Yoshida, K. Deguchi, H. Sato, S. Ito, T. Shiroishi, K. Takeyasu, T. Noda and T. Fujita

- (2014). "Autoimmune disorders associated with gain of function of the intracellular sensor MDA5." *Immunity* **40**(2): 199-212.
- Gack, M. U., Y. C. Shin, C. H. Joo, T. Urano, C. Liang, L. Sun, O. Takeuchi, S. Akira, Z. Chen, S. Inoue and J. U. Jung (2007). "TRIM25 RING-finger E3 ubiquitin ligase is essential for RIG-I-mediated antiviral activity." *Nature* **446**(7138): 916-920.
- Gall, A., P. Treuting, K. B. Elkon, Y. M. Loo, M. Gale, Jr., G. N. Barber and D. B. Stetson (2012). "Autoimmunity initiates in nonhematopoietic cells and progresses via lymphocytes in an interferon-dependent autoimmune disease." *Immunity* **36**(1): 120-131.
- Gao, P., M. Ascano, Y. Wu, W. Barchet, B. L. Gaffney, T. Zillinger, A. A. Serganov, Y. Liu, R. A. Jones, G. Hartmann, T. Tuschl and D. J. Patel (2013). "Cyclic [G(2',5')pA(3',5')p] is the metazoan second messenger produced by DNA-activated cyclic GMP-AMP synthase." *Cell* **153**(5): 1094-1107.
- Gao, P., M. Ascano, T. Zillinger, W. Wang, P. Dai, A. A. Serganov, B. L. Gaffney, S. Shuman, R. A. Jones, L. Deng, G. Hartmann, W. Barchet, T. Tuschl and D. J. Patel (2013). "Structure-function analysis of STING activation by c[G(2',5')pA(3',5')p] and targeting by antiviral DMXAA." *Cell* **154**(4): 748-762.
- Garcia, F., N. Climent, A. C. Guardo, C. Gil, A. Leon, B. Autran, J. D. Lifson, J. Martinez-Picado, J. Dalmau, B. Clotet, J. M. Gatell, M. Plana, T. Gallart and D. M. O. S. Group (2013). "A dendritic cell-based vaccine elicits T cell responses associated with control of HIV-1 replication." *Sci Transl Med* **5**(166): 166ra162.
- Gentili, M., J. Kowal, M. Tkach, T. Satoh, X. Lahaye, C. Conrad, M. Boyron, B. Lombard, S. Durand, G. Kroemer, D. Loew, M. Dalod, C. Thery and N. Manel (2015). "Transmission of innate immune signaling by packaging of cGAMP in viral particles." *Science* **349**(6253): 1232-1236.
- Gilbert, P. B., I. W. McKeague, G. Eisen, C. Mullins, N. A. Gueye, S. Mboup and P. J. Kanki (2003). "Comparison of HIV-1 and HIV-2 infectivity from a prospective cohort study in Senegal." *Stat Med* **22**(4): 573-593.
- Goldstone, D. C., V. Ennis-Adeniran, J. J. Hedden, H. C. Groom, G. I. Rice, E. Christodoulou, P. A. Walker, G. Kelly, L. F. Haire, M. W. Yap, L. P. de Carvalho, J. P. Stoye, Y. J. Crow, I. A. Taylor and M. Webb (2011). "HIV-1 restriction factor SAMHD1 is a deoxynucleoside triphosphate triphosphohydrolase." *Nature* **480**(7377): 379-382.
- Goujon, C., O. Moncorge, H. Bauby, T. Doyle, C. C. Ward, T. Schaller, S. Hue, W. S. Barclay, R. Schulz and M. H. Malim (2013). "Human MX2 is an interferon-induced post-entry inhibitor of HIV-1 infection." *Nature* **502**(7472): 559-562.
- Grandvaux, N., B. R. tenOever, M. J. Servant and J. Hiscott (2002). "The interferon antiviral response: from viral invasion to evasion." *Curr Opin Infect Dis* **15**(3): 259-267.
- Grieves, J. L., J. M. Fye, S. Harvey, J. M. Grayson, T. Hollis and F. W. Perrino (2015). "Exonuclease TREX1 degrades double-stranded DNA to prevent spontaneous lupus-like inflammatory disease." *Proc Natl Acad Sci U S A* **112**(16): 5117-5122.

- Hasan, M., C. S. Fermaintt, N. Gao, T. Sakai, T. Miyazaki, S. Jiang, Q. Z. Li, J. P. Atkinson, H. C. Morse, 3rd, M. A. Lehrman and N. Yan (2015). "Cytosolic Nuclease TREX1 Regulates Oligosaccharyltransferase Activity Independent of Nuclease Activity to Suppress Immune Activation." *Immunity* **43**(3): 463-474.
- Hasan, M., J. Koch, D. Rakheja, A. K. Pattnaik, J. Brugarolas, I. Dozmorov, B. Levine, E. K. Wakeland, M. A. Lee-Kirsch and N. Yan (2013). "Trex1 regulates lysosomal biogenesis and interferon-independent activation of antiviral genes." *Nat Immunol* **14**(1): 61-71.
- He, J., Y. Chen, M. Farzan, H. Choe, A. Ohagen, S. Gartner, J. Busciglio, X. Yang, W. Hofmann, W. Newman, C. R. Mackay, J. Sodroski and D. Gabuzda (1997). "CCR3 and CCR5 are co-receptors for HIV-1 infection of microglia." *Nature* **385**(6617): 645-649.
- Herzner, A. M., C. A. Hagmann, M. Goldeck, S. Wolter, K. Kubler, S. Wittmann, T. Gramberg, L. Andreeva, K. P. Hopfner, C. Mertens, T. Zillinger, T. Jin, T. S. Xiao, E. Bartok, C. Coch, D. Ackermann, V. Hornung, J. Ludwig, W. Barchet, G. Hartmann and M. Schlee (2015). "Sequence-specific activation of the DNA sensor cGAS by Y-form DNA structures as found in primary HIV-1 cDNA." *Nat Immunol* **16**(10): 1025-1033.
- Hornung, V., J. Ellegast, S. Kim, K. Brzozka, A. Jung, H. Kato, H. Poeck, S. Akira, K. K. Conzelmann, M. Schlee, S. Endres and G. Hartmann (2006). "5'-Triphosphate RNA is the ligand for RIG-I." *Science* **314**(5801): 994-997.
- Hou, F., L. Sun, H. Zheng, B. Skaug, Q. X. Jiang and Z. J. Chen (2011). "MAVS forms functional prion-like aggregates to activate and propagate antiviral innate immune response." *Cell* **146**(3): 448-461.
- Ishii, K. J., C. Coban, H. Kato, K. Takahashi, Y. Torii, F. Takeshita, H. Ludwig, G. Sutter, K. Suzuki, H. Hemmi, S. Sato, M. Yamamoto, S. Uematsu, T. Kawai, O. Takeuchi and S. Akira (2006). "A Toll-like receptor-independent antiviral response induced by double-stranded B-form DNA." *Nat Immunol* **7**(1): 40-48.
- Ishikawa, H. and G. N. Barber (2008). "STING is an endoplasmic reticulum adaptor that facilitates innate immune signalling." *Nature* **455**(7213): 674-678.
- Ishikawa, H., Z. Ma and G. N. Barber (2009). "STING regulates intracellular DNA-mediated, type I interferon-dependent innate immunity." *Nature* **461**(7265): 788-792.
- Jakobsen, M. R., R. O. Bak, A. Andersen, R. K. Berg, S. B. Jensen, J. Tengchuan, A. Laustsen, K. Hansen, L. Ostergaard, K. A. Fitzgerald, T. S. Xiao, J. G. Mikkelsen, T. H. Mogensen and S. R. Paludan (2013). "IFI16 senses DNA forms of the lentiviral replication cycle and controls HIV-1 replication." *Proc Natl Acad Sci U S A* **110**(48): E4571-4580.
- Jiang, X., L. N. Kinch, C. A. Brautigam, X. Chen, F. Du, N. V. Grishin and Z. J. Chen (2012). "Ubiquitin-induced oligomerization of the RNA sensors RIG-I and MDA5 activates antiviral innate immune response." *Immunity* **36**(6): 959-973.

- Kadowaki, N., S. Ho, S. Antonenko, R. W. Malefyt, R. A. Kastelein, F. Bazan and Y. J. Liu (2001). "Subsets of human dendritic cell precursors express different toll-like receptors and respond to different microbial antigens." *J Exp Med* **194**(6): 863-869.
- Kane, M., S. S. Yadav, J. Bitzegeio, S. B. Kutluay, T. Zang, S. J. Wilson, J. W. Schoggins, C. M. Rice, M. Yamashita, T. Hatzlioannou and P. D. Bieniasz (2013). "MX2 is an interferon-induced inhibitor of HIV-1 infection." *Nature* **502**(7472): 563-566.
- Kato, H., K. Takahasi and T. Fujita (2011). "RIG-I-like receptors: cytoplasmic sensors for non-self RNA." *Immunol Rev* **243**(1): 91-98.
- Kato, H., O. Takeuchi, S. Sato, M. Yoneyama, M. Yamamoto, K. Matsui, S. Uematsu, A. Jung, T. Kawai, K. J. Ishii, O. Yamaguchi, K. Otsu, T. Tsujimura, C. S. Koh, C. Reis e Sousa, Y. Matsuura, T. Fujita and S. Akira (2006). "Differential roles of MDA5 and RIG-I helicases in the recognition of RNA viruses." *Nature* **441**(7089): 101-105.
- Kawai, T., K. Takahashi, S. Sato, C. Coban, H. Kumar, H. Kato, K. J. Ishii, O. Takeuchi and S. Akira (2005). "IPS-1, an adaptor triggering RIG-I- and Mda5-mediated type I interferon induction." *Nat Immunol* **6**(10): 981-988.
- Kawane, K., H. Fukuyama, G. Kondoh, J. Takeda, Y. Ohsawa, Y. Uchiyama and S. Nagata (2001). "Requirement of DNase II for definitive erythropoiesis in the mouse fetal liver." *Science* **292**(5521): 1546-1549.
- Kawane, K., M. Ohtani, K. Miwa, T. Kizawa, Y. Kanbara, Y. Yoshioka, H. Yoshikawa and S. Nagata (2006). "Chronic polyarthritis caused by mammalian DNA that escapes from degradation in macrophages." *Nature* **443**(7114): 998-1002.
- Kinter, A., A. Catanzaro, J. Monaco, M. Ruiz, J. Justement, S. Moir, J. Arthos, A. Oliva, L. Ehler, S. Mizell, R. Jackson, M. Ostrowski, J. Hoxie, R. Offord and A. S. Fauci (1998). "CC-chemokines enhance the replication of T-tropic strains of HIV-1 in CD4(+) T cells: role of signal transduction." *Proc Natl Acad Sci U S A* **95**(20): 11880-11885.
- Kranzusch, P. J., A. S. Lee, J. M. Berger and J. A. Doudna (2013). "Structure of human cGAS reveals a conserved family of second-messenger enzymes in innate immunity." *Cell Rep* **3**(5): 1362-1368.
- Kruger, A., M. Oldenburg, C. Chebrolu, D. Beisser, J. Kolter, A. M. Sigmund, J. Steinmann, S. Schafer, H. Hochrein, S. Rahmann, H. Wagner, P. Henneke, V. Hornung, J. Buer and C. J. Kirschning (2015). "Human TLR8 senses UR/URR motifs in bacterial and mitochondrial RNA." *EMBO Rep*.
- Laguette, N., B. Sobhian, N. Casartelli, M. Ringeard, C. Chable-Bessia, E. Segéral, A. Yatim, S. Emiliani, O. Schwartz and M. Benkirane (2011). "SAMHD1 is the dendritic- and myeloid-cell-specific HIV-1 restriction factor counteracted by Vpx." *Nature* **474**(7353): 654-657.
- Lahaye, X., T. Satoh, M. Gentili, S. Cerboni, C. Conrad, I. Hurbain, A. El Marjou, C. Lacabarat, J. D. Lelievre and N. Manel (2013). "The capsids of HIV-1 and HIV-2 determine immune detection of the viral cDNA by the innate sensor cGAS in dendritic cells." *Immunity* **39**(6): 1132-1142.

- Lanzetta, P. A., L. J. Alvarez, P. S. Reinach and O. A. Candia (1979). "An improved assay for nanomole amounts of inorganic phosphate." *Anal Biochem* **100**(1): 95-97.
- Lartigue, A., P. Courville, I. Auquit, A. Francois, C. Arnoult, F. Tron, D. Gilbert and P. Musette (2006). "Role of TLR9 in anti-nucleosome and anti-DNA antibody production in lpr mutation-induced murine lupus." *J Immunol* **177**(2): 1349-1354.
- Le Bon, A. and D. F. Tough (2002). "Links between innate and adaptive immunity via type I interferon." *Curr Opin Immunol* **14**(4): 432-436.
- Le Goffic, R., V. Balloy, M. Lagranderie, L. Alexopoulou, N. Escriou, R. Flavell, M. Chignard and M. Si-Tahar (2006). "Detrimental contribution of the Toll-like receptor (TLR)3 to influenza A virus-induced acute pneumonia." *PLoS Pathog* **2**(6): e53.
- Lee-Kirsch, M. A., M. Gong, D. Chowdhury, L. Senenko, K. Engel, Y. A. Lee, U. de Silva, S. L. Bailey, T. Witte, T. J. Vyse, J. Kere, C. Pfeiffer, S. Harvey, A. Wong, S. Koskenmies, O. Hummel, K. Rohde, R. E. Schmidt, A. F. Dominiczak, M. Gahr, T. Hollis, F. W. Perrino, J. Lieberman and N. Hubner (2007). "Mutations in the gene encoding the 3'-5' DNA exonuclease TREX1 are associated with systemic lupus erythematosus." *Nat Genet* **39**(9): 1065-1067.
- Lehtinen, D. A., S. Harvey, M. J. Mulcahy, T. Hollis and F. W. Perrino (2008). "The TREX1 double-stranded DNA degradation activity is defective in dominant mutations associated with autoimmune disease." *J Biol Chem* **283**(46): 31649-31656.
- Levinsohn, J. L., Z. L. Newman, K. A. Hellmich, R. Fattah, M. A. Getz, S. Liu, I. Sastalla, S. H. Leppla and M. Moayeri (2012). "Anthrax lethal factor cleavage of Nlrp1 is required for activation of the inflammasome." *PLoS Pathog* **8**(3): e1002638.
- Li, L., Q. Yin, P. Kuss, Z. Maliga, J. L. Millan, H. Wu and T. J. Mitchison (2014). "Hydrolysis of 2'3'-cGAMP by ENPP1 and design of nonhydrolyzable analogs." *Nat Chem Biol* **10**(12): 1043-1048.
- Li, X., C. Shu, G. Yi, C. T. Chaton, C. L. Shelton, J. Diao, X. Zuo, C. C. Kao, A. B. Herr and P. Li (2013). "Cyclic GMP-AMP synthase is activated by double-stranded DNA-induced oligomerization." *Immunity* **39**(6): 1019-1031.
- Li, X. D., L. Sun, R. B. Seth, G. Pineda and Z. J. Chen (2005). "Hepatitis C virus protease NS3/4A cleaves mitochondrial antiviral signaling protein off the mitochondria to evade innate immunity." *Proc Natl Acad Sci U S A* **102**(49): 17717-17722.
- Li, X. D., J. Wu, D. Gao, H. Wang, L. Sun and Z. J. Chen (2013). "Pivotal roles of cGAS-cGAMP signaling in antiviral defense and immune adjuvant effects." *Science* **341**(6152): 1390-1394.
- Liddicoat, B. J., R. Piskol, A. M. Chalk, G. Ramaswami, M. Higuchi, J. C. Hartner, J. B. Li, P. H. Seburg and C. R. Walkley (2015). "RNA editing by ADAR1 prevents MDA5 sensing of endogenous dsRNA as nonself." *Science* **349**(6252): 1115-1120.
- Liu, S., X. Cai, J. Wu, Q. Cong, X. Chen, T. Li, F. Du, J. Ren, Y. T. Wu, N. V. Grishin and Z. J. Chen (2015). "Phosphorylation of innate immune adaptor proteins MAVS, STING, and TRIF induces IRF3 activation." *Science* **347**(6227): aaa2630.

- Liu, S., J. Chen, X. Cai, J. Wu, X. Chen, Y. T. Wu, L. Sun and Z. J. Chen (2013). "MAVS recruits multiple ubiquitin E3 ligases to activate antiviral signaling cascades." *Elife* **2**: e00785.
- Loo, Y. M., J. Fornek, N. Crochet, G. Bajwa, O. Perwitasari, L. Martinez-Sobrido, S. Akira, M. A. Gill, A. Garcia-Sastre, M. G. Katze and M. Gale, Jr. (2008). "Distinct RIG-I and MDA5 signaling by RNA viruses in innate immunity." *J Virol* **82**(1): 335-345.
- Lund, J. M., L. Alexopoulou, A. Sato, M. Karow, N. C. Adams, N. W. Gale, A. Iwasaki and R. A. Flavell (2004). "Recognition of single-stranded RNA viruses by Toll-like receptor 7." *Proc Natl Acad Sci U S A* **101**(15): 5598-5603.
- Maino, V. C., M. A. Suni and J. J. Ruitenberg (1995). "Rapid flow cytometric method for measuring lymphocyte subset activation." *Cytometry* **20**(2): 127-133.
- Manel, N., B. Hogstad, Y. Wang, D. E. Levy, D. Unutmaz and D. R. Littman (2010). "A cryptic sensor for HIV-1 activates antiviral innate immunity in dendritic cells." *Nature* **467**(7312): 214-217.
- Mazur, D. J. and F. W. Perrino (1999). "Identification and expression of the TREX1 and TREX2 cDNA sequences encoding mammalian 3'-->5' exonucleases." *J Biol Chem* **274**(28): 19655-19660.
- Medzhitov, R. and C. A. Janeway, Jr. (1997). "Innate immunity: the virtues of a nonclonal system of recognition." *Cell* **91**(3): 295-298.
- Melchjorsen, J., S. B. Jensen, L. Malmgaard, S. B. Rasmussen, F. Weber, A. G. Bowie, S. Matikainen and S. R. Paludan (2005). "Activation of innate defense against a paramyxovirus is mediated by RIG-I and TLR7 and TLR8 in a cell-type-specific manner." *J Virol* **79**(20): 12944-12951.
- Meylan, E., J. Curran, K. Hofmann, D. Moradpour, M. Binder, R. Bartenschlager and J. Tschopp (2005). "Cardif is an adaptor protein in the RIG-I antiviral pathway and is targeted by hepatitis C virus." *Nature* **437**(7062): 1167-1172.
- Monroe, K. M., Z. Yang, J. R. Johnson, X. Geng, G. Doitsh, N. J. Krogan and W. C. Greene (2014). "IFI16 DNA sensor is required for death of lymphoid CD4 T cells abortively infected with HIV." *Science* **343**(6169): 428-432.
- Morita, M., G. Stamp, P. Robins, A. Dulic, I. Rosewell, G. Hrvnak, G. Daly, T. Lindahl and D. E. Barnes (2004). "Gene-targeted mice lacking the Trex1 (DNase III) 3'-->5' DNA exonuclease develop inflammatory myocarditis." *Mol Cell Biol* **24**(15): 6719-6727.
- Motani, K., S. Ito and S. Nagata (2015). "DNA-Mediated Cyclic GMP-AMP Synthase-Dependent and -Independent Regulation of Innate Immune Responses." *J Immunol* **194**(10): 4914-4923.
- Murphy, K. M. and S. L. Reiner (2002). "The lineage decisions of helper T cells." *Nat Rev Immunol* **2**(12): 933-944.
- Muzio, M., N. Polentarutti, D. Bosisio, P. P. Manoj Kumar and A. Mantovani (2000). "Toll-like receptor family and signalling pathway." *Biochem Soc Trans* **28**(5): 563-566.

- Neil, S. J., T. Zang and P. D. Bieniasz (2008). "Tetherin inhibits retrovirus release and is antagonized by HIV-1 Vpu." *Nature* **451**(7177): 425-430.
- Nissen, S. K., J. F. Hojen, K. L. Andersen, E. Kofod-Olsen, R. K. Berg, S. R. Paludan, L. Ostergaard, M. R. Jakobsen, M. Tolstrup and T. H. Mogensen (2014). "Innate DNA sensing is impaired in HIV patients and IFI16 expression correlates with chronic immune activation." *Clin Exp Immunol* **177**(1): 295-309.
- Pawaria, S., K. Moody, P. Bustos, K. Nundel, C. H. Choi, T. Ghayur and A. Marshak-Rothstein (2015). "Cutting Edge: DNase II deficiency prevents activation of autoreactive B cells by double-stranded DNA endogenous ligands." *J Immunol* **194**(4): 1403-1407.
- Peisley, A., B. Wu, H. Xu, Z. J. Chen and S. Hur (2014). "Structural basis for ubiquitin-mediated antiviral signal activation by RIG-I." *Nature* **509**(7498): 110-114.
- Pertel, T., S. Hausmann, D. Morger, S. Zuger, J. Guerra, J. Lascano, C. Reinhard, F. A. Santoni, P. D. Uchil, L. Chatel, A. Bisiaux, M. L. Albert, C. Strambio-De-Castillia, W. Mothes, M. Pizzato, M. G. Grutter and J. Luban (2011). "TRIM5 is an innate immune sensor for the retrovirus capsid lattice." *Nature* **472**(7343): 361-365.
- Pichlmair, A., O. Schulz, C. P. Tan, T. I. Naslund, P. Liljestrom, F. Weber and C. Reis e Sousa (2006). "RIG-I-mediated antiviral responses to single-stranded RNA bearing 5'-phosphates." *Science* **314**(5801): 997-1001.
- Plataniatis, L. C. (2005). "Mechanisms of type-I- and type-II-interferon-mediated signalling." *Nat Rev Immunol* **5**(5): 375-386.
- Rasaiyaah, J., C. P. Tan, A. J. Fletcher, A. J. Price, C. Blondeau, L. Hilditch, D. A. Jacques, D. L. Selwood, L. C. James, M. Noursadeghi and G. J. Towers (2013). "HIV-1 evades innate immune recognition through specific cofactor recruitment." *Nature* **503**(7476): 402-405.
- Rathinam, V. A., Z. Jiang, S. N. Waggoner, S. Sharma, L. E. Cole, L. Waggoner, S. K. Vanaja, B. G. Monks, S. Ganesan, E. Latz, V. Hornung, S. N. Vogel, E. Szomolanyi-Tsuda and K. A. Fitzgerald (2010). "The AIM2 inflammasome is essential for host defense against cytosolic bacteria and DNA viruses." *Nat Immunol* **11**(5): 395-402.
- Reikine, S., J. B. Nguyen and Y. Modis (2014). "Pattern Recognition and Signaling Mechanisms of RIG-I and MDA5." *Front Immunol* **5**: 342.
- Rice, G. I., J. Bond, A. Asipu, R. L. Brunette, I. W. Manfield, I. M. Carr, J. C. Fuller, R. M. Jackson, T. Lamb, T. A. Briggs, M. Ali, H. Gornall, L. R. Couthard, A. Aeby, S. P. Attard-Montalto, E. Bertini, C. Bodemer, K. Brockmann, L. A. Brueton, P. C. Corry, I. Desguerre, E. Fazzi, A. G. Cazorla, B. Gener, B. C. Hamel, A. Heiberg, M. Hunter, M. S. van der Knaap, R. Kumar, L. Lagae, P. G. Landrieu, C. M. Lourenco, D. Marom, M. F. McDermott, W. van der Merwe, S. Orcesi, J. S. Prendiville, M. Rasmussen, S. A. Shalev, D. M. Soler, M. Shinawi, R. Spiegel, T. Y. Tan, A. Vanderver, E. L. Wakeling, E. Wassmer, E. Whittaker, P. Lebon, D. B. Stetson, D. T. Bonthron and Y. J. Crow (2009). "Mutations involved in Aicardi-Goutieres syndrome implicate SAMHD1 as regulator of the innate immune response." *Nat Genet* **41**(7): 829-832.

- Rice, G. I., Y. del Toro Duany, E. M. Jenkinson, G. M. Forte, B. H. Anderson, G. Ariaudo, B. Bader-Meunier, E. M. Baildam, R. Battini, M. W. Beresford, M. Casarano, M. Chouchane, R. Cimaz, A. E. Collins, N. J. Cordeiro, R. C. Dale, J. E. Davidson, L. De Waele, I. Desguerre, L. Faivre, E. Fazzi, B. Isidor, L. Lagae, A. R. Latchman, P. Lebon, C. Li, J. H. Livingston, C. M. Lourenco, M. M. Mancardi, A. Masurel-Paulet, I. B. McInnes, M. P. Menezes, C. Mignot, J. O'Sullivan, S. Orcesi, P. P. Picco, E. Riva, R. A. Robinson, D. Rodriguez, E. Salvatici, C. Scott, M. Szybowska, J. L. Tolmie, A. Vanderver, C. Vanhulle, J. P. Vieira, K. Webb, R. N. Whitney, S. G. Williams, L. A. Wolfe, S. M. Zuberi, S. Hur and Y. J. Crow (2014). "Gain-of-function mutations in IFIH1 cause a spectrum of human disease phenotypes associated with upregulated type I interferon signaling." *Nat Genet* **46**(5): 503-509.
- Rice, G. I., P. R. Kasher, G. M. Forte, N. M. Mannion, S. M. Greenwood, M. Szynkiewicz, J. E. Dickerson, S. S. Bhaskar, M. Zampini, T. A. Briggs, E. M. Jenkinson, C. A. Bacino, R. Battini, E. Bertini, P. A. Brogan, L. A. Brueton, M. Carpanelli, C. De Laet, P. de Lonlay, M. del Toro, I. Desguerre, E. Fazzi, A. Garcia-Cazorla, A. Heiberg, M. Kawaguchi, R. Kumar, J. P. Lin, C. M. Lourenco, A. M. Male, W. Marques, Jr., C. Mignot, I. Olivieri, S. Orcesi, P. Prabhakar, M. Rasmussen, R. A. Robinson, F. Rozenberg, J. L. Schmidt, K. Steindl, T. Y. Tan, W. G. van der Merwe, A. Vanderver, G. Vassallo, E. L. Wakeling, E. Wassmer, E. Whittaker, J. H. Livingston, P. Lebon, T. Suzuki, P. J. McLaughlin, L. P. Keegan, M. A. O'Connell, S. C. Lovell and Y. J. Crow (2012). "Mutations in ADAR1 cause Aicardi-Goutieres syndrome associated with a type I interferon signature." *Nat Genet* **44**(11): 1243-1248.
- Rosa, A., A. Chande, S. Ziglio, V. De Sanctis, R. Bertorelli, S. L. Goh, S. M. McCauley, A. Nowosielska, S. E. Antonarakis, J. Luban, F. A. Santoni and M. Pizzato (2015). "HIV-1 Nef promotes infection by excluding SERINC5 from virion incorporation." *Nature* **526**(7572): 212-217.
- Ryoo, J., J. Choi, C. Oh, S. Kim, M. Seo, S. Y. Kim, D. Seo, J. Kim, T. E. White, A. Brandariz-Nunez, F. Diaz-Griffero, C. H. Yun, J. A. Hollenbaugh, B. Kim, D. Baek and K. Ahn (2014). "The ribonuclease activity of SAMHD1 is required for HIV-1 restriction." *Nat Med* **20**(8): 936-941.
- Satoh, T., H. Kato, Y. Kumagai, M. Yoneyama, S. Sato, K. Matsushita, T. Tsujimura, T. Fujita, S. Akira and O. Takeuchi (2010). "LGP2 is a positive regulator of RIG-I- and MDA5-mediated antiviral responses." *Proc Natl Acad Sci U S A* **107**(4): 1512-1517.
- Sauer, J. D., K. Sotelo-Troha, J. von Moltke, K. M. Monroe, C. S. Rae, S. W. Brubaker, M. Hyodo, Y. Hayakawa, J. J. Woodward, D. A. Portnoy and R. E. Vance (2011). "The N-ethyl-N-nitrosourea-induced Goldenticket mouse mutant reveals an essential function of Sting in the in vivo interferon response to Listeria monocytogenes and cyclic dinucleotides." *Infect Immun* **79**(2): 688-694.
- Schroder, K. and J. Tschopp (2010). "The inflammasomes." *Cell* **140**(6): 821-832.

- Seth, R. B., L. Sun, C. K. Ea and Z. J. Chen (2005). "Identification and characterization of MAVS, a mitochondrial antiviral signaling protein that activates NF-kappaB and IRF 3." *Cell* **122**(5): 669-682.
- Sollberger, G., G. E. Strittmatter, M. Garstkiewicz, J. Sand and H. D. Beer (2014). "Caspase-1: the inflammasome and beyond." *Innate Immun* **20**(2): 115-125.
- Stanley, S. A., J. E. Johndrow, P. Manzanillo and J. S. Cox (2007). "The Type I IFN response to infection with Mycobacterium tuberculosis requires ESX-1-mediated secretion and contributes to pathogenesis." *J Immunol* **178**(5): 3143-3152.
- Stavrou, S., K. Blouch, S. Kotla, A. Bass and S. R. Ross (2015). "Nucleic acid recognition orchestrates the anti-viral response to retroviruses." *Cell Host Microbe* **17**(4): 478-488.
- Stetson, D. B., J. S. Ko, T. Heidmann and R. Medzhitov (2008). "Trex1 prevents cell-intrinsic initiation of autoimmunity." *Cell* **134**(4): 587-598.
- Stopak, K., C. de Noronha, W. Yonemoto and W. C. Greene (2003). "HIV-1 Vif blocks the antiviral activity of APOBEC3G by impairing both its translation and intracellular stability." *Mol Cell* **12**(3): 591-601.
- Stremlau, M., C. M. Owens, M. J. Perron, M. Kiessling, P. Autissier and J. Sodroski (2004). "The cytoplasmic body component TRIM5alpha restricts HIV-1 infection in Old World monkeys." *Nature* **427**(6977): 848-853.
- Sun, L., J. Wu, F. Du, X. Chen and Z. J. Chen (2013). "Cyclic GMP-AMP synthase is a cytosolic DNA sensor that activates the type I interferon pathway." *Science* **339**(6121): 786-791.
- Sun, Q., L. Sun, H. H. Liu, X. Chen, R. B. Seth, J. Forman and Z. J. Chen (2006). "The specific and essential role of MAVS in antiviral innate immune responses." *Immunity* **24**(5): 633-642.
- Suthar, M. S., H. J. Ramos, M. M. Brassil, J. Netland, C. P. Chappell, G. Blahnik, A. McMillan, M. S. Diamond, E. A. Clark, M. J. Bevan and M. Gale, Jr. (2012). "The RIG-I-like receptor LGP2 controls CD8(+) T cell survival and fitness." *Immunity* **37**(2): 235-248.
- Swain, S. L. and L. M. Bradley (1992). "Helper T cell memory: more questions than answers." *Semin Immunol* **4**(1): 59-68.
- Sze, A., S. M. Belgnaoui, D. Olagnier, R. Lin, J. Hiscott and J. van Grevenynghe (2013). "Host restriction factor SAMHD1 limits human T cell leukemia virus type 1 infection of monocytes via STING-mediated apoptosis." *Cell Host Microbe* **14**(4): 422-434.
- Tabeta, K., P. Georgel, E. Janssen, X. Du, K. Hoebe, K. Crozat, S. Mudd, L. Shamel, S. Sovath, J. Goode, L. Alexopoulou, R. A. Flavell and B. Beutler (2004). "Toll-like receptors 9 and 3 as essential components of innate immune defense against mouse cytomegalovirus infection." *Proc Natl Acad Sci U S A* **101**(10): 3516-3521.
- Tabeta, K., K. Hoebe, E. M. Janssen, X. Du, P. Georgel, K. Crozat, S. Mudd, N. Mann, S. Sovath, J. Goode, L. Shamel, A. A. Herskovits, D. A. Portnoy, M. Cooke, L. M.

- Tarantino, T. Wiltshire, B. E. Steinberg, S. Grinstein and B. Beutler (2006). "The Unc93b1 mutation 3d disrupts exogenous antigen presentation and signaling via Toll-like receptors 3, 7 and 9." *Nat Immunol* **7**(2): 156-164.
- Tanaka, Y. and Z. J. Chen (2012). "STING specifies IRF3 phosphorylation by TBK1 in the cytosolic DNA signaling pathway." *Sci Signal* **5**(214): ra20.
- Tolmie, J. L., P. Shillito, R. Hughes-Benzie and J. B. Stephenson (1995). "The Aicardi-Goutieres syndrome (familial, early onset encephalopathy with calcifications of the basal ganglia and chronic cerebrospinal fluid lymphocytosis)." *J Med Genet* **32**(11): 881-884.
- Tominaga, K., T. Yoshimoto, K. Torigoe, M. Kurimoto, K. Matsui, T. Hada, H. Okamura and K. Nakanishi (2000). "IL-12 synergizes with IL-18 or IL-1beta for IFN-gamma production from human T cells." *Int Immunol* **12**(2): 151-160.
- Tschopp, J. and K. Schroder (2010). "NLRP3 inflammasome activation: The convergence of multiple signalling pathways on ROS production?" *Nat Rev Immunol* **10**(3): 210-215.
- Tudor, D., S. Riffault, C. Carrat, F. Lefevre, M. Bernoin and B. Charley (2001). "Type I IFN modulates the immune response induced by DNA vaccination to pseudorabies virus glycoprotein C." *Virology* **286**(1): 197-205.
- Usami, Y., Y. Wu and H. G. Gottlinger (2015). "SERINC3 and SERINC5 restrict HIV-1 infectivity and are counteracted by Nef." *Nature* **526**(7572): 218-223.
- Vollmer, J., S. Tluk, C. Schmitz, S. Hamm, M. Jurk, A. Forsbach, S. Akira, K. M. Kelly, W. H. Reeves, S. Bauer and A. M. Krieg (2005). "Immune stimulation mediated by autoantigen binding sites within small nuclear RNAs involves Toll-like receptors 7 and 8." *J Exp Med* **202**(11): 1575-1585.
- Walunas, T. L., D. S. Bruce, L. Dustin, D. Y. Loh and J. A. Bluestone (1995). "Ly-6C is a marker of memory CD8+ T cells." *J Immunol* **155**(4): 1873-1883.
- Wang, Q., M. J. Moore, G. Adelman, J. A. Marto and P. A. Silver (2013). "PQBP1, a factor linked to intellectual disability, affects alternative splicing associated with neurite outgrowth." *Genes Dev* **27**(6): 615-626.
- Wang, T., T. Town, L. Alexopoulou, J. F. Anderson, E. Fikrig and R. A. Flavell (2004). "Toll-like receptor 3 mediates West Nile virus entry into the brain causing lethal encephalitis." *Nat Med* **10**(12): 1366-1373.
- Wassermann, R., M. F. Gulen, C. Sala, S. G. Perin, Y. Lou, J. Rybniker, J. L. Schmid-Burgk, T. Schmidt, V. Hornung, S. T. Cole and A. Ablasser (2015). "Mycobacterium tuberculosis Differentially Activates cGAS- and Inflammasome-Dependent Intracellular Immune Responses through ESX-1." *Cell Host Microbe* **17**(6): 799-810.
- Watson, R. O., S. L. Bell, D. A. MacDuff, J. M. Kimmey, E. J. Diner, J. Olivas, R. E. Vance, C. L. Stallings, H. W. Virgin and J. S. Cox (2015). "The Cytosolic Sensor cGAS Detects Mycobacterium tuberculosis DNA to Induce Type I Interferons and Activate Autophagy." *Cell Host Microbe* **17**(6): 811-819.

- Watson, R. O., P. S. Manzanillo and J. S. Cox (2012). "Extracellular M. tuberculosis DNA targets bacteria for autophagy by activating the host DNA-sensing pathway." *Cell* **150**(4): 803-815.
- Wu, B., A. Peisley, C. Richards, H. Yao, X. Zeng, C. Lin, F. Chu, T. Walz and S. Hur (2013). "Structural basis for dsRNA recognition, filament formation, and antiviral signal activation by MDA5." *Cell* **152**(1-2): 276-289.
- Wu, B., A. Peisley, D. Tetrault, Z. Li, E. H. Egelman, K. E. Magor, T. Walz, P. A. Penczek and S. Hur (2014). "Molecular imprinting as a signal-activation mechanism of the viral RNA sensor RIG-I." *Mol Cell* **55**(4): 511-523.
- Wu, J., L. Sun, X. Chen, F. Du, H. Shi, C. Chen and Z. J. Chen (2013). "Cyclic GMP-AMP is an endogenous second messenger in innate immune signaling by cytosolic DNA." *Science* **339**(6121): 826-830.
- Xu, H., X. He, H. Zheng, L. J. Huang, F. Hou, Z. Yu, M. J. de la Cruz, B. Borkowski, X. Zhang, Z. J. Chen and Q. X. Jiang (2014). "Structural basis for the prion-like MAVS filaments in antiviral innate immunity." *Elife* **3**: e01489.
- Xu, H., X. He, H. Zheng, L. J. Huang, F. Hou, Z. Yu, M. J. de la Cruz, B. Borkowski, X. Zhang, Z. J. Chen and Q. X. Jiang (2015). "Correction: Structural basis for the prion-like MAVS filaments in antiviral innate immunity." *Elife* **4**.
- Xu, L. G., Y. Y. Wang, K. J. Han, L. Y. Li, Z. Zhai and H. B. Shu (2005). "VISA is an adapter protein required for virus-triggered IFN-beta signaling." *Mol Cell* **19**(6): 727-740.
- Yan, N., A. D. Regalado-Magdos, B. Stiggebout, M. A. Lee-Kirsch and J. Lieberman (2010). "The cytosolic exonuclease TREX1 inhibits the innate immune response to human immunodeficiency virus type 1." *Nat Immunol* **11**(11): 1005-1013.
- Yang, Y. G., T. Lindahl and D. E. Barnes (2007). "Trex1 exonuclease degrades ssDNA to prevent chronic checkpoint activation and autoimmune disease." *Cell* **131**(5): 873-886.
- Yoneyama, M., M. Kikuchi, T. Natsukawa, N. Shinobu, T. Imaizumi, M. Miyagishi, K. Taira, S. Akira and T. Fujita (2004). "The RNA helicase RIG-I has an essential function in double-stranded RNA-induced innate antiviral responses." *Nat Immunol* **5**(7): 730-737.
- Yoshida, H., Y. Okabe, K. Kawane, H. Fukuyama and S. Nagata (2005). "Lethal anemia caused by interferon-beta produced in mouse embryos carrying undigested DNA." *Nat Immunol* **6**(1): 49-56.
- Zeng, M., Z. Hu, X. Shi, X. Li, X. Zhan, X. D. Li, J. Wang, J. H. Choi, K. W. Wang, T. Purrington, M. Tang, M. Fina, R. J. DeBerardinis, E. M. Moresco, G. Pedersen, G. M. McInerney, G. B. Karlsson Hedestam, Z. J. Chen and B. Beutler (2014). "MAVS, cGAS, and endogenous retroviruses in T-independent B cell responses." *Science* **346**(6216): 1486-1492.

- Zeng, W., L. Sun, X. Jiang, X. Chen, F. Hou, A. Adhikari, M. Xu and Z. J. Chen (2010). "Reconstitution of the RIG-I pathway reveals a signaling role of unanchored polyubiquitin chains in innate immunity." *Cell* **141**(2): 315-330.
- Zhang, S. Y., E. Jouanguy, S. Ugolini, A. Smahi, G. Elain, P. Romero, D. Segal, V. Sancho-Shimizu, L. Lorenzo, A. Puel, C. Picard, A. Chapgier, S. Plancoulaine, M. Titeux, C. Cognet, H. von Bernuth, C. L. Ku, A. Casrouge, X. X. Zhang, L. Barreiro, J. Leonard, C. Hamilton, P. Lebon, B. Heron, L. Vallee, L. Quintana-Murci, A. Hovnanian, F. Rozenberg, E. Vivier, F. Geissmann, M. Tardieu, L. Abel and J. L. Casanova (2007). "TLR3 deficiency in patients with herpes simplex encephalitis." *Science* **317**(5844): 1522-1527.
- Zhang, X., H. Shi, J. Wu, X. Zhang, L. Sun, C. Chen and Z. J. Chen (2013). "Cyclic GMP-AMP containing mixed phosphodiester linkages is an endogenous high-affinity ligand for STING." *Mol Cell* **51**(2): 226-235.
- Zhang, X., J. Wu, F. Du, H. Xu, L. Sun, Z. Chen, C. A. Brautigam, X. Zhang and Z. J. Chen (2014). "The cytosolic DNA sensor cGAS forms an oligomeric complex with DNA and undergoes switch-like conformational changes in the activation loop." *Cell Rep* **6**(3): 421-430.
- Zhao, Y., J. Yang, J. Shi, Y. N. Gong, Q. Lu, H. Xu, L. Liu and F. Shao (2011). "The NLRC4 inflammasome receptors for bacterial flagellin and type III secretion apparatus." *Nature* **477**(7366): 596-600.
- Zhu, J., H. Yamane and W. E. Paul (2010). "Differentiation of effector CD4 T cell populations (*)." *Annu Rev Immunol* **28**: 445-489.